STUDY OF SYNTHESIS AND CHARACTERIZATION OF POLYMER ELECTROLYTE NANOCOMPOSITE FOR DYE-SENSITIZED SOLAR CELL

Thesis Submitted for the Award of the Degree of

DOCTOR OF PHILOSOPHY

in

Electronics and Communication Engineering

By

Palvinder Singh

Registration Number: 41900064

Supervised By

Dr. Amit Sachdeva (16701)

Professor

School of Electronics and Electrical Engineering

Co-Supervised by

Dr. Cherry Bhargava

Senior Engineer

Centre for Reliability and Safety, Eaton India Innovation Centre Eaton, Magarpatta SEZ IT City, Pune-4110284

LOVELY PROFESSIONAL UNIVERSITY, PUNJAB

2024

DECLARATION

I, hereby declared that the presented work in the thesis entitled "Study Of Synthesis and Characterization of Polymer Electrolyte Nanocomposite for Dye-Sensitized Solar Cell" in fulfilment of degree of **Doctor of Philosophy (Ph. D.)** is outcome of research work carried out by me under the supervision Dr. Amit Sachdeva, working as Associate Professor, in the School of Electronics and Electrical Engineering of Lovely Professional University, Punjab, India. In keeping with the general practice of reporting scientific observations, due acknowledgements have been made whenever work described here has been based on the findings of another investigator. This work has not been submitted in part or full to any other University or Institute for the award of any degree.

(Signature of Scholar)

Palvinder Singh
Registration No.: 41900064
School of Electronics and Electrical Engineering, Lovely Professional University,
Punjab, India

CERTIFICATE

This is to certify that the work reported in the Ph. D. thesis entitled "Study of Synthesis and Characterization of Polymer Electrolyte Nanocomposite for Dye-Sensitized Solar Cell" submitted in fulfillment of the requirement for the reward of degree of **Doctor of Philosophy (Ph.D.)** in the School of Electronics and Electrical Engineering, is a research work carried out by Palvinder Singh, Regn. No: 41900064, is bonafide record of his/her original work carried out under my supervision and that no part of thesis has been submitted for any other degree, diploma, or equivalent course.

(Signature of Supervisor)
Dr. Amit Sachdeva
Professor
School of Electronics and Electrical Engineering, Lovely Professional University, Punjab, India

(Signature of Co-Supervisor)
Dr. Cherry Bhargava
Senior Engineer
Centre for Reliability and Safety,
Eaton India Innovation Centre
Eaton, Magarpatta SEZ IT City,
Pune-4110284.

ACKNOWLEDGEMENT

I would like to express my deepest gratitude to the following individuals and organizations who have contributed to the successful completion of this Ph.D. thesis:

My supervisor, Dr. Amit Sachdeva, Professor, School of Electronics and Electrical Engineering, Lovely Professional University, Phagwara for their invaluable guidance, support, and encouragement throughout the entire duration of my research. Their expertise, insightful feedback, and unwavering commitment to excellence have been instrumental in shaping this thesis.

I would be thankful to the members of the Research Advisory Committee, for their expertise, critical evaluation, and constructive suggestions, which have significantly enhanced the quality and rigor of this work.

I am grateful to the Lovely Professional University, Phagwara, Chandigarh University, Gharuan, Mohali, for providing the necessary resources, infrastructure, and academic environment that fostered a conducive research atmosphere.

We would like to thank Dr. Parmod K. Singh from Sharda University in Greater Noida, India for their technical support in carrying out experiments, giving us access to specialized tools, and helping us with data analysis.

I would like to extend my appreciation to Dr. Rajinder Singh Rana, Principal, Sanatan Dharma College, Ambala Cantt., Haryana who motivate me to do higher education for career growth. I would be thankful to my colleagues and friends who have supported me throughout this journey, both academically and personally. Their camaraderie, discussions, and shared experiences were invaluable.

I would like to thank my family for their unwavering love, understanding, and continuous encouragement. Their belief in my abilities has been my greatest motivation, and I am grateful for their presence in my life.

ABSTRACT

Poly (ethyl Methacrylate) (PEMA) based electrolyte was prepared using Solution Casting Technique. Poly (ethyl Methacrylate) conductivity was increased by adding Potassium Iodide as salt in different weight percentage variations. After that sample had ionic conductivity 3.80 x 10^{-6} S/cm at 40% weight percentage of Potassium Iodide (KI). Further amorphicity enhancement and mechanical strength was increased by adding Ethylene Carbonate (EC) as plasticizer. Ethylene carbonate was added (EC) in different weight percentage variation and got maximum conducting sample at 60% weight percentage of EC i.e., 4.64 x 10^{-5} S/cm. Maximum conducting sample was investigated using various characterization approaches such as X-ray Diffraction (XRD), Scanning Electron Microscopy (SEM), Complex Impedance Spectroscopy (CIS), Fourier Transform Infrared Spectroscopy (FTIR). Further enhancement of conductivity incorporation of multiwalled carbon nanotubes was used. Carbon nanotubes were added into maximum conducting polymer electrolyte of Poly (ethyl Methacrylate) (PEMA) +40% wt. percentage of KI+ 60% wt. percentage of EC for further enhancement of conductivity of composite electrolyte. Carbon nanotubes were added into maximum conducting composite electrolyte with respect to different weight percentage. At 9% wt. percentage of CNT, polymer composite sample had maximum conducting sample having conductivity 3.5x10^{-4} S/cm. After that Polymer electrolyte maximum conducting sample was used to prepare DSSC solar cell electrolyte. DSSC solar cell prepared using doctor blade technique. The DSSC solar cell model was tested using Sun Simulator and Keysight instruments under Sun 1 condition. After 72 hours it again tested and fill factor value obtained 81.12 and energy conversion efficiency 2.26%.

Table of Contents

List of Figures

List of Tables

Chapter 1. : Introduction

1.1. GENERAL INTRODUCTION

Now a days many advanced portable devices have being invented, for that purpose there has been a requirement of high-performance energy devices. So that researchers have focused on developing advanced energy /battery systems. Early 1830 Michael Faraday discovered conduction of ions in liquid and solid electrolytes that field known as "Solid StateIonics". In this field Ionics fast, ionic conduction takes place through Bulk/solid materials. For that reason, research is focused in exploring the chemical and physical properties of these solids known as "Supersonic Solids" or [1] "Fast Ion conductors" or "Solid electrolytes"

1.2. TYPE OF SOLID ELECTROLYTES

Firstly, depending upon ions the solid electrolytes are classified into following groups:

i. Solid electrolytes are conductible by silver ion (Ag+).
ii. Solid electrolytes are conductible by copper ion (Cu^{+})
iii. Solid electrolytes are conductible by Lithium ion (Li^{+}).
iv. Solid electrolytes are conductible by Sodium ion (Na^{+}).
v. Solid electrolytes are conductible by Hydrogen ion (H^{+}).
vi. Solid electrolytes are conductible by Oxygen ion (O^{-2}).
vii. Solid electrolytes are conductible by Fluoride ion (F^{-}).
viii. A few divalent cations, including Ba++, Cd++, and Sr++

But it observed that their conductivity is very small. Additionally, solid electrolytes are classified into several groups according to their microstructure and physical characteristics.

i. Crystalline solid electrolytes.
ii. Glass solid electrolytes.
iii. Gel solid electrolytes.

iv. Composite or dispersed phase solid electrolytes.

v. Polymer solid electrolytes or Polymer electrolytes

All these electrolytes have high ionic conductivity so that these electrolytes are used in electrochemical devices such as batteries, Dye sensitized solar cell (DSSCs).

1.3. POLYMERS BASICS:

The notation “polymer" originates from the language Greek “POLY" means many and "MEROS," means parts. respectively. It is a material that is made of numerous components. For polymers, some scientists prefer to use the term "macromolecules." The practical impact of polymers on daily life is significant and very direct. The "polymer age” are currently experiencing. As a result, one of the most significant and expanding fields of science is that of macromolecules and polymers. [2]. As mentioned above type, Polymer electrolytes are suitable for energy devices due to light weight, flexibility, chemical stability, good processability and ease of film forming ability. Solid polymer electrolytes have flexible mechanical properties with ionic conductivity. So that these are used in rechargeable batteries, fuel cells, supercapacitors, electrochemical sensors etc. [2]–[4]. So, there has been a challenge to choose a host polymer for preparation of polymer electrolyte due to availability of various type of polymers. Below figure 1.1 shows chain structure of polymer.

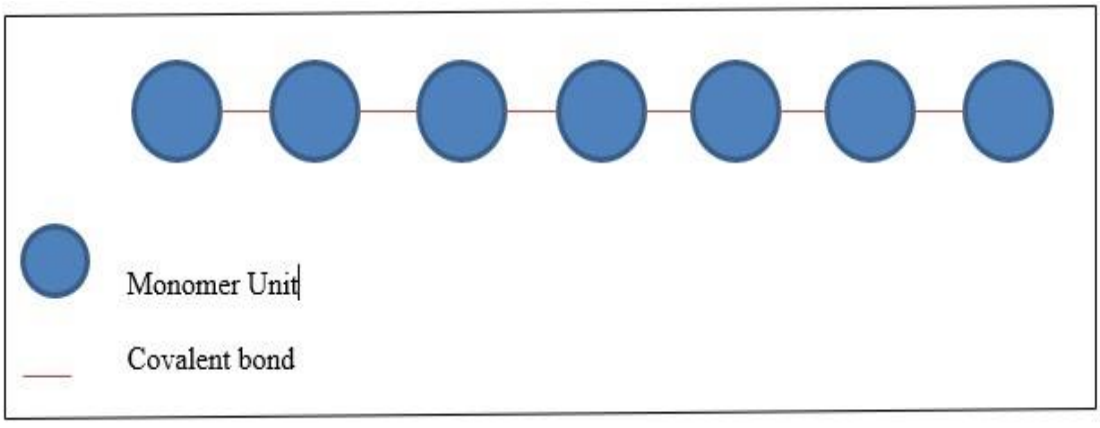

Figure 1.1: Chain structure of Polymer.

1.3.1 CLASSIFICATION OF POLYMERS

Polymers are classified in various categories depending upon nature of origin, thermal behavior, formation route, and crystalline nature, occurrence of polarity, physical properties, and type of chain, structural organization, and tacticity polymers. [5]. Some type of polymer are shown in Figure 1.2.

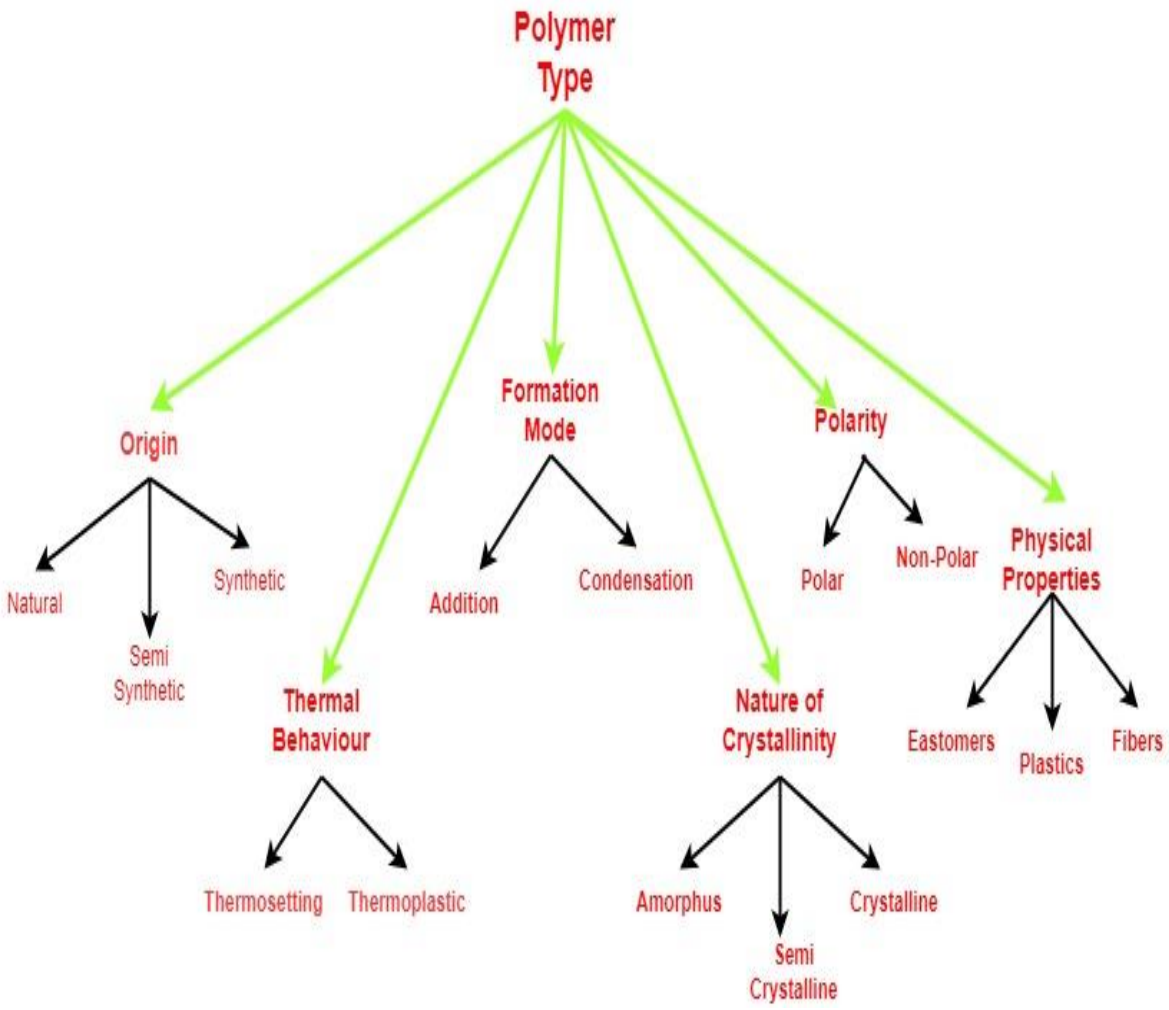

Figure 1.2: Classification of polymers.

Origin

Depending on the nature of origin, polymers are grouped as Natural, Semi Synthetic and Synthetic.

(i) Natural polymers: Name suggests that polymers that free available in environment are acknowledged as Natural Polymers. (e.g.) Rubber, Silk, Protein and so many.

(ii) Semi Synthetic Polymers: Polymers are obtained because of chemical modification of natural Polymers. (e.g.) methyl cellulose, cellulosic.

(iii) Synthetic Polymers: The polymers that are prepared in the lab/research laboratory using some thermal techniques come under this category. (e.g.) Polyethyl oxide, polyvinyl alcohol.

. *Thermal Activation*

Depending on the thermal behavior, polymers fall under two categories.

(i) Thermoplastic Polymers: Polymers that become plastic when subjected to thermal energy and on removal of heat if the soft plastic gets harden, then the polymers are said to be Thermoplastic polymers. (e.g.) Nylon, Polyvinyl chloride.

(ii) Thermosetting Polymers: On heating if polymers undergo certain chemical reactions and get converted into an infusible, insoluble polymer network, then the polymers are known as Thermosetting Polymers. (e.g.) Epoxy Resin, Urea formaldehyde.

Formation Route

The mode of formation of polymers also decides their type.

(i) Addition Polymers: The monomer molecules add to each other and form a chain-by-chain mechanism. The product formed is the Addition Polymer. The above process by which Addition Polymers are obtained is termed Addition Polymerisation. (e.g.) Teflon, Polyethylene.

(ii) Condensation Polymers: The polymers formed by condensation reaction are known as Condensation Polymers. In this case, the molecule fuses to form macromolecules with some loss of small molecules as by-products. (e.g.) Cellulose, Polypeptide chains of proteins.

Nature of Crystallinity

Polymers exist in three forms - Amorphous, Semi Crystalline and Crystalline forms. For specific applications, the state of polymers plays a vital role. Thus, polymers have been

classified based on their crystallinity. Some polymers have a high degree of ordered crystalline structures whereas certain polymers have disordered non crystalline arrangements occurring in powdered form. There are some polymers having a mixture of crystalline and powdery nature. Accordingly, the polymers have been classified as Crystalline, Amorphous and Semi Crystalline polymers respectively.

Polarity

If the molecules of polymers are not completely bonded to each other by covalent bond, then a slight imbalance in the charge distribution occurs. Thus, some molecules of the polymers are electronegative, and some are electropositive. This type of polymer is known as polar polymers (e.g.) PVC, polyacrylic acid.

In certain polymers, molecules have full covalent bonds and charge symmetry exists. Such polymers are termed as non-polar polymers (e.g.) polyolefines.

Physical Properties

Due to physical properties polymers are classified in the following categories:

(i) Elastomers: Polymers with weak intermolecular forces, possessing both viscosity (e.g.) Synthetic rubber, Natural rubber.

(ii) Plastic: Synthetic or Organic polymers of high molecular mass are called plastics. On application of heat and pressure, plastics can be moulded into the required articles. (e.g.) PMMA, PVC**.**

(iii) Fibers: Polymers having long filamentous thread and length is longer than its diameter are said to be Fibers. (e.g.) PAN, Asbestos.

Structural Organization

Depending on the structural arrangement of monomer units in polymers, they are categorized as follows.

(i) Linear Polymer: Polymer's monomer unit are arranged in a linear orientation; it is a linear polymer.

(ii) Branched Polymer: If the polymer consists of monomer units which are joined as branches, then the polymer is known as Branched Polymer.

(iii)Cross linked Polymer: This type of polymer comprises of monomer units that are connected to each other in a chain like manner.

Chain Formation

Based on the composition of monomer units, there are two divisions of polymer.

(i) Homo Polymers: The monomer units of the same chemical composition or structure join to form Homopolymers.

(ii) Hetero Polymers: The polymers made of different types of monomer units are known as hetero polymers.

Tacticity

Tacticity means the configurational orderliness of repeating units in the main chain of the polymers. On this basis, polymers are classified into three types.

(i) Isotactic Polymer: The presence of substituent groups on the same side of the macro-molecular backbone constitutes Isotactic Polymer.

(ii) Syndiotactic Polymer: In this type of polymer, the characteristic groups are attached in an alternate way.

(iii) Atactic Polymer: when polymer substituents groups are arranged alongside chain known as Atactic Polymer

Thus, based on the application, the host polymers are to be chosen carefully. Then the polymer electrolytes are prepared with these host polymers.

1.4. POLYMER ELECTROLYTES

Ion incorporated polymer-based materials serve as electrolytes in electrochemical devices such as supercapacitor, battery, and solar cell etc. The ionic salts are dissolved in a polymer matrix to create the polymer electrolytes. The PE serves as a divider between the two electrodes in this instance and acts as a conduit for ionic migration. They are ion conducting but electrical insulators thus, preventing the short circuit between the anode and the cathode.

The polymers favour the easy dissociation of salt resulting in cations and anions. The dissociation takes place due to the coordinating effects of neighboring polymer segments

consisting of hetero atoms such as N, O etc. Ionic conduction is caused by a covalent bond between the salt and the polymer backbone. The reorganization of the polymer segments' positions and configuration increases ionic mobility. Table 1.1 lists the characteristics, benefits, and various uses of polymers. The polymers in the polymer electrolyte typically exhibit two different motions.

(i) Segmental motion: It is also known as internal Brownian motion. This motion is the result of movement of each monomer segment.

(ii) Molecular motion: This is due to the motion of molecule. Molecular motion is also known as External Brownian motion.

1.4.1 Categories of Polymer electrolytes

Based on the preparation strategies followed during the film casting, the polymer electrolytes have been categorized into the following four types [6]

- Solvent Free/Dry PE
- Gel based PE.
- Rubbery PE
- Composite PE

Table 1-1: Characteristics, benefits, and use of polymer

S. No	Properties	Advantage	Industrial Application
1	Transparent	Easy of fabrication	Electrochromic window
2	Light weight	restricts the application of corrosive bonds	DSSC, Solar cells, fuel cells
3	Solvent free	Extended lifespan	Solid state batteries
4	High safety	Reduce flammability	Analog meter devices
5	Ionic conductivity high	Non-toxic	Electrochromic display equipment's
6	Versatility	Cheaper	Electric Automobiles
7	Reliability	consistency of the parameters	Solid –state batteries
8	Self-discharging low	internal shorting does not	Solid –state batteries

exist

Dry / Solvent Free Polymer Electrolytes

These polymer electrolytes contain both polymer and lithium salt. The lithium salt is dissolved in the polymer matrix to create them. In this case, the polymer supports ionic conduction by serving as a conducting host. These electrolytes can be easily made into free-standing films and are highly compatible with the electrodes because of their flexibility. A tremendous interest is shown in developing various types of dry polymer electrolytes for their potential applications in rechargeable lithium based cell/batteries since of its high density energy content and safety [7]. In rechargeable lithium-ion batteries, poly (ethylene oxide) (PEO) based polymers with lithium salts are the most frequently used dry polymer electrolyte. Because the polar groups in the polymer chains aid in dissolving the ionic salts, PEO-based polymer electrolytes have higher ionic conductivity than those made of other polymers. [8]. The PEO-based polymer electrolyte system generated a poor ionic conductivity of the order of 10^{-7} S/cm at ambient temperatures. Lithium salts and polymers' lattice energies are key factors in determining ionic conductivity. By combining lithium salts that have small lattice energies and polymer hosts with high dielectric constants, high performance dry polymer electrolytes can be created [9].

Gel /Plasticized Polymer Electrolytes

By adding a low molecular weight organic solvent with a high dielectric constant and low viscosity to the polymer-salt complexes, Gel Polymer Electrolytes are created [4]–[6]. Since gels have the cohesive properties of solids and the diffusive properties of liquids, they have a special quality that makes them extremely useful in electrochemical devices. The plasticizer aids in lowering crystallinity and enhancing segmental mobility of the polymer. It also promotes ion dissociation, resulting in the emergence of numerous species of charges for ionic transport. [10]. The plasticizer facilitates ionic mobility by softening the polymer's backbone. The polymer electrolyte system's expansion of free volume is made possible by the addition of plasticizer. Gel polymer electrolytes have poor mechanical as well as thermal stability despite having a high ion conductivity at room

temperature.

Rubbery Polymer Electrolytes

This polymer electrolyte consists of a small amount of polypropylene oxide and polyethylene oxide and a large amount of salt. These materials' glass transition temperatures are so low that they can still exist in a rubbery state at ambient temperature. [11], [12]. To maintain high conductivity as well as the rubbery state, these electrolytes must satisfy the following conditions: To produce rubbery when polymer hosts are added, the salt's glass transition temperature (Tg) needs to be much lower than the surrounding air temperature. The salt melt should have good polymer solubility. The Rubbery Polymer electrolyte should be a single (Li+) ion conductor. The electrolyte should exhibit high electrochemical stability. The preparation of such polymer electrolytes satisfying the above conditions becomes quite difficult. These types of polymer electrolytes show appreciable conductivity at the expense of their rubbery state.

Composite Polymer Electrolytes

CPEs are ceramic fillers that are micro- or nanosized like MgO, Al_2O_3, SiO_2, TiO_2, $LiAlO_2$, CeO_2, and $BaTiO_3$. Due to their high mechanically stable, excellent conductivity, and good interfacial compatibility with the electrodes, numerous researchers are interested in studying these polymer electrolytes. [11]–[13]. Composite Polymer electrolytes may be regarded as continuous phase materials and the flow mechanism here is purely decided by the composition and the size of the filler [14]. The fillers increase ionic mobility and decrease the polymer electrolyte system's crystallinity. The host polymer's segmental chain motion is accelerated by the ceramic fillers, which also helps the ionic transport. [15].

1.4.2 Requirements of Polymer electrolytes

A polymer electrolyte should possess the following properties to be used in Batteries, solar panel. etc. Various types of polymers are reported in literature and examples of host polymers used widely are shown in table 1.2.

- ❖ High ionic conductivity at ambient temperature.
- ❖ They ought to possess thermal stability within the -30 °C to 80 °C range.

- ❖ Good dimensional stability to function as a separator in batteries.
- ❖ Better mechanical strength for the preparation of free-standing films.
- ❖ Chemically compatible with the anode and cathode.
- ❖ Poor electrical conductivity to avoid short circuit.

Table 1-2: Polymer host generally used with unit and examples.

S. No	Polymer	formula	Examples	Conductivity (S/cm)	Ref.
1	Poly (acrylic acid)	$-(CH_2-CH-(-COOH))_n-$	PAA-LiTFSI-Sb_2O_3	2.15 X 10^{-4}	[16]
2	Poly(acrylonitrile)	$-(CH_2-CH-(-CN))_n-$	PAN-$LiClO_4$-α-Al_2O_3	5.7 X 10^{-4}	[17]
3	Poly (ethyl methacrylate)	$-(CH_2-C(-CH3)(-COOCH_2CH_3))_n-$	PEMA-LiTf-lL	1.17 X 10^{-4}	[2]
4	Poly (ethylene oxide)	$-(CH_2CH_2O)_n-$	(PEO-HBP)-$LiN(CF_3SO_2)_2$-$BaTiO_3$	2.6 X 10^{-4}	[18]
5	Poly(ε-caprolactone)	$-(O-(CH_2)_5-CO)_n-$	PCL-NH_4SCH-EC	3.8 X 10^{-5}	[17]
6	Poly (methyl methacrylate)	$-(CH_2-C(-CH_3)(-COOCH_3))_n-$	PMMA-$LiClO_4$-DMP-CeO_2	7.3 X 10^{-6}	[19]
7	Poly (vinylidene fluoride)	$-(CH_2-CF_2)_n-$	PVdF-PEGDA-PMMA	4.5 X 10^{-3}	[20]
8	Poly (vinylidene fluoride-Hexafluoro propylene)	$-[(CH_2-CF_2-)-(CF_2-CF-(CF_3)]_n-$	PVdF-HFP)-SiO2-LiTFSl-RTIL	4.3 X 10^{-3}	[21]
9	Poly (vinyl chloride)	$-(CH_2-CHCl)_n-$	PVC-$Li_2B_4O_7$-DBP	2.83 X 10^{-6}	[22]
10	Poly (vinyl alcohol)	$-(CH_2-CH(-OH))_n-$	PVA-PEO-glass-fibre-mat	4.75 X 10^{-2}	[23]

The properties of polymer electrolytes must be tuned for better performance of batteries. Thus, various approaches to improve the properties of polymer electrolytes are fellow:

- Blending of two polymers [24], [25]
- Cross - linking two polymers [26], [27]
- Incorporation of organic solvents (plasticizers) to prepare Gel/Plasticized polymer electrolytes [4], [14], [28]

- Addition of fillers to form composite polymer electrolytes [29]–[31]
- New polymer synthesis [32]

1.5. POLYMER-SALT COMPLEX

The dissolution of salt in a polymer produces conductive solid solution and through this solution the interaction of the salt's cation and the electron pairs carried by a hetero atom, typically O or N. The type of salt added, the method of reparation, and the environment in which the polymer-salt complex is prepared determine whether the complex is crystalline or amorphous. Ion transport prefers the phase of amorphous nature. The structural relaxation of the employed polymer host has an impact on ionic mobility as well. The polymer-salt complexes are controlled by the solvation energy and lattice energy of the salt. Only when is it possible for polymer-salt complexes to form.

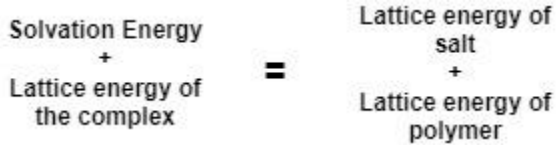

1.5.1 Criteria for the formation of polymer-salt complex

- Ionic salts can dissolve in a solvent only if the solvation energy of the ions in solution is higher than the salt's lattice energy.
- If the polymer matrix completely dissolves the ions and defeats the ionic salt's lattice energy, the effective polymer-salt complex can form.
- The polymer should be highly flexible and have a low cohesive energy.

1.5.2 Characteristics of polymer host

- For the atoms of polymers to establish coordinate bonds with cations they should possess sufficient electron donor power.
- To enable segmental motion, the host polymer's glass transition temperature should be low.
- To enable a sudden segmental motion of the polymer chain in response to a small temperature change, the barrier to bond rotation should be as low as possible.

- The appropriate distance between the coordinating centers of the polymer host allows for the establishment of multiple interpolymer ion bonds.

1.6. ADVANTAGES OF POLYMER ELECTROLYTE

- The polymer electrolyte acts as a binder and hence the interfacial stability with the electrodes is high.
- The need to incorporate an inert porous separator has been eliminated as the polymer electrolyte acts as an electrolyte as well as separator.
- Due to their flexibility, they can be fabricated into thin films.
- The formation of gas during charging and discharging processes has been avoided by polymer electrolyte.

1.7. APPROACHES

. Figure 1.3 depicts a variety of approaches that have been offered in the literature to improve the PEs' performance and characteristics [3].

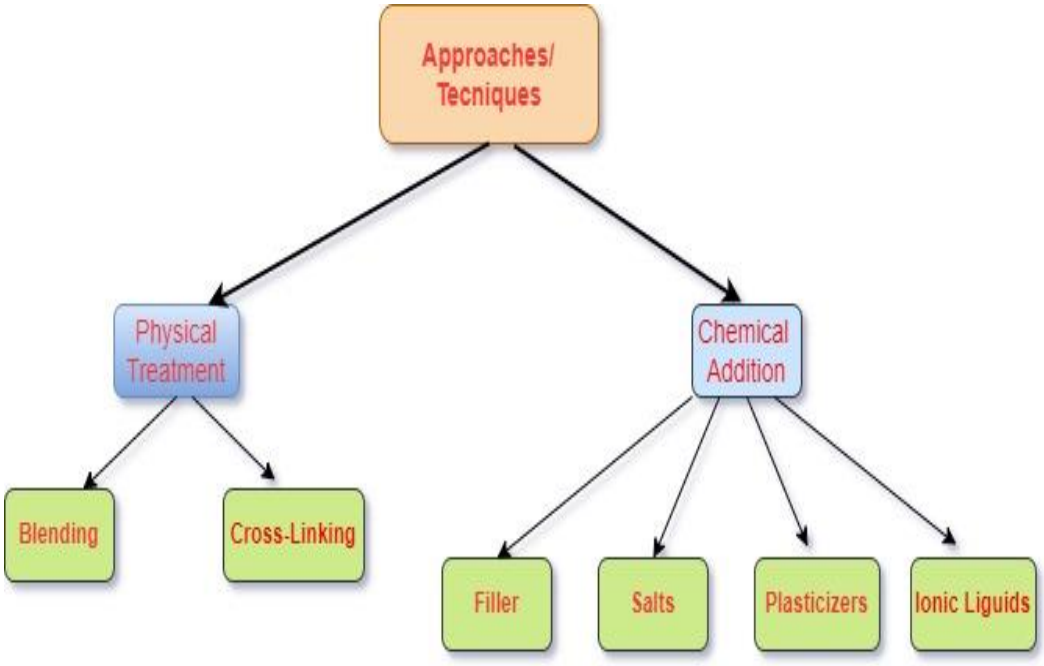

Figure 1.3: Techniques for improving performance of polymer.

1.7.1 Blending

Polymer mixing is the strategy that is most useful among the alternatives. Polymer blending is the process of physically or chemically combining two or more polymers. A polymer blend is produced by physically combining two or more polymers or copolymers. Since polymer blends have unique properties that make them superior to their component polymers, they are highly valuable items for commercial and industrial applications. With this technology, mechanical stability, ionic conductivity, and strength are all increased. It is a typical technique for shrinking a polymer matrix's crystallite. [2]. It is a conventional technique to reduce the crystallite nature of polymer solution.

1.7.2 Cross-linking

At room temperature, SPEs exhibit high electrochemical performance due to the polymer's amorphous state. The cross-linked PEs are completely amorphous and have a high ionic conductivity at room temperature. Cross-linked polymers, on the other hand, are frequently inflexible, rigid, and difficult to manufacture [2]. The monomer content influences the PEs' ionic conductivity and flexibility, according to the research. An example of a cross-linking polymer is shown in the following diagram.

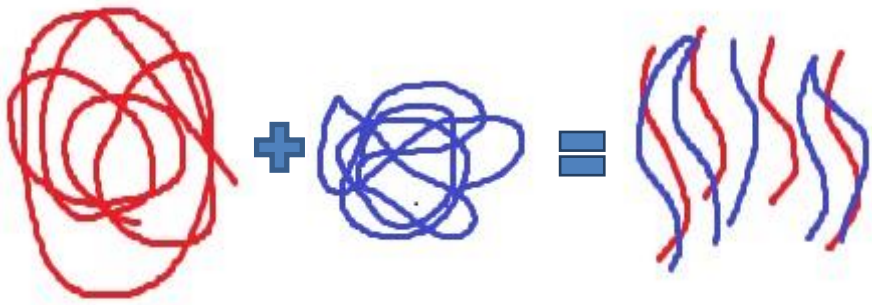

Figure 1.4: Polymer blends pictorial model.

1.7.3 Fillers:

Another way to improve SPE performance is to fill polymer matrices with tiny and

small particle size nanomaterial fillers. Figure 1.5 depicts a visual depiction of filler doping in a polymer electrode. The electrical conductance of PEs is improved by filler doping. Surface stability, high heat stability, decreased crystallite size and glass change temperatures, amendment of the conducting polymers in amorphous zone, and enhanced interfacial stability in contact with a variety of electrode materials are just a few of the benefits.

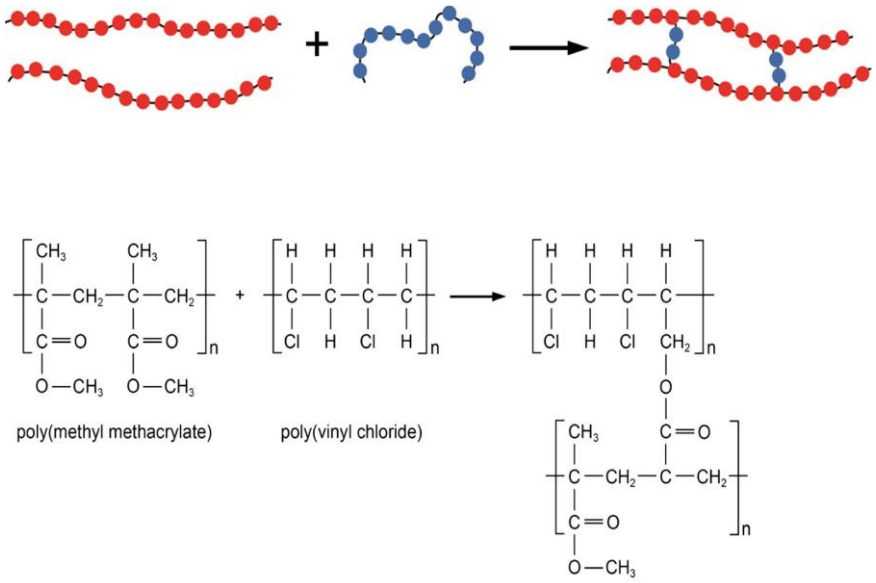

Figure 1.5: Polymer crosslink pictorial model [21]

Polymers' crystallinity is reduced, which prevents them from recrystallizing, while their amorphicity is increased, which improves ionic conductivity. The fillers lower the crystalline nature of the polymers, preventing them from recrystallizing, and increase amorphicity, which improves electrical characteristics. Small particles are more efficient because they have a larger surface area-to-volume ratio and less crystal formation. Fillers may alter the lattice structure of polymer matrices. The procedure results in the development of interfacial layers between the filler grains. As a result, charge carriers, such as electrode materials, become trapped at the grain boundary of the polymer chain lattice. Aluminum oxide (Al_2O_3), titanium oxide (TiO_2), zirconium oxide (ZrO_2), and

hydrophobic-fumed silica are all high surface area materials.[13], [34], [35]

1.7.4 Nanofillers:

Nanomaterials can be used as fillers in nanocomposite polymer electrode. The nanoparticles interaction with the polymer host boosts the PE's physical and electrical conductance[40] . Capiglia and colleagues [34, p. 2] developed a nanomaterial-based PE in 1999 by inserting silica in the form of nanomaterial (SiO_2) into PEO-$LiClO_4$ polymer electrolytes. The ionic conductivities of PEs were similarly increased by nanosized aluminiumoxide (Al_2O_3), according to another study [35].

1.7.5 Copolymers

A copolymer is a polymer that is made up of at least two distinct monomers. The cross-linking method can be used to make copolymers. The most commonly composite is PVdF-HFP, which is synthesized through polymerizing PVdF and HFP together, as shown in Figure 1.6. Because of synergistic effects in the mixed structure, the copolymer has superior properties than the components alone. Electrolytes made of epichlorohydrin, and ethylene oxide copolymer were investigated for usage in electrochemical devices [2].

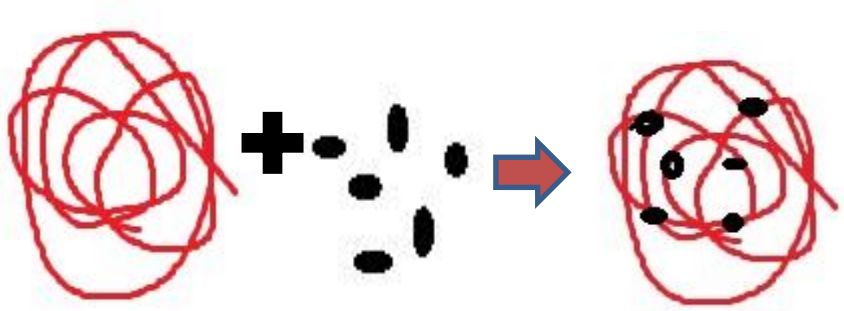

Figure 1.6: Example of Complex Polymer Electrolyte adding filler.

1.8 Sample preparation technique:

The increasing use of polymer electrolytes in a variety of uses required the development of high-quality film technology. Various sample preparation techniques are

listed below.

1.8.1 Solution casting approach

It is a traditional approach for making solid polymer electrolytes bendable (Figure. 1.7). It could also develop polymer films ranging in size from 50 to 300 micrometers. The following are the steps in this procedure:

1. To achieve homogenous mixing, a preset amount of polymer is added to a solvent and stirred.

2. A salt solution is added to the polymer matrix, which is then agitated at atmosphere temperature until the polymer–salt complexation develops.

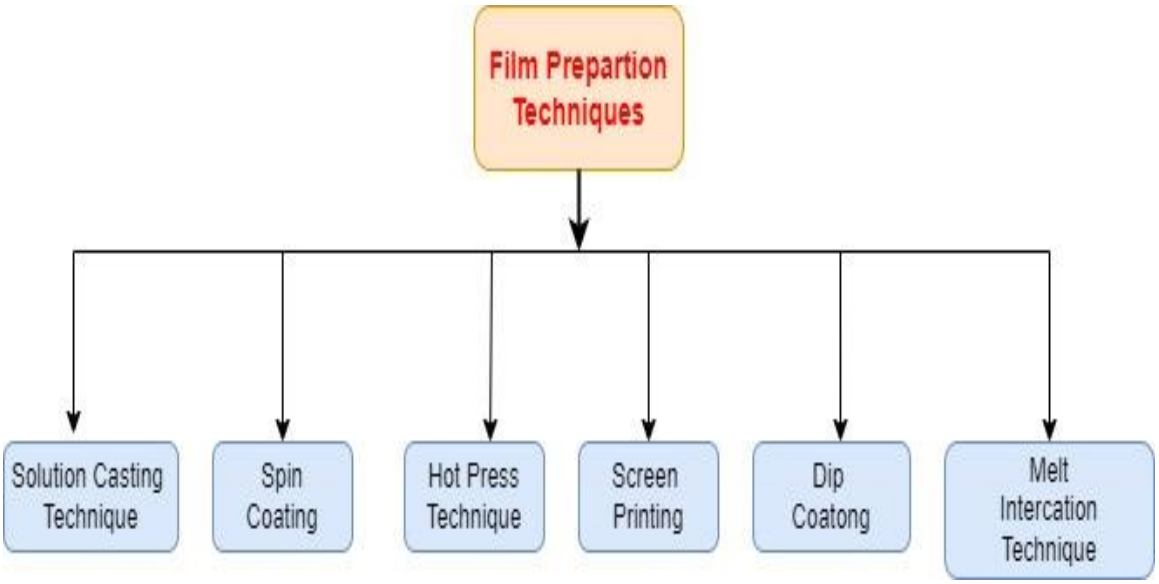

Figure 1.7: Sample preparation techniques.

3. The nanofillers/clay/plasticizer are then added, and the mixture is well mixed.

4. Pour the viscous solution into glass or Teflon Petri plates and let it sit at atmosphere temperature for 2-4 days to gently evaporate.

5. The result is a thin, uniformly thick layer.

1.8.2 Spin coating.

The spin-coating method and solution casting analysis have common features. A

tiny amount of the chemical mixture is dropped on a mechanical stirrer that rotates at an appropriate velocity to create a smooth film rather than casting the film on a surface. The rotating axis of the substance must be the opposite of the surface being coated. Due to centripetal acceleration, the mixture will spread out on the substrate. The detergent is subsequently evaporated with the help of spread heating. Spin coating's simplicity and relative ease of preparation, as well as its ability to swiftly make homogenous films ranging in thickness a few microns to a few nanometers, are all advantages.

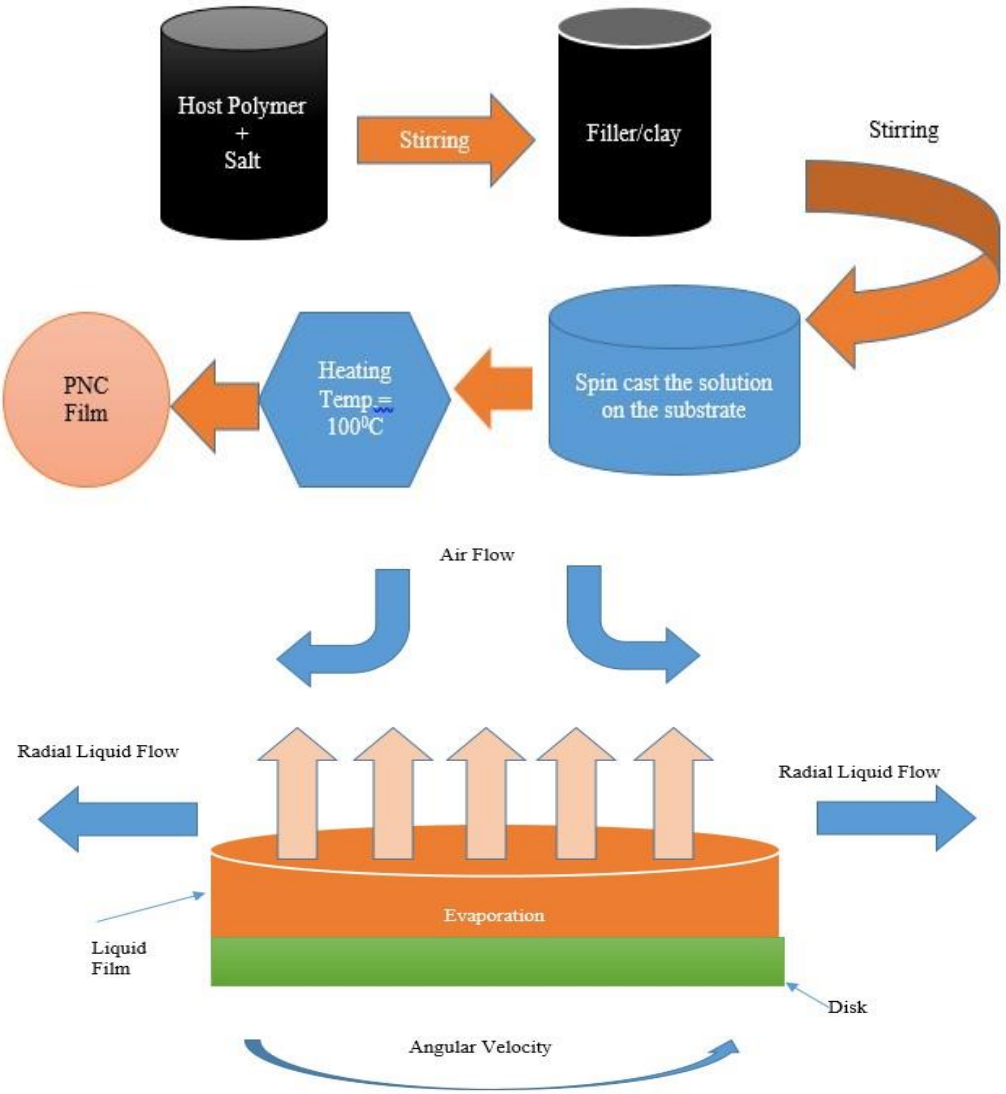

Figure 1-8: Spin Coating Technique and its systemic arrangement.

The viscosity (concentration), adhesion strength, rotational time, and speed of rotation of the mixture can all be easily modified to adjust the film thickness.

Because it has a direct impact on the force applied to the mixture, the rotating speed is critical. However, this procedure only works with highly viscosity mixtures, not very viscous ones. The spin coater's rotation is insufficient to properly distribute the gel mixture droplets and produce a thin sheet [3]. Figure 1.8 shows arrangement.

1.8.3 Tape casting technique:

In the container, the host polymer and salt are dissolved in the proper ratios with an appropriate solvent, like DMF or acetone, and the mixture is stirred continuously for 10 to 12 hours. The dispersion of the nanofiller in various weight percentages relative to the host polymer is now carried out in the correct ratio and combined for the same time as before in the polymer-salt complex. The viscous solution is now tape-cast and allowed to air-dry after being briefly heated on a hot plate.

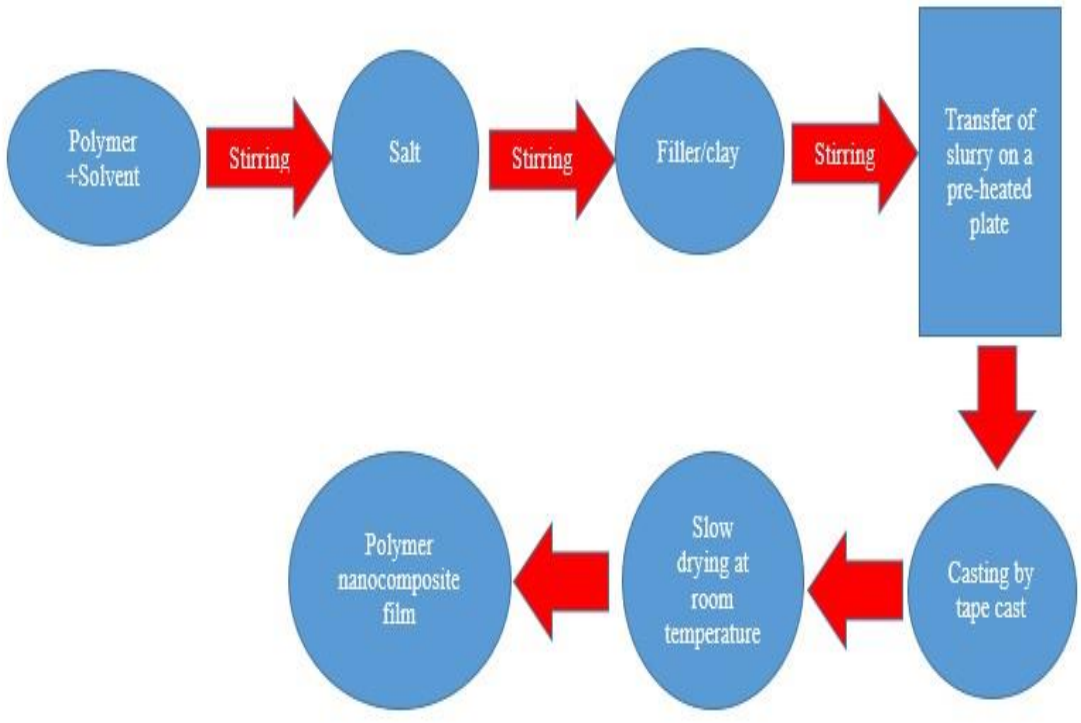

Figure 1-9: Tape casting technique.

As a result, a self-supporting conductive polymer nanocomposite film can be made with desired thickness. The amount of slurry at the blade edge, as well as the pressure, are kept constant. The full technique is depicted in Figure 1.9. A slurry-filled steel container is hooked up to a gaseous metal tank. Gas pressure is used to regulate the slurry flow rate, which maintains a constant amount of slurry at the scraper edge. The edge of the scraper and the carrier split apart to generate a slit when the carrier (tape) is run through a solution at a certain value. The membrane is obtained and rolled into a container after the slurry has dried on the carrier with a slit-sized opening. The thickness of the membranes can be altered by adjusting the slit. This technology is perfect for manufacturers because it can easily handle the sample's width and size.[3].

1.8.4 Hot press technique:

It is substituting the standard solution cast process, is a one-of-a-kind technology that provides advantages including speed, cheap cost, solvent-free operation, and the ability to work with thick materials. The advantage of this method is that it can compound a large variety of metallic particles and alkali salts with a large variety of polymer candidates.

The apparatus consists of a temperature sensor, a utility room, a heating chamber, and a weighing cylinder. An ideal powdery mixture of polymer, salt, and filler/plasticizer is firmly pounded for one to two hours at room temperature in an agate pestle and mortar. To change the pressure, the sample is pressed using a weighing cylinder [3]. To create a hot slurry for later use, stainless steel (SS) blocks are separated from the mixture of polymer, salt, and filler compositions (Fig. 1.10). The environment's reactive lithium salts make it challenging for lithium ions to operate in the hot press, necessitating special processing conditions.

1.9 Dye-Sensitized Solar Cell Overview:

Nearly 80% of the energy used globally is provided by fossil fuels, which are quickly running out. So, a potential energy crisis may arise soon. Numerous initiatives have been made worldwide to develop some alternative energy sources to address this issue. Direct solar energy use is the best course of action in this situation to generate electricity. On the

surface of the earth, solar radiation and energy are unending and constant. The photosphere of the Sun, which is at 6000 K, is where it is released. The solar constant, also referred to as "solar constant," is the value for the average solar radiation (or solar power) intensity that the earth's surface experiences on an annual basis. The "Photovoltaic effect" was first noticed by French scientist Edmond Bequerel in 1839 after he noticed the potential difference between two electrodes attached to a solid/liquid system on its two opposite faces when exposed to light. This breakthrough made it possible to transform solar energy into electrical energy [39].

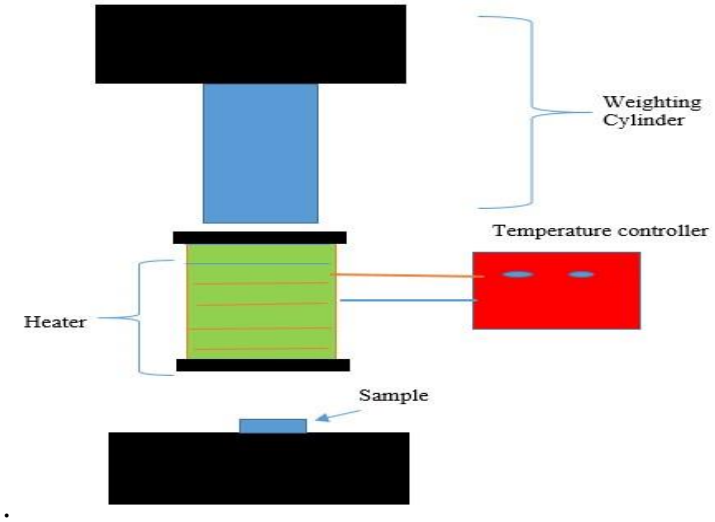

Figure 1-10: Hot Press Technique

Since then, several fresh ideas have emerged to create photovoltaics or solar cells, which turn solar energy into electricity directly. Solar cells or photovoltaics have been discovered in three generations so far. First-generation solar cells have been developed with both crystallized and amorphous silicon as their materials. Crystalline and amorphous silicon, copper indium gallium diselenide, cadmium telluride, and several semiconductors including GaAs, GaInAsP, GaAlAs, InAs, and InP make up the second-generation solar cells. These solar cells, also referred to as photo electrochemical solar cells, are more expensive than the thermal and hydroelectric power currently in use, according to research. Using the nanocrystalline material TiO_2. The first third-generation solar cells, also referred

to as dye-sensitized solar cells (DSSCs) or Grätzel cells, were invented in 1991 by B. O'Regan and M. Grätzel. The first and second generations of solar cells are semiconductors that separate charge carriers created by light using p-n hetrojunction. However, DSSC operation is based on a number of different fundamental principles [40]. To separate photogenerated charge carriers, these do not use a p-n hetrojunction. The DSSCs are superior to semiconductor thin film solar cells in many ways, including ease of fabrication and the use of low cast materials. Therefore, currently, extensive research is being done on a global scale to develop the theory and real-world applications of DSSCs [40]–[44]. The following critical discussions are also provided because DSSCs are the subject of this investigation.

1.9.1 Working principle of DSSC

Figure 1.11 depicts the DSSC's configuration, and it consists of a porous nanocrystalline TiO_2 coating on a conducting transparent glass sheet that serves as the working electrode. The colourant molecules are adhered to the TiO_2 surface. A redox pair, a counter electrode plated with platinum, and an electrolyte with a cathode are also present., for example I^-/I^{3-}. An external load is connected to the two electrodes. A current is drawn from the cell by the external load when the cell is illuminated, creating a potential difference between the two electrodes. In DSSC, dye molecules absorb incident light, which causes them to release electrons that separate charges in the TiO_2 at the semiconductor electrolyte interface [45]. Only 1% of the incident light can be absorbed by a single layer of dye molecules [40]. To improve the absorption of incident light, a porous nanocrystalline titanium oxide electrode structure is used. More dye molecules can be attached to the electrode because of the increased internal surface area. Clearly, this improves charge separation at the interface between the electrolyte and the TiO_2. [46]. If the electrode has a thickness of 10 m and particle and pore sizes that are typically in the range of 20 nm, the inner surface area of the TiO_2 electrode becomes 103 times larger than the flat surface area of the electrode..[40], [47]. Additionally, the TiO_2 porous electrode is a semiconductor with a large band gap that only absorbs solar radiation below 400 nm,

allowing dye molecules to absorb most of the solar radiation that is available. The DSSC is a regenerative type of photo electrochemical solar cell. In figure 1.11, its working cycle is depicted. The dye molecule that is present on the surface of the porous TiO_2 electrode absorbs the incident visible light photon of energy hv. As a result, in the dye molecule, an electron gets excited from a molecular ground state S to a higher lying excited state S* (1). The dye molecule is left behind in the oxidized state S+ as this excited electron is soon injected into the TiO_2 molecule's conduction band (2). As a result, this injected electron travels through the porous TiO_2 space before reaching the glass substrate's conducting layer, which acts as a working electrode.

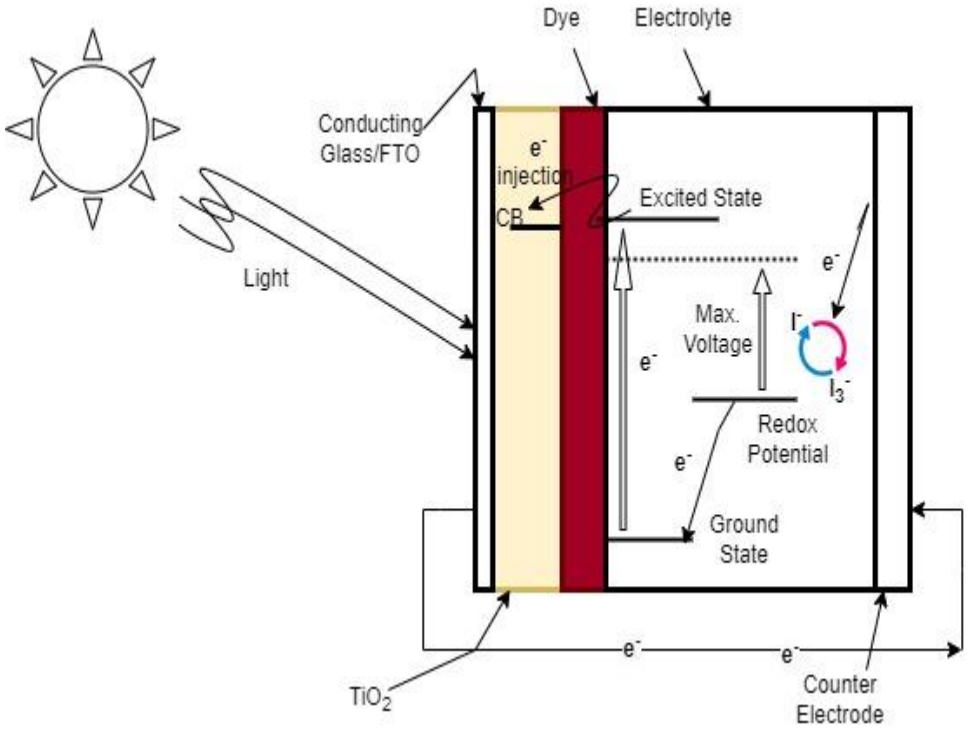

Figure 1-11: Construction and working of solar cell.

It then moves to the counter electrode (cathode) of the cell through an external load that is attached to the cell (3). In the presence of a platinum catalyst, this electron gets transferred to the triiodide (I_3^-) ion in the electrolyte at the cathode to produce iodide (I^-)

ion. (4).

The terminology of chemical reactions can be used to summarize the working cycle. [48] as-

Anode: $hv + S = S^*$ (Absorption) ….(1.10)

$S^+ + S^* + e^- = TiO_2$ (Electron Injection) …(1.11)

$2S^+ + 3I^- = I_3^- + 2S$ (Regeneration) …..(1.12)

Cathode: $I_3^- + 2e^- = 3I^-$ …. (1.13)

Cell: $e^-(Pt) + hv = e^-TiO_2$ ….(1.14)

It has been found by researchers that the potential difference between the TiO2 conduction band edge and the predicted maximum photovoltaic under open circuit conditions and the redox potential of the I^-/ I_3^- pair in the electrolyte solution [44]. Potential variations between the DSSC's electrodes and, consequently, across the external load can be produced. that is attached because of the different positions of energy levels at the cathode and anode as shown in figure 1.8. The net cell reaction is depicted in equation 1.14. Which clearly implies that no permanent chemical changes in the cell's involved species take place; instead, incident light energy is only converted into electricity. DSSC is a photo electrochemical solar cell that is regenerative in nature. [40], [46].

1.9.2 Performance parameters of a DSSC

Light energy is converted into electrical energy by the DSSC. Depending on its capabilities,it might be able to simultaneously generate a photocurrent (I) across it and a potential difference (V) across an external loadconnected to it. For a variety of loads, V and J measurements are taken with fixed illumination and constant temperature. Figure 1.11 illustrates the plot of the current density(J) versus voltage (V) curve. The DSSC's (J–V) characteristic curve is what this is known as.(A). These are the defined DSSC parameters.

Open circuit Voltage (V_{OC}):

It has been defined to be the cell voltage when the DSSC does not generate any current.

Current density in short circuits (Jsc):

It is a current density that can be determined when the DSSC is shorted under light, or when the DSSC voltage is V=0.

Fill factor (FF):

It serves as the main DSSC photo performance criterion. Its equation is the reciprocal of the product of the maximum power output (Pmax), the short circuit current density (Jsc), and the open circuit voltage (Voc).

$$FF = P_{max}/J_{sc}V_{oc}$$
$$= J_{max}V_{max}/J_{sc}V_{oc} \quad \ldots (1.18)$$

where the maximum power output, Pmax, equals Jmax. Vmax is the product of the maximum current density (Jmax) and the maximum voltage (Vmax) at the point of highest power on the J-V curve that is characteristic of a DSSC.

Efficiency (η):

It is the ratio of Pmax at MPP on J-V curve to Pin (incident photo power) on the DSSC.

$$\eta = P_{max} / P_{in} \times 100 \quad \ldots (1.19)$$
$$\eta = J_{max}. V_{max} / P_{in} \times 100 \quad \ldots (1.20)$$
$$\eta = J_{sc}. V_{oc}. FF / P_{in} \times 100 \quad \ldots (1.21)$$

As for as η is concerned, some important points to be noted are -

(i) η depends upon J_{sc}, V_{oc} and FF. Jsc, Voc, and FF. The photo performance of DSSC can be enhanced by optimizing these parameters.

(ii) The efficiency of a DSSC is also influenced by the cell's temperature, the total amount of incident light intensity, and the light's spectral composition.

As a result, each of these needs to be mentioned whenever is reported. Considering these facts, DSSC testing should be standardized across all laboratories globally. There are some accepted standard conditions. The incident light intensity is 1000 W/m^2, the incident light source's spectrum is the AM1.5 global standard solar spectrum, as shown in figure 1.12, and the cell's temperature is 25 ^oC.[41].

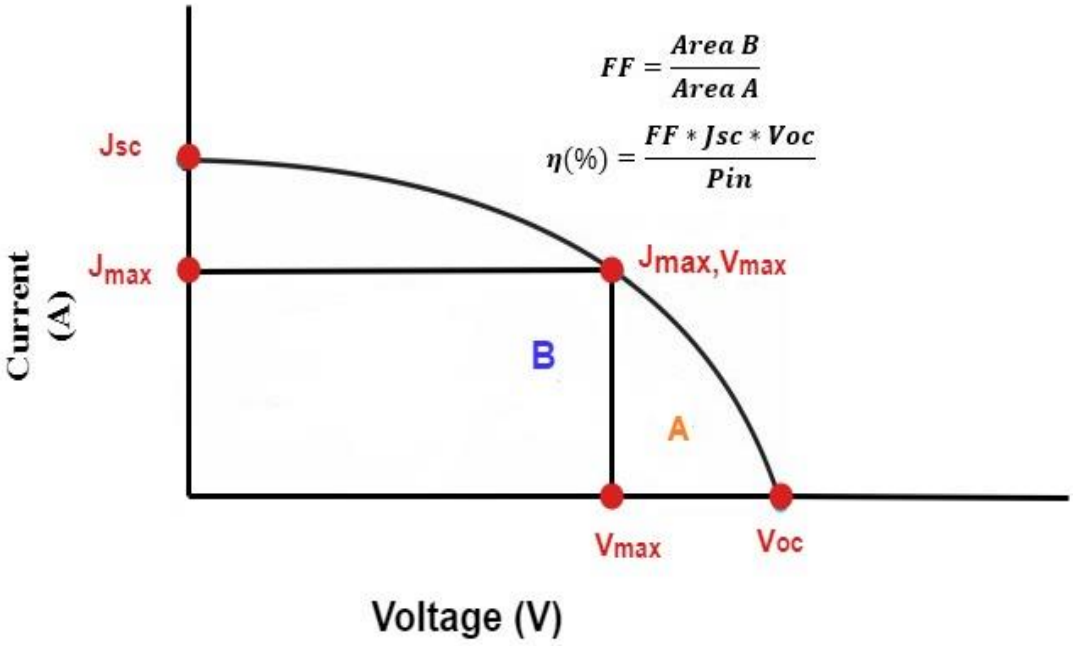

Figure 1-12: Standard I-V curve to calculate efficiency of solar cells.

Chapter 2. : Literature Review

2.1. POLYMER

First decade of the 1970s, materials with solid states such as ceramic, glass, crystalline, and polymer electrolytes were produced [5]. Fenton et al.'s first publication of polymer electrolyte in 1973 and awareness of the significance of its scientific use in the early1980s [49]. A membrane known as an electrolyte composed of polymers (PE) is made up of salt dissolving in a high-molecular-weight polymer matrix [9]. Because of their solid, solvent-free structure's high ionic conductivity, electrochemical appliances like solid-state battery packs, rechargeable batteries, and lithium-ion batteries frequently use them. Supercapacitors, fuel cells, dye-sensitive solar cells, rechargeable batteries, electrochemical sensors, analogue memory devices, and electrochromic windows are some of the more recent examples of cutting-edge electrochemical and electronic devices that PEs may be used [10-14].

2.2 PEMA AS POLYMER HOST

A methacrylic ester polymer is called Poly (ethyl methacrylate) (PEMA). It offers great optical transparency, strong surface resistance, good ionic conductivity, and chemical resistance.

Rajendran et al. [50] used PEMA polymer using EC as a plasticizer and $LiClO_4$ as a dopant. It was noted that the polymer mix electrolyte with 8 weight percent lithium salt was reported to have the highest ionic conductivity, which was found to be 3.454×10^{-3} Scm^{-1} at room temperature. It was discovered that ion aggregates that impede ionic transport occurred above 8 %. wt. of salt. It was discovered that the electrolyte with 8 wt.% salt has a thermal stability of 231 °C.

Thermal analysis used by Kwei et al. [51] to confirm the compatibility in PVdF and PEMA mixes. Due to the polymer PEMA's predominately amorphous nature, the DSC spectra showed that combinations containing 80% or more of PEMA displayed a single glass transition temperature. Furthermore, the temperatures for glass transition and melting were

established.

Han et al. [52] described the synthesized polymer blend electrolytes based on a 1:1 mixing of EC/PC and PVC/PEMA host polymer blend and 1 M of $LiPF_6$. The PVC/PEMA polymer was found to have two phases: one that was rich in electrolytes and the other that was rich in polymers. While the polymer-rich phase assisted in the increase of mechanical strength, the electrolyte-rich phase served as a conducting channel for ion transport. The PVC/PEMA polymer blend electrolyte offered a mechanical strength that was significantly higher than a PVC/PMMA polymer blend electrolyte that had previously been reported. The conductivity of the electrolyte system was greater than 10^{-3} Scm^{-1}.

The optical morphology of annealed PVC, PEMA, and PVC/PEMA blends was investigated by Fahmy et al. [53]. The morphology of the annealed polymers changed, as was seen. The polymer PEMA revealed minute round-shaped domains after annealing, but the annealed PVC showed a rod-like structure. For the prepared samples, various characterization procedures including FTIR, XRD, and TSDC were carried out to investigate the temperature-induced morphological changes.

Ramesh Prabhu et al. [54]examined the ionic conductivity of the nano composite PVC/PEMA$LiClO_4$- PC-TiO_2. Using various characterization techniques, they investigated the conductivity, thermal responsiveness, and surface morphology of the created electrolyte membranes. For the membrane containing 15 wt.% TiO2, the AC impedance spectra produced a conductivity value of $7.179x10^{-3}$ Scm^{-1}. Ion motion was helped by the creation of a new kinetic channel by the polymer-ceramic filler, where ceramic particles act as nucleation centers. For 15 wt.% of TiO_2, it was discovered that the glass transition temperature (Tg) was decreased, promoting segmental mobility, which in turn helps with ionic transport. Ionic diffusion was significantly improved by the positive contact between the polymer chains and the cations. The Scanning Electron Microscopy image proved that the polymer electrolyte system was in a homogenous phase. The XRD examination showed that the blend had both crystalline and amorphous phases.

2.3 PMMA AS POLYMER HOST

Poly (methyl methacrylate) (PMMA) is a highly transparent polymer with good stiffness and dimensional stability. The polymer's ease of handling, processing, and low cost make it a popular ingredient in polymer blends.

The PGR-NMR method was used by Nicotera et al. [55] to measure the lithium self-diffusion coefficient and ionic conductivity of PMMA/ PVdF+ EC/PC +lithium . The results showed that the sample with 60% PMMA and 40% PVdF exhibited the highest ionic conductivity. The interaction between the EC and lithium cations was controlled by the PMMA/PVdF mix ratios, and it was verified by Raman Spectroscopy.

Using blends of PVdF+ and PEO-b-PMMA copolymers made using a phase inversion approach, Xiao et al. [56] evaluated the conductivity of a novel macroporous polymer electrolyte. The DSC study proved that as the PEO-b-PMMA content rose, the polymer blend's crystalline phase changed to an amorphous phase. It was discovered that adding block copolymers to PVdF enhanced the electrolyte system's porosity and interconnectivity. The ionic conductivity at room temperature was 2.79 $x10^{-3}$ Scm^{-1}, according to the AC impedance test. The prepared sample's electrochemical stability window was reported to be 5.0 V.

Kuo et al.[57] produced PMMA-based polymer electrolytes utilizing various $LiClO_4$ salt ratios with constant concentrations of the plasticizer PC and another system of polymer electrolytes by adjusting the PC content in PMMA-$LiClO_4$-SiO_2 composite polymer electrolytes. The FTIR investigation supported the development of polymer-salt-plasticizer-filler complexes. The thermal behavior of the electrolytes was examined using thermogravimetric analysis (TGA) and differential scanning calorimetry (DSC) (DSC). The electrolyte systems had excellent thermal properties, which were confirmed by TGA and DSC experiments. At 80 °C, the electrolyte membrane with 14 wt.% LiClO4 salt had a maximum conductivity of $1.39x10^{-3}$ Scm^{-1}. The conductivity value for the composite

polymer electrolyte system with 7 wt.% SiO_2 filler was $8.91x10^{-3}$ Scm^{-1} at 90 °C.

Conductivity of poly (vinyl chloride)/poly (methyl methacrylate)-LiBF4-EC/PC and poly(vinyl chloride)/poly(methyl methacrylate)-$LiClO_4$-DEP plasticized polymer blend electrolytes were reported by Stephan et al. [58]. The kind and concentration of plasticizers and lithium salt had a significant impact on the conduction in the plasticized polymer blend electrolytes. The results of an AC impedance investigation identified the variables that influence ionic conductivity. Contrary to the plasticizer EC/PC, it was discovered that adding DEP reduced conductivity. The decrease in conductivity demonstrated that the primary determinant of ion dynamics was determined by the molecular interactions between the plasticizer and ions. The polymer electrolytes' amorphous phase with EC/PC and crystalline phase with DEP were both validated by XRD spectra.

Electrolytes constructed of PVdF-HFP/PMMA-LiTf polymer blend were studied by Gebreyesus et al.[59] . For the produced polymer blend electrolytes, several characterization procedures including XRD, FTIR, SEM, DSC, and AC impedance tests were carried out. Ionic conductivity was determined by the PVdF-HFP/PMMA polymer blend's composition and temperature. With 22.5 wt.% of PMMA, the greatest ionic conductivity measured at room temperature was $7.4x10^{-5}$ Scm^{-1}. This value was attributed to the polymer's amorphous rich phase, which facilitated ionic mobility.

2.4 CATEGORIES OF PES

The PEs have been divided down into three categories in an extensive literature review, as shown in figure 2.1.

2.4.1 Liquid polymer electrolyte

Liquid electrolytes are made up of a short-circuit-preventive separator and lithium-salt that has been dissolved in an organic solvent. According to the solvent, it is divided into two categories: electrolyte in aqueous liquid (ALE) and non-aqueous liquid (NALE). NALE can be produced by dissolving solvents in alkaline salts which include ethylene carbonate (EC), dimethyl carbonate (DMC), diethyl carbonate (DEC), and propylene

carbonate (PC), which act as a solid polymer electrolyte with a high ionic conductivity. Some of our appealing qualities include high ionic conductivity, thermal stability in ambient and sub-environmental conditions, relatively large electrochemical conditions, a stable lock, and simplicity of use. [23]– [30]. Since ALE is more conductive than NALE and has qualities, such as having inexpensive and flammable in addition to being safe, it is a good potential applicant for practical use even at temperatures that are higher.

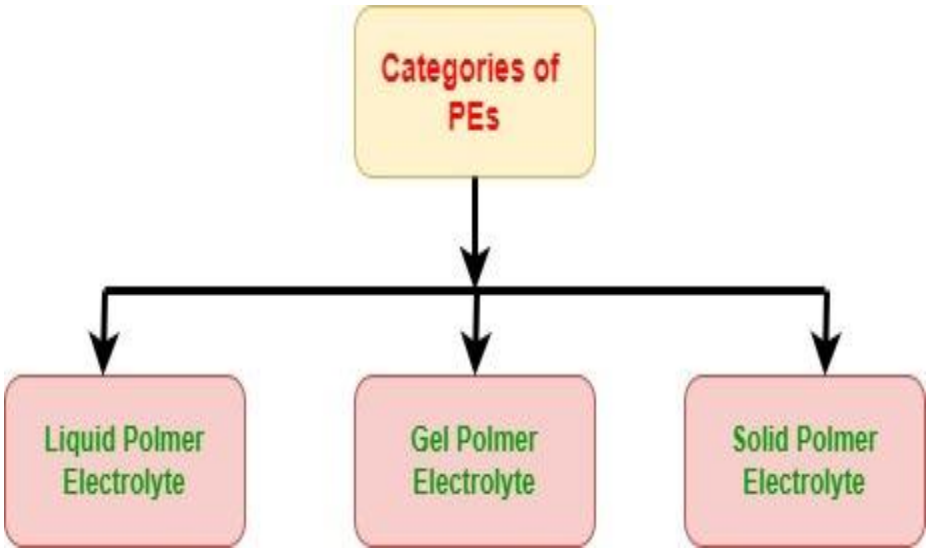

Figure 2.1:Categories of polymers.

Ionic liquids (ILs) are primarily in a generation in organic salts such as minerals and present in liquid form in the environment temperature because of low ion interaction / inadequate packaging atoms. These ionic liquids are suitable for use due to their electrochemical stability and solvability properties, making them candidates for the development of organic electrolytes to replace inorganic ones. Supercapacitors, batteries, fuel tanks, and other advanced electrochemical devices. Using different cations or anions and adjusting the cation-to-anion ratio in ionic liquids can significantly change the properties of solvents. Some liquid polymer electrolytes (LPEs) are shown in Table 2.3 along with their conductivity.

2.4.2 Gel polymer electrolytes

A low-molecular-weight solvent, dissolved salt, and an inert polymer matrix are all components of third-generation materials known as GPEs. Based on the method employed, gels can be grouped into two categories [43,14]

- Physical gels are limited to a polymer matrix without the possibility of bonding the polymer with solvent e.g., $LiClO_4$ / EC / PC (PMMA).
- Chemical gel crosslinkers assist in the development of a chemical relationship between the crosslinker agent and the polymer feature group.

Table 2-1: Polymer, salt, solvents as LPE and their parameters.

S. No	Polymer	Salt/ILs	Solvent	Conductivity	Ref.
1	PEO-PVdF	LiTFSI	Acetone/DMAc	4.9×10^{-3}	[60]
2	PVdF-HFP	[BMIM][BF_4]	Acetone	1.6×10^{-2}	[61]
3	PVA	$LiClO_4$/[EMIM][$EtSO_4$]	DMSO	1.9×10^{-6}	[62]
4	PVdF-HFP	PAni-MMT/BMIMBr	Acetone	7.7×10^{-3}	[10]
5	PEO	LiTFSI/BMITFSI	Solvent free	3.2×10^{-4}	[63]
6	PEMA	$NH_4CF_3SO_3$/BMATSFI	THF	10^{-4}	[64]
7	PEO	LiTf/EMITf	ACN	3×10^{-4}	[65]
8	PVA	CH_3COONH_4/(BmlMCl)	Distilled water	7.3×10^{-3}	[66]
9	PVA	Li_2So_4/BMIMCI	-	37×10^{-3}	[67]
10	PEO	$LiPF_6$/MMPIPF_6	-	1.13×10^{-3}	[68]
11	PEO	EMIM-TY	Solvent free	10^{-4}	[69]
12	PEO	$LiClO_4$/[BMIM][PF_6]	Anhydrous methanol	8×10^{-6}	[70]
13	PEO	Al_2O_3/EMIM-TY	Distilled methanol	5.8×10^{-5}	[71]
14	PEO	LiTFSi[Pyr_{14}TFSI]	-	1.1×10^{-4}	[72]

Cohesive and diffusive solid properties are carried by GPEs. properties of liquids and high mechanical strength. The polymer in GPEs serves to maintain a solid-state matrix with an approximate conductivity value of 10^{-3} Scm^{-1} at room temperature and permits ion migration in solvents. GPEs make our lives easier due to advantages like their many different shapes, faster charging and discharging rates, light weight, low cost, and high-

power density. Additionally, ionic conductivity increased, but mechanical reliability declined.

Table 2-2: Polymer, salt, solvent as GPEs and their parameters

S. No	Polymer+Salt/ILs	Solvent	conductivity	Ref.
1	PVdF-HFP+ $NaClO_4$-EC/DMC/DEC	DMF	$0.60X\ 10^{-3}$	[73]
2	P(EO-co-PO) + $LiPF_6$	DMF+distilled water	$2.8\ X\ 10^{-3}$	[74]
3	P(MMA-AN-VAc)+ $LiPF_6$	DMF	$3.48\ X\ 10^{-3}$	[75]
4	PMMA+ ZnTr	EC/PC	$1.67\ X\ 10^{-3}$	[76]
5	LiBF4-EC/PC	-	$6\ X\ 10^{-3}$	[77]
6	PMMA+ $LiN(CF_3SO_2)_2$	EC/DMC	10^{-3}	[78]
7	PVdF-HFP+ $LiN(CF_3SO_2)_2$	EC/DEC	10^{-3}	[79]
8	$LiN(CF_3SO_2)_2$	EC/PC	$1.74\ X\ 10^{-3}$	[28]
9	PVdF+ SiO_2-PAALi-EC/EMC/DMC	DMF/acetone	$35\ X\ 10^{-3}$	[80]
10	P(HFBMA-co-PEGMA)/PVDF	-	$3.19\ X\ 10^{-3}$	[81]
11	PVdF+ LiPVAOB	-	$0.26\ X\ 10^{-3}$	[26]
12	PAN-PMMA+ PYR14TFSI	-	$3.6\ X\ 10^{-3}$	[82]
13	PVDF-HFP	DMF	$0.45\ X\ 10^{-3}$	[83]
14	PECA-PET+ $LiPF_6$	Acstone	$2.54\ X\ 10^{-3}$	[84]
15	PVdF-PEO+ $LiClO_4$-EC/PC/DVB	-	$3.03\ X\ 10^{-4}$	[85]
16	PEMA+ LIBF-EC/EMC/PC	THF	$5.8\ X\ 10^{-4}$	[86]
17	PVDF-PEMA+ LICIO-EC/PC	THF	$1.47\ X\ 10^{-3}$	[87]
18	PVA+ NH_4SCN	DMSO	$2.58\ X\ 10^{-3}$	[88]
19	P(MA-co-AN)/PVA+ $LIPF_6$-EC/DM/CDEC	-	$0.98\ X\ 10^{-3}$	[89]
20	PVB+ $LIPF_6$	-	$4.09\ X\ 10^{-4}$	[90]
21	PVDF-HFP+ Urea/PVP	DMF	$2.823\ X\ 10^{-3}$	[91]

2.4.3 Solid polymer electrolytes

For several reasons, including their high durability, extended shelf life, high energy density, decreased weight, isolation from solvent, exceptional cell size stability, low electrode reactivity., SPEs have been favored over LPEs and GPEs. For operations above the ambient temperature and less expensive packaging, toxic gas leakage occurs. More

substantial electrochemical, some thermal stability, and low volatility are also present. [64].

Table 2-3: Various SPEs and its properties

S. No	Polymer	Salt	Solvent	Filler/plasticizer	Conductivity	Ref.
1	PVA	$Mg(NO_3)_2$	Triply distilled water	-	$7.36X\ 10^{-7}$	[92]
2	PAN	$LiClO_4$	DMF	ALA-MMT	$2.44\ X\ 10^{-4}$	[52]
3	PVC-PEMA	$LiPF_6$	THF	-	10^{-3}	[93]
4	PEO	LiTf	-	EC/sepiolite	10^{-4}	[94]
5	PEO-PMMA	$LiClO_4$	NMP	PA	$1.59\ X\ 10^{-5}$	[90]
6	PVA-PVdF	$LiClO_4$	DMF	-	$3.03\ X\ 10^{-5}$	[95]
7	PEO-PMMA	LiTFSI	THF	Al_2O_3	$3.24\ X\ 10^{-4}$	[96]
8	PVdF-PVA	LiTFSI	DMF	MMT	$4.31\ X\ 10^{-4}$	[97]
9	PAN	$LiPF_6$	DMF	DMMT	$3.7\ X\ 10^{-3}$	[98]
10	PAN	$LiCF_3SO_3$	DMF	DMMT	10^{-3}	[99]
11	PEO	$LiClO_4$	-	SiO_2	$1.2\ X\ 10^{-3}$	[100]
12	PEO	$LiAsF_6$	ACN	MMT	$4\ X\ 10^{-5}$	[101]
13	PEO	$LiCF_3SO_3$	-	Al_2O_3-DOP	$7.60\ X\ 10^{-4}$	[102]
14	PAN-PVA	$LiClO_4$	EC/DMC	EC/DMC	$2.5\ X\ 10^{-4}$	[103]
15	PVA-PVdF	$LiCF_3SO_3$	DMF	-	$2.7\ X\ 10^{-3}$	[104]
16	PEO	LiFSI	ACN	-	$1.3\ X\ 10^{-3}$	[105]
17	PVA	$NH_4Al(SO_4)_212H_2O$	Water	-	$1.73\ X\ 10^{-4}$	[106]
18	PVC-PEMA	$LiClO_4$	THF	PC	$3.45\ X\ 10^{-3}$	[107]
19	PVA	$Cu(NO_3)_2$	-	-	$1.6\ X\ 10^{-5}$	[57]
20	PMMA	$LiClO_4$	-	PC	$7.04\ X\ 10^{-3}$	[108]
21	PVB	$LiClO_4$	-	PEG	$2.15\ X\ 10^{-6}$	[109]
22	PVdF-PAN	$NaHCO_3$	-	SiO_2	$3.32\ X\ 10^{-3}$	[110]

Solid polymer electrolyte (SPEs), which is a decomposing of the salt in a matrix of polymers and has an electron donor group, has several benefits, including design flexibility,

the ability to miniaturize, increased safety, eased device manufacturing, etc. Additionally, the electrical conductivity and mechanical resistance of an ionically performing polymer membrane for electrochemical applications must be properly balanced. Due to their enhanced conductivity and environmental stability, SPEs may have applications in ionic solid-state products like supercapacitors, gasoline tanks, high-energy-density lithium-ion batteries, and other products [65]. Table 2.5 shows various SPEs and their properties.

2.5 DYE-SENSITIZED SOLAR CELL

Dye sensitized solar cell coverts solar energy or light energy into electrical energy. It is a 3rd generation solar cell having the advantage of low cost and easy fabrication. The first third-generation solar cells, also referred to as dye-sensitized solar cells (DSSCs) or Grätzel cells, were invented in 1991 by B. O'Regan and M. Grätzel. The 1^{st} and 2^{nd} generations solar cells are semiconductors that separate charge carriers created by light using p-n hetrojunction. However, DSSC operation is based on a number of different fundamental principles [40]. In the following section literature review of DSSC cell discussed.

Jihuai wu et al. [111] discusses the regenerative cycle of electrolytes in DSSCs and how it is completed by the conversion of I^3 to I^2. The paper explains the series of successive reactions that take place on the TiO_2 interface during the dye regeneration process. The paper proposes that the Grotthus-like mechanism can explain the high photocurrent density observed in DSSCs, independent of the viscosity of the electrolyte. The paper show that the relationship between conductivity and temperature in Grotthus-like mechanism follows the Arrhenius equation. The paper provides insights into the mechanisms involved in the operation of DSSCs, which can help in the development of more efficient and cost-effective devices.

Kumar et al. [112] prepared a natural dye from Balagidda leaves using different solvents and analyzing their properties using UV-spectrophotometer, pH-meter, colorimeter, and chromatography and prepared the photoanode using ZnO powder and the counter electrode using a combination of electrolyte (KI+ I2 + Acetonitrile) and carbon soot. Author applied

the natural dye paste onto the FTO coated glass substrate for effective sunlight harvesting, analyzed the structure of the ZnO coated with the dye using an optical microscope and measured the Voc (open circuit voltage), Isc (short circuit current), FF (fill factor), and efficiency of the DSSC using the Balagidda dye.

Gong et al., [113] offered a thorough analysis of the most recent advancements in dye-sensitized solar cells (DSSC) research, with a focus on device modeling, cutting-edge methods, and innovative device structure . The authors talked about how DSSCs are better than traditional silicon solar cells because they use cheap, abundant, and eco-friendly materials like titanium oxide, and they have comparable power conversion efficiency at low material and production costs. The paper also highlights the potential of DSSCs for indoor applications due to their better performance under lower light intensities. The authors additionally examined at how translucent and colorful thin layers can improve the DSSCs' aesthetic qualities. The paper concludes by discussing the future research directions and commercialization efforts in this promising technology.

Gong et al.,[114]examined the working of DSSC Cell. In this paper DSSC cell present development and future prospectus are also discussed. The paper discussed the limitations of traditional silicon-based solar cells and the advantages of DSSCs, which include low module cost, easy fabrication, lightweight, and flexibility. The study also covered the first dye-sensitized nanocrystalline solar cells developed in 1991 by Oregan and Gratzel, which had an incident photon to electrical current conversion efficiency of about 80% and a photoelectric energy conversion rate of 7.1%. The paper also discusses the evaluation of the overall performance of DSSCs in terms of cell efficiency and fill factor, and the dependence of active surface area on the geometry parameter.

Tandem-structured dye-sensitized solar cells (T-DSSCs), which are made up of a black dye-sensitized near-infrared-responsive bottom cell and a N719-sensitized UV-visible-responsive top cell, are optimized by Yanagida et al., [115].The performance of T-DSSC

for both parallel and series T-DSSCs is examined in relation to the thickness of TiO2 coating in the top cell. Under solar-simulating light circumstances (AM 1.5, 100 mWcmA^2), the optimized parallel T-DSSC yielded a photovoltaic conversion efficiency (Z) of 10.6% (aperture area: 0.188 cm^2, total area: 0.25 cm^2). This Z value was verified as the greatest value of the conversion efficiency for T-DSSCs.

Alhamed et al., [116] prepared DSSC cell using the study of natural dyes . To create a photosensitizer for DSSC, the contributors have investigated the optical and structural characteristics of pigments found in plants. To manufacture thin film components FTO/TiO_2 / Natural Dye / Electrolyte / Pt / FTO, they employed a variety of natural dyes that are classified as anthocyanins, including berries, shami-berries, grapes, hibiscus, and a combination of colors. They also prepared the DSSC using the SOL-GEL approach. The efficiency of DSSC obtained 3.04%, having fill factor = 60% for cell area a = 4cm^2, short circuit current 0.6 mA/cm^2 and open circuit voltage 0.42 V. The authors have also isolated anthocyanins pigments from natural plants and extracted Chlorophyll from green leaves for the study.

Sharma et al., [117] included a comprehensive review of the current state and developments in the area of photoelectrode, photosensitizer, and electrolyte for DSSCs till 2015. The paper also discusses the highest efficiency 11.2% for N719 achieved by DSSCs. The performance of DSSC modules is found to be superior to Si modules when the paper also conducts a comparison between the two types of modules. To create more affordable, flexible, stable, and lightweight DSSCs with improved efficiency, the study also emphasizes the need for novel, thin, inexpensive, and easily synthesized materials.

Iftikhar et al.,[118] provided a comprehensive review of the progress made in the development and application of electrolytes for DSSC solar cells. The review covers various types of electrolytes and their role in enhancing the photovoltaic performance and long-term stability of DSSCs. The advantages and disadvantages of recently disclosed innovative electrolyte compositions to produce inexpensive and industrially scalable solar

cell technology were also covered in the research. The literature review of the research includes a variety of electrolyte formulations that have been developed and tested in different DSSC configurations to address the challenges of long-term stability and photovoltaic performance.

Sokolsky and Cirak [119] discussed the history and development of dye-sensitized solar cells (DSSCs). It mentions the first panchromatic film that used dyes and silver halide grains to produce black and white images. The operating principle of DSSCs was recognized in the 1960s when researchers used organic dyes to sensitize a ZnO photoelectrode. However, these cells had low efficiency due to the use of single crystals and polycrystalline materials. The performance of DSSCs improved with the introduction of mesoporous materials such as TiO_2 and synthesized dyes. The paper also mentions the use of porous TiO_2 electrodes with a roughness factor to improve the efficiency of DSSCs.

Gu et al., [120] discussed the performance of dye-sensitized solar cells (DSSC) is influenced by the type of electrolyte used, with organic solvents showing better performance than inorganic solvents.. The best performance DSSC can be obtained with an electrolyte solution containing 0.6 mol/L KI and 0.075 mol/L I2, and After being left at room temperature for 72 hours, a solvent mixture consisting of ethylene glycol and acetonitrile demonstrated superior stability.

In the above literature review information got that selection of materials used to prepare WE/CE/Dye also affects the efficiency and fill factor of DSSC cell. Table 2.4 shows the comparison of different materials used to prepare WE/CE/Dye.

2.6 RESEARCH GAP

As per literature review electrochemical application of polymer-based composites have been studied on account of their flexibility, shelf life, leak proof and ease of fabrication. Numerous polymers, including PEO, PVA, PVC, PVDF, PMMA, and PEMA, are mentioned in the literature.

In the present investigation PEMA based composites used as a host polymer offers several advantages as mentioned below.

1. It offers high optical transparency, excellent chemical resistance, superior surface stability, and simple ion movement through the polymer segments.
2. It has electrochemical stability up to 4.3V.
3. It exists in semicrystalline form.
4. Very less literature is available for PEMA.

As per available literature, composites based on PEMA mainly consist of lithium-based salts like $LiClO_4$, $LiBF_4$, LiFSI, $LiPF_6$ etc. This results in an unstable composite apart from preventing repeatability of the results. Potassium iodide as a salt used in PEMA polymer that made it more stable composite and will ensure repeatability of result.

Also, very less literature is available on amorphous PEMA as a polymer electrolyte. In the present research, the mobility of polymer chain enhanced by adding plasticizers so that maximum space is available for ions to move in the host polymer. Conductivity will further be enhanced by adding nanoparticles.

2.7 OBJECTIVES

i. Synthesis of polyethyl methacrylate-based polymer electrolyte by adding potassium iodide (Kl) as salt using solution casting method.
ii. Amorphicity enhancement by using ethylene carbonate (EC) as plasticizer.
iii. Incorporation of multiwalled carbon nanotubes for further enhancement of ionic conductivity.
iv. Characterization of the maximum conducting sample using Scanning electron microscopy (SEM), X-ray diffraction (XRD), Complex impedance spectroscopy (CIS), Fourier transform infrared spectroscopy (FTIR)
v. Application of the prepared nanocomposite in Dye-Sensitized solar cell

Table 2-4. Different Strategies for Enhancing DSSC Efficiency

S.NO.	WE/CE/DYE	Material	J_{SC} (mAcm^{-2})	V_{OC}(V)	FF (%)	Ƞ(%)	Ref.
1	WE	TiO_2 doped fluorine	11	0.754	76	6.31	[121]
2	WE	ONT/FTO	10.65	0.700	70	5.32	[122]
3	WE	TiO_2 doped with scandium	19.10	0.752	68	9.6	[123]
4	WE	TiO_2 doped with tungsten	15.10	0.730	67	7.42	[124]
5	WE	TiO_2 doped with boron	7.85	0.660	66	3.44	[125]
6	WE	TiO_2 doped with indium	16.97	0.716	61	7.48	[126]
7	WE	TiO_2 doped with carbon	20.38	0.730	57	8.55	[127]
8	WE	Nanographite TiO_2	1.69	0.720	35	0.44	[128]
9	CE	PtCo	16.96	0.717	66	7.64	[129]
10	CE	PtMo	15.48	0.697	62	6.75	[130]
11	CE	PtCuNi	18.30	0.758	69	9.66	[131]
12	CE	FeN/N-doped graphene	18.83	0.740	78	10.86	[132]
13	CE	$NiCo_2S_4$	2.98	0.148	55.8	0.24	[133]
14	CE	SS: Graphene	1.46	0.524	26	1.98	[134]
15	CE	AC/MWCNTs	16.07	0.753	83	10.05	[135]
16	CE	Cu_2O	11.35	0.680	47	3.62	[136]
17	Dye	Y123+$CO^{3+/2+}$			74	8.81	[42]
18	Dye	YA422+$CO^{3+/2+}$			74	10.65	[137]
19	Dye	N3+$I^{3-/I-}$			71	9.25	[138]
20	Dye	N3+Pentacence			49	0.8	[139]
21	Dye	Mangosteen+PEG			14.5	0.01	[140]
22	Dye	D102+VM5C9			38	0.47	[141]
23	Dye	N719+PET membrane			83	10.24	[142]
24	Dye	SQ+TVT			64	0.19	[143]

Chapter 3. : Research Methodology

3.1. PEMA

PEMA, or poly (ethyl methacrylate), is a methacrylic ester. The material has exceptional optical transparency and strong chemical resistance. PEMA films also exhibit outstanding mechanical strength, good adherence to the substrate, and good elastic properties [30]. PEMA has a high surface resistance and ionic conductivity. Due to the superior mechanical properties of PEMA, which are higher than the mechanical properties of polymer PMMA [31], the polymer PEMA can be blended with other polymers where the boost in the mechanical strength is necessary. The oxygen electron pairs in PEMA's oxygen atoms can coordinate with lithium ions, which makes it easier to build polymer salt complexes. The PEMA's carboxylic group (-COOH) can facilitate easier ion flow along the polymer segments by enhancing the interconnecting routes. The PEMA's characteristics are listed below:

Molecular Formula: $C_6H_{10}O_2$

Molecular weight: 51.5×10^4 g mol^{-1}

Nature: Semicrystalline

Density: 1.119 g/cm^3

Glass Transition Temperature: 66 °C

Melting temperature: 210 °C

Appearance: Powder

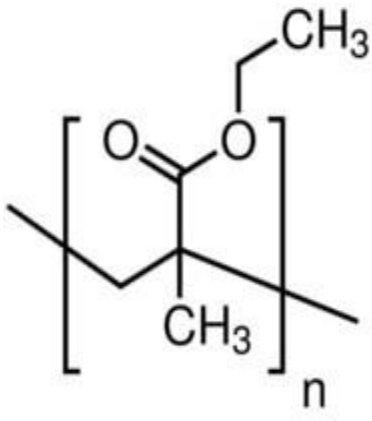

3.2. Plasticizers

Plasticizers are naturally occurring solvents that are not volatile having lower atomic weights, high dielectric constants, and low viscosities. The natural rubberiness and brittleness of polymers is greatly diminished when plasticizers are added. This is because adding plasticizer weakens the binding forces of attraction between polymer chains, which significantly lowers the Tg of the polymers. Due to their small size, the plasticizer molecules can remain attached to the polymer chain segments and create an adhesive force of attraction within the polymer matrix. This increases the flexibility of the polymer chains by reducing the cohesive force between them. As a result, segmental mobility increases, enhancing ionic conductivity. Ionic conductivity of the polymer-salt mixture is increased by the addition of plasticizers. Several studies [34–36] have documented how plasticizers affect the ionic conductivity of polymer electrolytes. The properties of the plasticizers, including gamma-butyrolactone (GBL), propylene carbonate (PC), and ethylene carbonate (EC), which have been introduced into the polymer-salt complexes, are listed in Table 3.1.

Table 3-1: Properties of different Plasticizers

Properties	EC	PC	GBL
Molecular Formula	$C_3H_4O_3$	$C_4H_6O_3$	$C_4H_6O_2$
Density (g/cm^3)	1.320	1.205	1.125
Melting Point(°C)	34-37	-55	-43
Boiling Point (°C)	260.7	240	202
Dielectric Constant	89.6	64.4	39.1
Viscosity	2.53	1.85	1.75

3.3. SAMPLES STUDIED

In this research topic, Polymer PEMA, salt KI, plasticizer EC and CNT were used to make maximum conductivity sample that act as polymer electrolyte in preparation of DSSC solar cell.

1. Poly (ethyl methacrylate, or PEMA), doped with KI salt at various concentrations; specifically, PEMA +x wt% KI, where x = 10, and increment by 10 up to 90.

2. Poly (ethyl methacrylate) (PEMA) doped with 40wt.% KI salt at different concentrations of Ethylene carbonate (EC) i.e., PEMA+ 40 wt.% KI+ x wt.% EC where x = 10, 20….90

3. Poly (ethyl methacrylate) (PEMA) doped with 40wt.% KI+60wt.% EC +x wt.% Carbon Nano Tubes at different concentration. i.e., PEMA+ 40 wt.% KI+60wt.% EC +x wt.% CNT where x = 1, 2, …….20.

Each of the polymer electrolytes' materials used and sample preparation methods are discussed in separate chapters along with their characterization.

3.4. SAMPLE PREPARATION

Spin coating, sputtering, chemical/physical vapour deposition, and solution casting are a few well-known methods for fabricating free-standing polymer electrolyte films. In our laboratory, these polymer electrolytes were prepared to obtain thin film by solution cast method. The complete process is explained in the next section.

3.4.1 Solution cast technique

It is the most straightforward, affordable, and well-liked method for preparing polymer electrolytes. Using this technique, various samples were prepared in the form of thin film. This technique described as follow:

1. For complete dissolution at room temperature, a decided fix quantity of polymer is continuously magnetically steered into the predetermined solvent.
2. The predetermined salt quantity is added to the above- mentioned polymer solution.
3. For 4 hours, the mixture is continuously mixed or stirring using a magnetic stirrer until ahomogeneous viscous solution of "polymer-salt complex" is obtained.
4. The solvent from this viscous solution is then allowed to slowly evaporate at roomtemperature for several days in polypropylene petri

dishes.

5. Free self-standing polymer-salt thin complex films are ultimately produced after drying at room temperature.

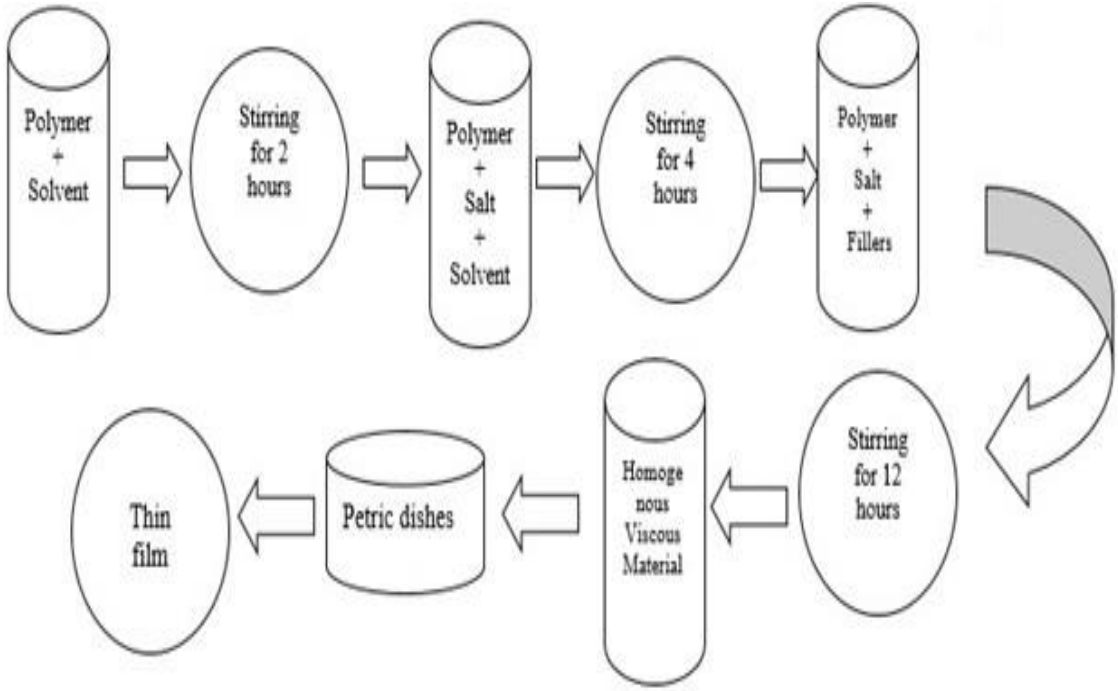

Figure 3.1: Solution Casting Technique

These complex films of free-standing polymer salts with varying salt weight percentages have been used to characterize the films' structural, electrical, and optical properties. For structural characterization, XRD and Fourier transform infrared (FTIR) methodologies have been used. Optically scanned studies have been carried out to better understand the surface morphology of the prepared films. Electrical characterization has been carried out using dc polarization studies and impedance spectroscopy.

3.5. STRUCTURAL CHARACTERIZATION

3.5.1 X- ray diffraction

In the research study, the complexation of the sample was investigated by x-ray diffraction (XRD) method. The films that were created were relatively amorphous. The justification is provided below.

The atoms present throughout the planes scatter the monochromatic x-ray when it collides with a collection of equidistant parallel planes with an interplanar distance of d. The intensity variations that show up as maxima and minima in the diffraction patterns are caused by interference between various scattered x-rays from subsequent planes. According to Bragg's law, the nth order maximum condition is as follows:

$$2d * Sin\theta = \lambda n \quad \text{…. (3.1)}$$

Where n value varies up to infinity. Offers the order of the diffraction maximum values and is the material-specific glancing angle or scattered angle on an individual plane. Additionally, it has been observed that while samples are non-crystalline type or amorphous type materials show few broad hallows at maximum, crystalline materials show clearly defined narrow peaks at each maximum. The XRD patterns of semicrystalline solids will exhibit sharp peaks crossing a hollow. Utilizing XRD analysis, the polymer-salt complexes have been thoroughly investigated. This research made use of the Rigaku D/max-2500 x-ray diffractometer (figure 3.2). A highly efficient technique for figuring out the vibrations of various structural groups found in both simple and complex molecules is IR vibrational spectroscopy, which studies molecular vibrations. The near range from 0.75 μm to 2.5 μm and mid infrared range from 2.5 μm to 50 μm in μm is the most practical range because most molecular vibrations take place in this range. In essence, IR spectra serve as molecular structures' digital fingerprints. This method is appropriate for the study of proton conductors because A-H stretching modes (A = O, N, or halogen) produce strong absorption bands in the 4000-1700 cm^{-1} range where there is not much interference from other groups.

3.5.2 FTIR Spectroscopy

FTIR spectroscopy can also be used to examine the structural change observed after the formation of the polymer-salt complex (or polymer electrolyte), which is the focus of this research problem. To achieve this, the IR spectra of films made of pure PEMA polymer, PEMA+ KI salt, PEMA+KI+EC and PEMA+KI+EC+CNT complex were all observed and compared. In this investigation polymer original spikes and their shifted spikes due to salt,

plastizer and CNT addition wavelength was studied. A Perkin Elmer IR spectrometer model 883 was used to record the FTIR spectrum for each sample (Figure 3.3)

Figure 3.2: Rigaku D/max- 2500 diffractometer.

3.5.3 Bulk ionic complex impedance spectroscopy

The scientific term in electrical conductivity is described below.

$$\sigma = Gl/A \qquad \ldots. (3.2)$$

Where G = 1/ R is referred to as the conductance and R is the sample's bulk resistance with a thickness of l and an area of cross-section of A. Typically, a single crystal sandwiched between two suitable electrodes, a membrane or film, or a pressed pellet is used to measure electronic conductivity, commonly employed geometry is,

Electrode / Electrolyte / Electrode

Figure 3.3: Perkin Elmer IR spectrometer model 883

The contributions from (i) electrode-electrolyte contact resistance make it difficult to interpret the measured ionic conductivity. (ii) Polarization at the electrode-electrolyte interface. Thus, the electrical conductivity that was measured cannot precisely represent the bulk conductivity. In the case of dc electrical conductivity measurements in particular, the unidirectional flow of current results in the formation of a gradient of concentration that cancels out the effect of the applied field. Therefore, solid electrolyte cannot be measured for dc electrical conductivity. The AC impedance technique is used for determining conductivity. To distinguish the true bulk conductivity in ionic solids from electrode, electrolyte, and grain boundary impedances, Bauerle [9] developed a sophisticated impedance method. A solid electrolyte-filled cell is exposed to a low amplitude sinusoidal a.c. signal in complex impedance spectroscopy. Over a broad frequency range, the real and imaginary components of the impedance and admittance are measured. Everyone can write the impedance (Z) / admittance. (Y) as

$$z(\omega) = z'(\omega) - jz''(\omega)$$

And

$$y(\omega) = G(\omega) + jB''(\omega) \ldots\ldots\ldots\ldots\ldots\ldots \quad (3.3)$$

z' real part, z'' imaginary part of impedance, G conductance, B susceptance and ω is frequency. The real parts and imaginary parts are plotted in complex planes to calculate frequency dispersion. These standard curves provide data on the effects of the grain boundary, bulk resistance, and electrode-electrolyte interface. The Nyquist (B-G) plots of a few practical simple circuits are shown in Figure 3.4

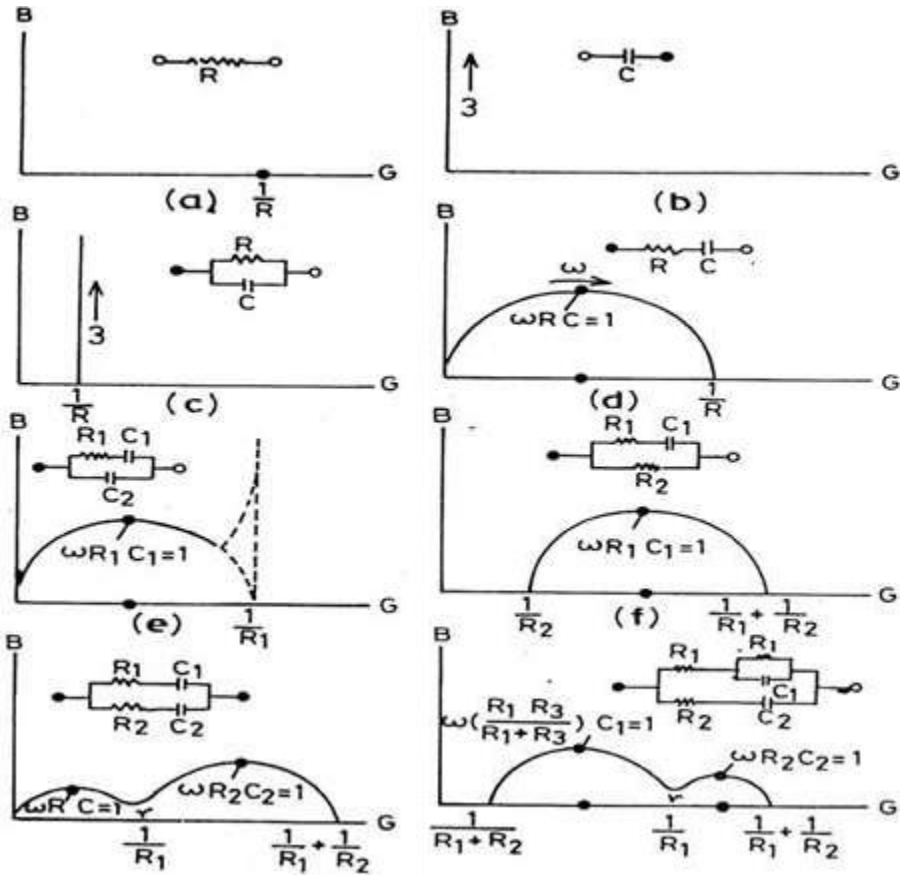

Figure 3.4: Nyquist plots of different RC combination.

The following three cases occur in practice when measuring the bulk ionic conductivity of polymer solid electrolytes, and each is discussed in turn.

- Sample using reversible/non-blocking electrodes:

Figure 3.5 shows a solid polymer electrolyte film enclosed between two non-blocking/reversible electrodes (a). In this circuit geometrical capacitance (Cg) parallel with

the bulk resistance R at the high-frequency range. The equivalent circuit is shown in Figure 3.5 (b), Figures 3.5(c) and (d) describe corresponding impedance and admittance plots respectively. At low frequency no division at electrode – electrolyte interface due to electrodes are non-blocking and reversible and result is no frequency dispersion. The intercept of the dispersion curve on the real axis provides the bulk resistance (R) / conductance (G = 1/R).

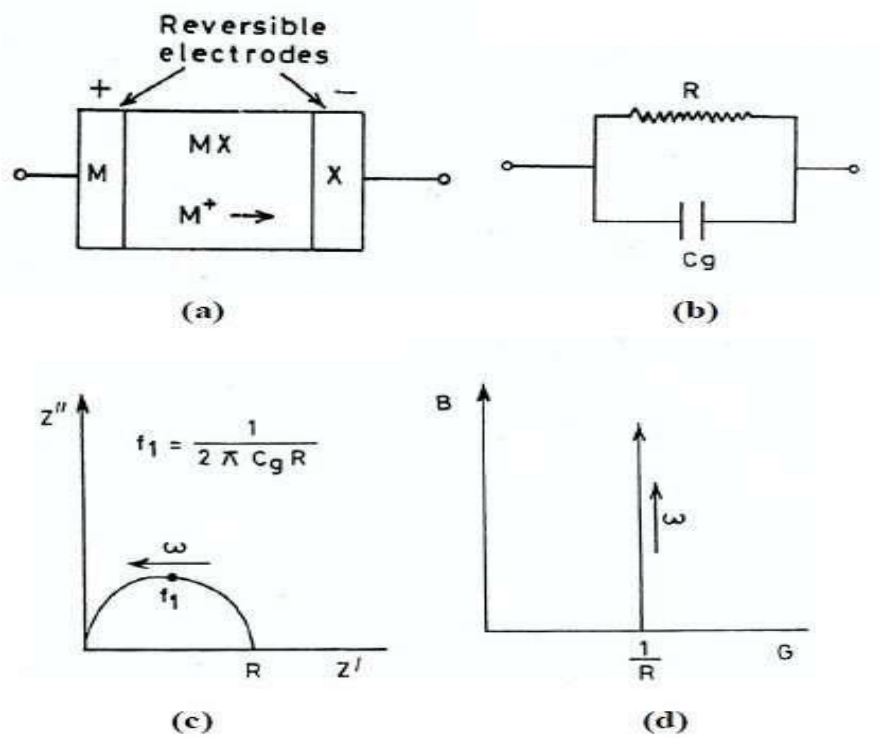

Figure 3.5: (a) non-blocking electrode, (b)Ideal Circuit, (c) Nyquist plot of respective circuit and (d) Nyquist plot respective circuit.

- Sample placed between blocking electrodes:

If the sample is placed between both blocking electrodes, the corresponding circuit illustrated in Figure 3.6 (a) has an additional double layer capacitance (Cd1) connected in series with the Cg-R where Cg-R are in parallel configuration. The corresponding impedance and admittance plots, shown in figures 3.6(b) and (c), respectively, show a further low frequency dispersion region. In this region, Cg has little impact, and double

layer capacitance is primarily responsible for polarization at the electrode-electrolyte interface. The electrode-electrolyte interface surfaces,however, have been presumably assumed to be ideal, that is, flat and immaculately smooth. Idealized interfaces cannot be implemented in practice because they change the impedance / admittance plots in figures 3.6(b) and (c) at the low frequency region. Finding the point where the low-frequency and high-frequency dispersion meet each other at real axis yields the sample's bulk resistance or conductance.

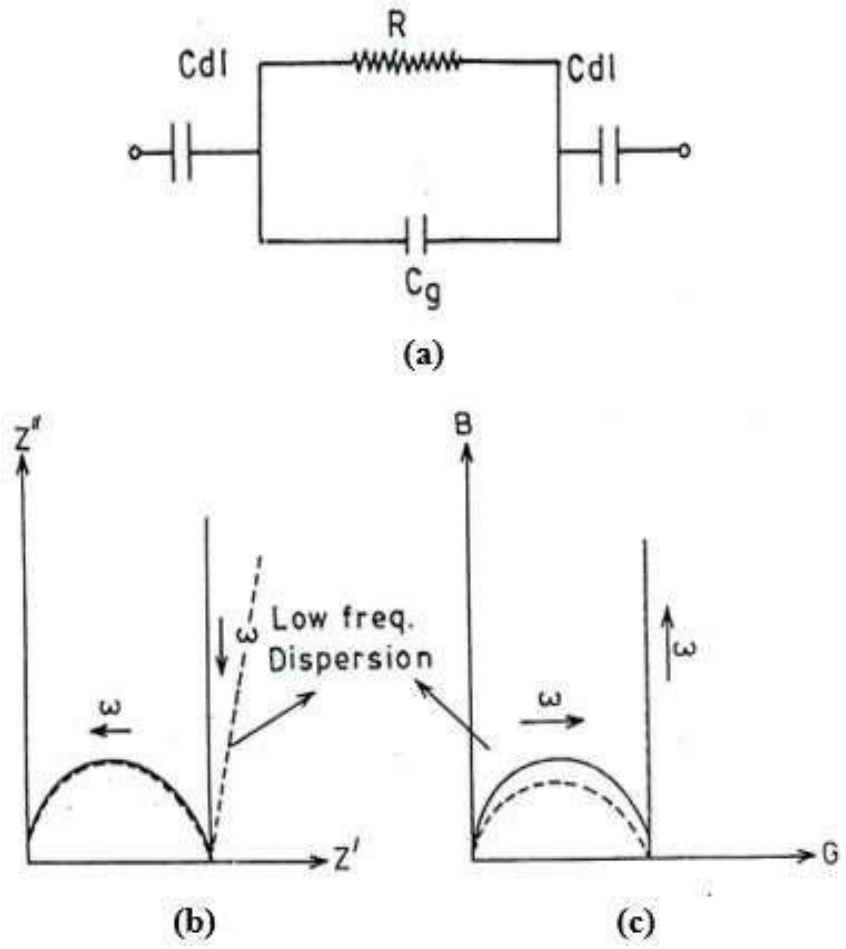

Figure 3.6: a) Ideal circuit of blocking electrode, (b) Respective Nyquist plot and (c) Respective Nyquist plot

- Polycrystalline sample having grain boundary effects:

Additionally, polycrystalline samples and samples having incredibly rough surfaces can contain grain boundaries. These grain boundaries may alter the conductivity depending on whether the activation energy for the conduction at the grain boundaries is lower or higher than the activation energy for conduction in the bulk. Polycrystalline with blocking electrode sample are shown in figure 3.7(a). In this diagram, the letters R_1-C_1 in parallel configuration known as electrode polarization, R_2-C_2 in parallel configuration known as bulk resistance, and R_3 with series configuration known as boundary resistance. The corresponding B-G plots are shown in Figure 3.7.

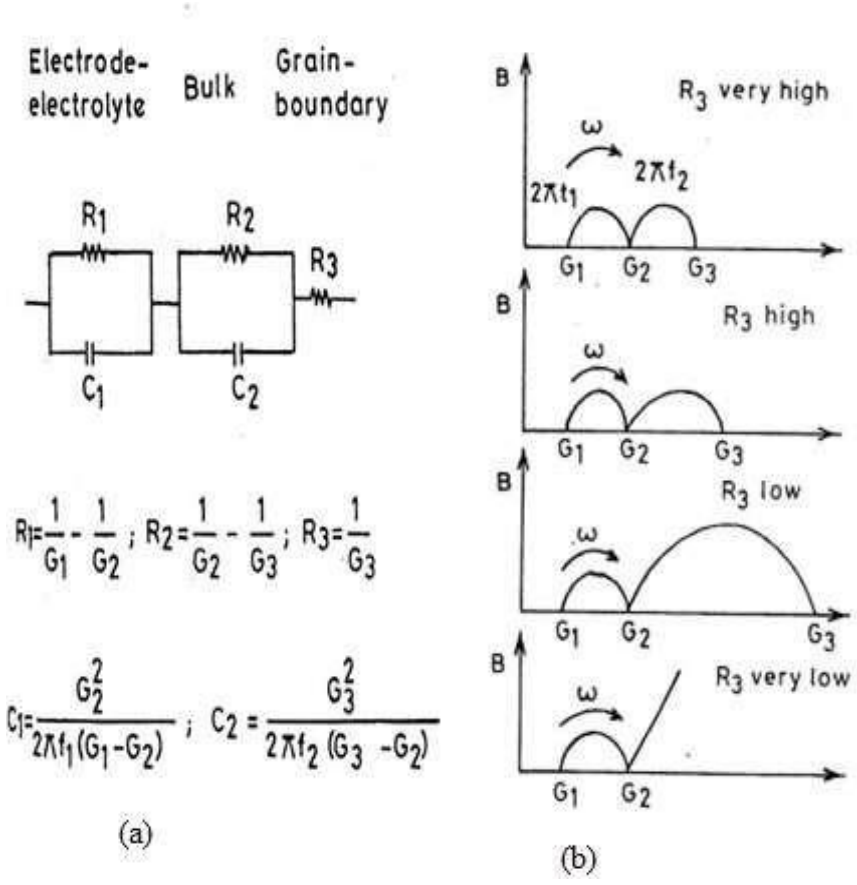

Figure 3.7: (a) Ideal circuit of polycrystalline sample and (b) Nyquist plots for different electrical/electronic components

The contribution of the active at high frequencies grain boundaries to conductivity is revealed by the high frequency intercepted on the real axis of the frequency distribution curve. The corresponding B-G plots for them (b) are shown in Figure 3.7. The contribution to conductivity made by the grain boundaries when they are active at high frequencies is revealed by the high frequency capture on the real axis of the frequency dispersion curve. Many other investigators have also investigated how electrochemical cells respond to changes in impedance and admittance. [10–14]. Polymer complex electrolyte sample bulk resistance was determined using the cell configuration Steel / Polymer electrolyte / Steel with the aid of a "CH instrument model 604 D, U.S.A." and formula 3.2 is used. An easy-to-use, spring-loaded sample holder, like the one in figure 3.8, was used for all measurements. In this case, steel electrodes were used to ensure proper electrode-electrolyte contact.

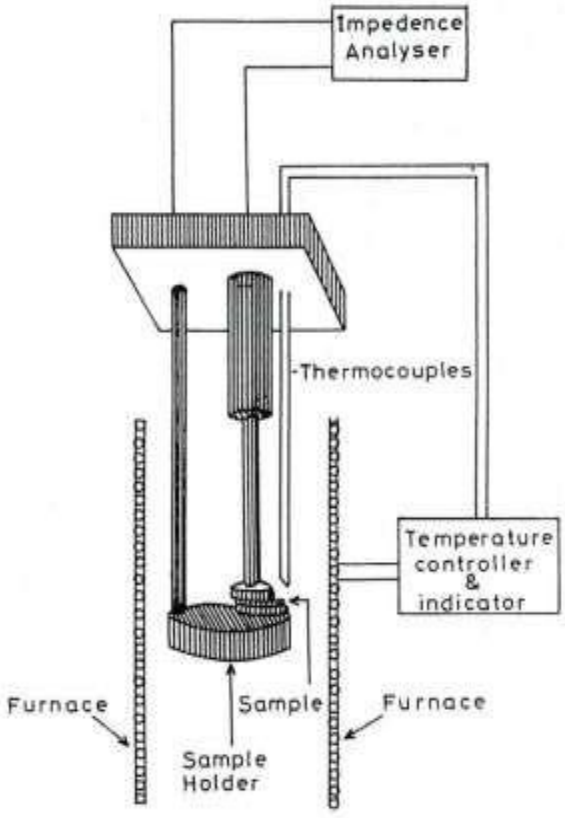

Figure 3.8: Conductivity measurement arrangement setup.

3.6. DSSC Solar Cell

DSSC stands for "dye-sensitized solar cell," which is a type of photovoltaic (PV) cell used to convert sunlight into electrical energy. DSSCs are also known as Grätzel cells, named after their inventor, Michael Grätzel. DSSCs have gained attention due to their potential for low-cost manufacturing and their ability to generate electricity under low-light conditions.

Here's how a DSSC works:

1. Absorption of light: The DSSC consists of a semiconductor layer made of titanium dioxide (TiO_2) nanoparticles that are coated with a photosensitive dye. When sunlight (photons) strikes the dye, it absorbs the light and transfers the energy to the TiO_2 layer.

2. Electron generation: The absorbed light energy causes the dye molecules to release electrons, creating electron-hole pairs. The electrons move from the dye molecules to the TiO_2 layer, leaving behind positively charged holes in the dye.

3. Electron transport: The TiO_2 layer acts as an electron conductor, allowing the electrons to move freely through the material. This electron transport is facilitated by the interconnected network of nanoparticles in the layer.

4. Redox couple: To maintain charge balance, a redox couple is introduced into the DSSC. Typically, an electrolyte containing a redox couple, such as iodide/triiodide (I^-/I_3^-), is used. The oxidized form (I_3^-) of the redox couple accepts the electrons from the TiO_2 layer, while the reduced form (I^-) shuttles electrons back to the dye.

5. Electricity generation: Electric current is produced when electrons move through an external circuit; this current can be used to power electronic devices or stored in a battery for later use.

Advantages of DSSCs include:

1. Cost-effective manufacturing: low-cost material and simple manufacturing processes like printing or coating, making them potentially less expensive than traditional silicon-based solar cells are used to prepare DSSC.
2. DSSCs can be fabricated using low-cost materials and simple manufacturing processes like printing or coating, making them potentially less expensive than traditional silicon-based solar cells.
3. High efficiency under low-light conditions: DSSCs can produce electricity even under diffuse or low-light conditions, making them suitable for indoor applications and cloudy environments.
4. Versatile design: DSSCs can be made flexible and transparent, allowing for various applications such as building-integrated photovoltaics (BIPV), portable electronics, and wearable devices.

However, DSSCs also have some limitations:

1. Lower efficiency: Despite significant efficiency improvements, DSSCs still have a lower overall conversion efficiency than conventional silicon-based solar cells. There are ongoing efforts to increase their effectiveness.
2. Durability concerns: The liquid electrolyte used in DSSCs can potentially leak or degrade over time, affecting the long-term stability and durability of the cells. Solid-state DSSCs using solid electrolytes are being developed to address this issue.
3. Sensitivity to moisture: DSSCs are sensitive to moisture ingress, which can degrade their performance. Proper encapsulation or use of moisture-resistant materials is necessary to protect the cells.

DSSCs are an active area of research and development, with ongoing efforts to improve their efficiency, stability, and commercial viability. They offer an alternative approach to harness solar energy and have the potential to contribute to the renewable energy landscape.

3.6.1 Doctor Blade Method

The doctor blade method is a specific technique used in the manufacturing process of dye-sensitized solar cells (DSSCs). It involves the deposition of the various layers of the DSSC structure using a doctor blade or a similar tool shown in figure 3.8.

Here's an overview of the doctor blade method in the context of DSSC manufacturing:

1. Substrate preparation: The process begins with preparing a suitable substrate, which is typically a conductive glass or plastic material coated with a transparent conductive oxide (TCO) layer, such as fluorine-doped tin oxide (FTO) or indium tin oxide (ITO). The substrate provides the foundation for the DSSC structure.

2. Preparation of the photoactive layer: The photoactive layer of the DSSC contains a mesoporous film made of titanium dioxide (TiO_2) nanoparticles. In the doctor blade method, a slurry or paste containing the TiO_2 nanoparticles is prepared. The slurry typically consists of the TiO_2 nanoparticles dispersed in a solvent, along with a binder material to enhance film cohesion. The slurry is spread onto the substrate using a doctor blade.

3. Doctor blade deposition: The doctor blade is a flat and straight-edged tool, often made of metal or plastic. It is used to spread the slurry evenly onto the substrate, creating a uniform layer of the TiO_2 film. The doctor blade is held at a fixed distance above the substrate, and as it is moved across the substrate, excess slurry is pushed away, leaving behind a controlled thickness of the TiO_2 layer. The speed and pressure of the doctor blade movement determine the thickness of the deposited layer.

4. Dye sensitization: After the TiO_2 layer is deposited, it is dried and then immersed in a solution containing a photosensitive dye. The dye molecules adsorb onto the surface of the TiO_2 nanoparticles, forming a monolayer that enables light absorption and electron transfer.

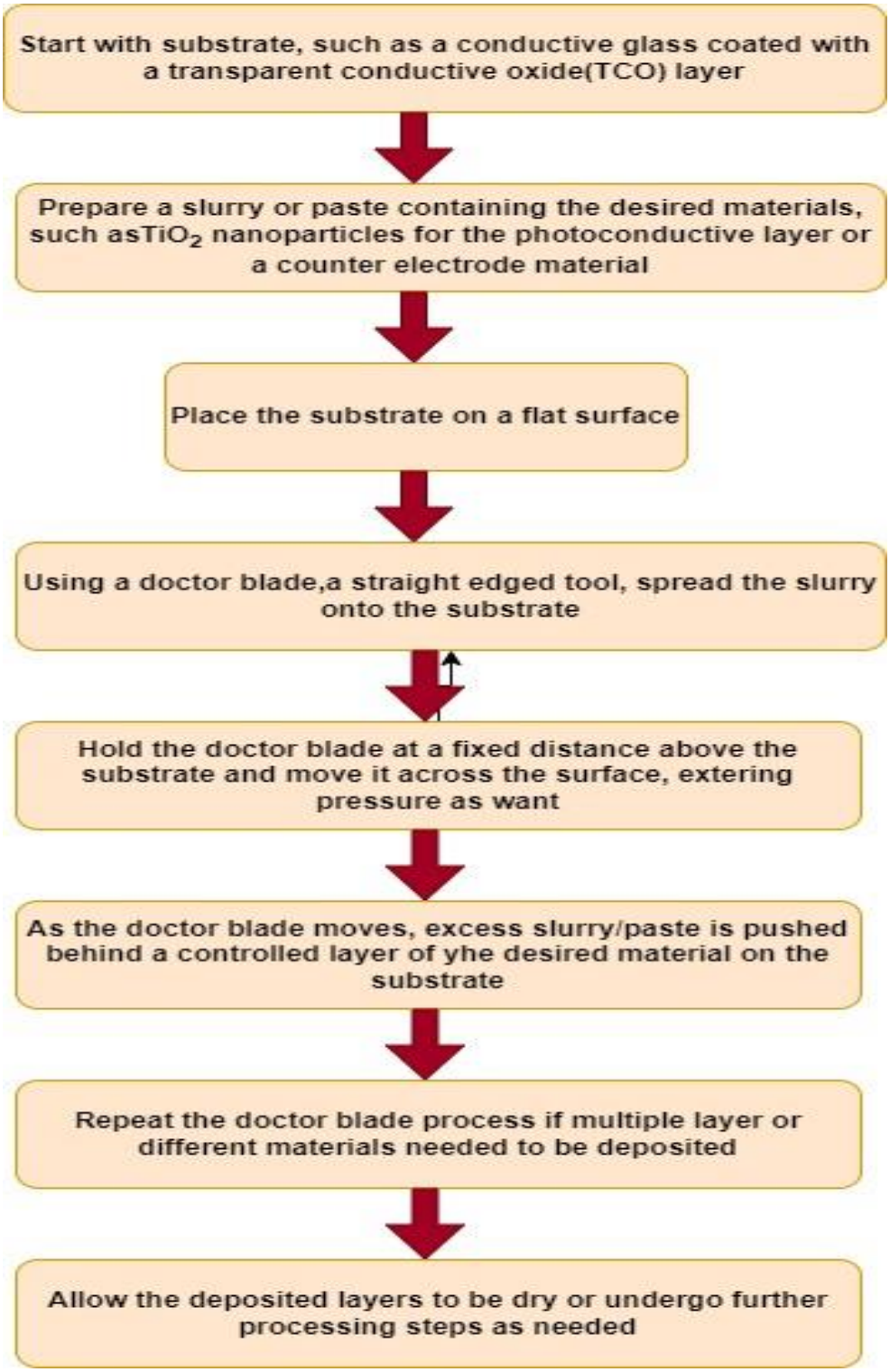

Figure 3.9: Doctor Blade Method

5. Counter electrode deposition: The counter electrode is typically made of a conductive material, such as platinum or carbon. In the doctor blade method, a paste or ink containing the counter electrode material is applied to another substrate using the same doctor blade technique. The substrate with the counter electrode is then carefully placed on top of the TiO_2 layer, creating a sandwich-like structure.

6. Electrolyte filling: A liquid electrolyte or a solid-state hole transport material is introduced into the DSSC structure to facilitate the flow of electrons and ions. For liquid electrolyte based DSSCs, a sealing layer is applied to encapsulate the cell and prevent electrolyte leakage.

The doctor blade method offers a simple and scalable approach to deposit the TiO_2 layer and other components of the DSSC structure. It allows for control over the film thickness and uniformity, which are crucial for achieving optimal performance. However, it's worth noting that other deposition techniques, such as screen printing, spin coating, or spray coating, are also employed in DSSC manufacturing, depending on the specific requirements and capabilities of the fabrication process.

Chapter 4.：Result and Discussion

4.1. Sample images

During the laboratory work various samples were prepared using solution casting techniques. Some sample images are shown in figure 4.1.

(a)Pure PEMA

(b)PEMA+40%KI

(c)Pure PEMA

(d) PEMA+10%KI

(e) PEMA+40%KI+60% EC

(e) PEMA+40%KI+50 %EC

Figure 4.1: Various sample images obtained after Solution Casting Techniques

4.2. Complex impedance spectroscopy

HIOKI 3522-50 LCR that is used in the frequency range of 50 Hz to 100 kHz, the prepared polymer composite electrolyte films were examined for their ionic conductivity. Separate cole-cole plots were used to determine the polymer composite electrolyte's ionic conductivityas a function of Kl and EC. Conductivity was measures using the stainless-steel electrodes and calculate it using the following formula:

$$\sigma = G\frac{l}{A}$$

G is conductance (l/Rb), l is sample the thickness, A is sample area, and is ionic conductivity.Rb is bulk resistance where the map of Nyquist intersects with the real axis.

Table 4-1: Conductivity variation in PEMA concerning Kl concentration.

S. No	Wt.%	Conductivity(S/cm)
Sample 1	10	$6.24x\ 10^{-8}$
Sample 2	20	$4.82x10^{-7}$
Sample 3	30	$9.33x10^{-7}$
Sample 4	40	$3.80x10^{-6}$
Sample 5	50	$2.40x10^{-6}$
Sample 6	60	$9.60x10^{-7}$
Sample 7	70	$7.20x10^{-7}$
Sample 8	80	$5.60x10^{-7}$
Sample 9	90	$2.34x10^{-7}$

Figure 4.2 shows the difference in polymer electrolyte ionic conductivity concerning the different concentrations of the scattered Kl phase. By doping the given polymer at 40% wt.Kl concentration, the maximum conducting sample was achieved. It was observed that the highest conductivity was 3.80×10^{-6} S/cm. The ionic conductivity is increased by adding Kl to the pure PEMA matrix.

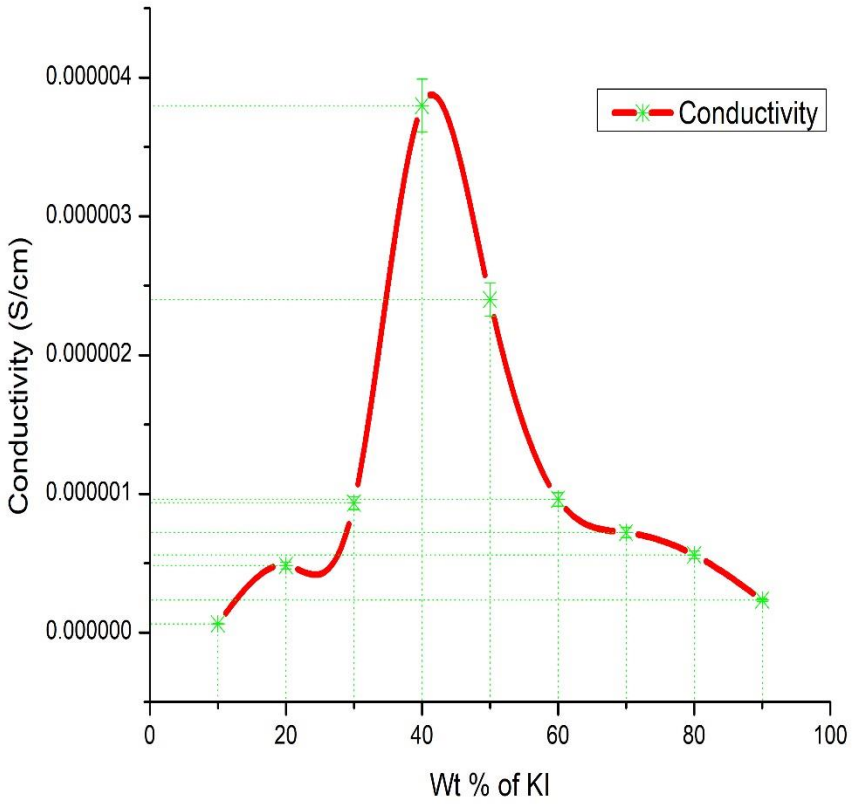

Figure 4.2: Conductivity variation in PEMA concerning Kl concentration.

The conductivity value observed 4.65 x 10^{-5} Scm^{-1} at 40 weight percent of Kl, where it reaches its peak, and then it starts to decline, as shown in Figure 4.2. The ionic conductivity related to KI concentration may decrease by more than 40 weight percent due to the formation of multiples of higher charge, while the ionic conductivity may increase with rising Kl concentration due to an increase in the number of mobile charge carriers. Figure 4.4 illustrates how variations in EC concentration affect the polymer electrolyte's ionic conductivity (PEMA + 40% Kl).

The graph clearly shows that increasing the amount of plasticizer by 60% increased conductivity by almost three orders in the maximally conducting sample. The highest conductivity was identified as 4.64 x 10^{-5} S/cm.

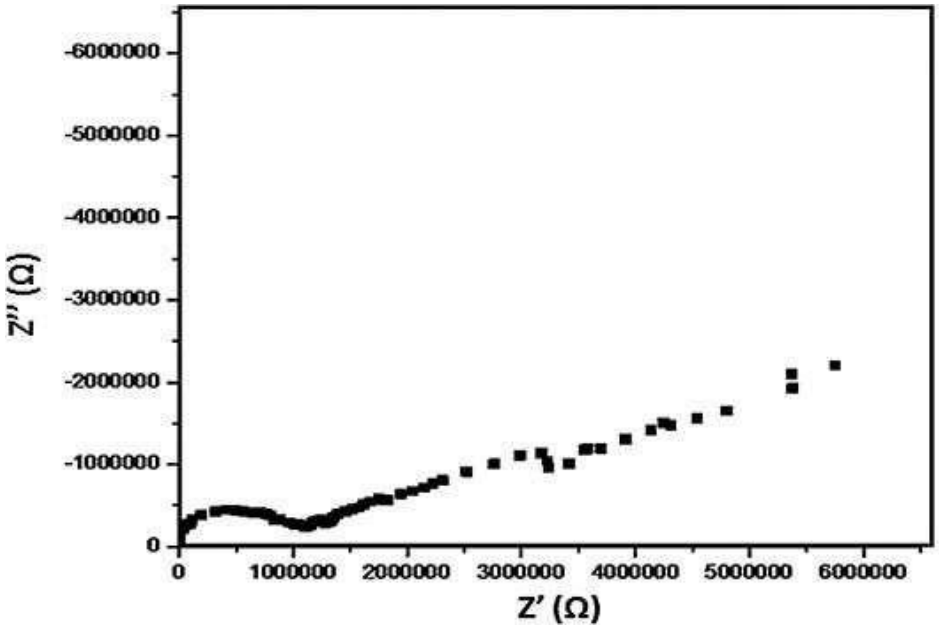

Figure 4.3: PEMA + 40% wt. KI maximum conductivity sample cole-cole plot.

Figure 4.3 displays the cole-cole plot of the salt polymer electrolyte and figure 4.5 displays the cole-cole plot of the plasticized polymer electrolyte device with full conducting. The addition of plasticizer makes the polymer electrolyte more amorphous, which enhances conductivity.

Table 4-2: EC wight percentage variation in PEMA+40% wt. KI.

S. No	Wt.%	Conductivity(S/cm)
Sample 1	20	6.82×10^{-6}
Sample 2	40	1.05×10^{-5}
Sample 3	50	3.76×10^{-5}
Sample 4	60	4.64×10^{-5}
Sample 5	70	4.53×10^{-5}
Sample 6	80	4.50×10^{-5}
Sample 7	90	2.40×10^{-5}

Comparing polymer molecules to plasticizer molecules, polymer molecules are relatively large. Thus, plasticizer molecules quickly and firmly bind to the chain fragments after entering the polymer matrix. Strong interactions between plasticizing agent molecules and

polymer chains decrease the forces that bind polymer chains together and increase the mobility of different polymer chain sectors, which further boosts the ionic conductivity and discharge time of the polymers. The main function of the plasticizer, according to the present study, is to reduce the viscosity of the electrolyte and help isolate KI, KI^{+}, and I. The ionic conductivity (s) for the electrolyte scheme is given as

$$\sigma = n.q.\mu$$

Where the density of the charge carrier is n, q is the carrier's charge, m is the carrier'smobility.

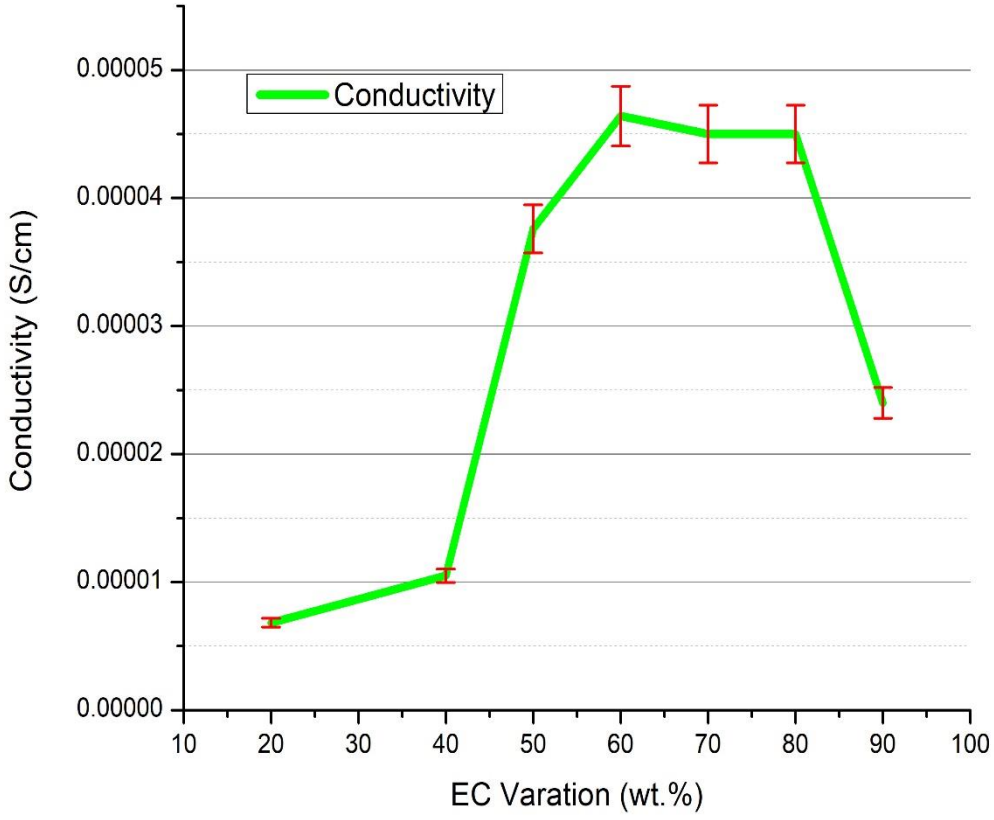

Figure 4.4: Conductivity vs EC weight percentage variation

Therefore, the importance of ionic conductivity would undoubtedly be influenced by any rise in any of the n or q parameters. Ionic conductivity increases when Kl is added to the PEMA +EC solution matrix form, and ionic conductivity decreases can be explained using the model of charge pairs. In the present case, Kl causes the production of

additional mobile charge species, which are KI^+ cation and I^- anion. Ion conduction in PEMA polymerelectrolytes is also brought on by the ionic hopping process.

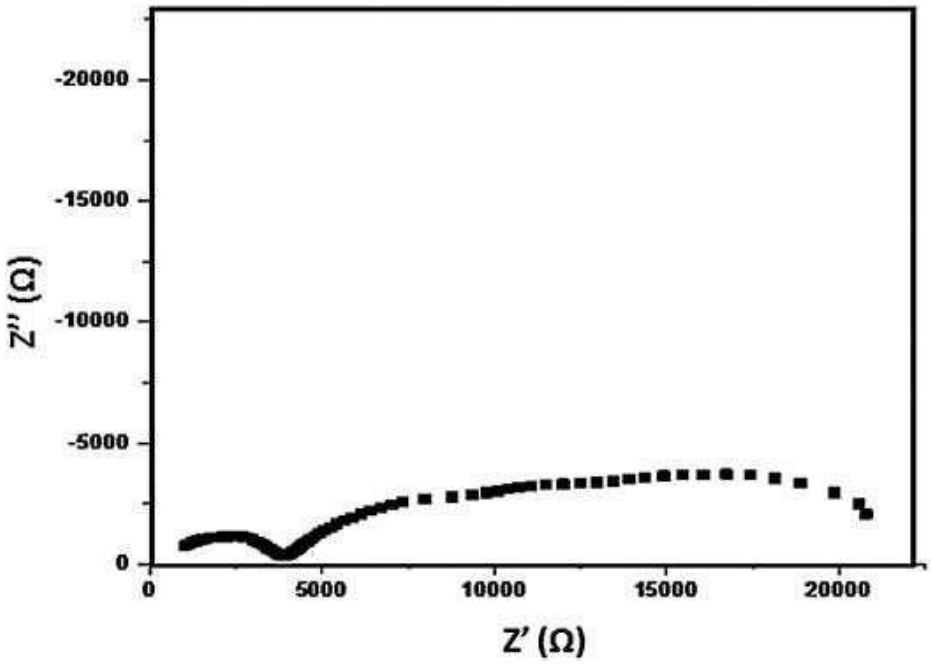

Figure 4.5: PEMA + 40% Kl + 60% EC maximum conductive sample cole-cole plot.

4.3. FTIR

From 500 and 4500 cm^{-1} wavenumbers, the FTIR spectra of pure PEMA and salt doped PEMA (PEMA+40% KI+60% EC) were obtained using the Perkin-Elmer spectrophotometer (model 833). This method is crucial for examining the composition of the polymer because it provides a thorough understanding of the composite and coordination between various materials in a composite electrolyte polymer device. In Figure 4.6, the vibrational bands at 2990 and 2945 cm^{-1} are attributed to the asymmetric and symmetric C- H stretching of the methylene group of PEMA. The modes of C-H_2 scissoring, C-H_2 wagging, and -CH_2 rocking are indicated by the heights of 1484, 950, and 755cm^{-1},respectively. At 1718cm^{-1}, the C = O carbonyl stretching was seen. The vibration of the C = CH_2 group band was observed at 941 cm^{-1}. The peaks found in the range of 3000 to 3550 cm^{-1} display classes of -OH and -OOH. At 1800cm^{-1} wavelength peak exist due to Kl salt. At 1774 cm^{-1} and 1804 cm^{-1} C=O stretching band exist due to

EC [144].

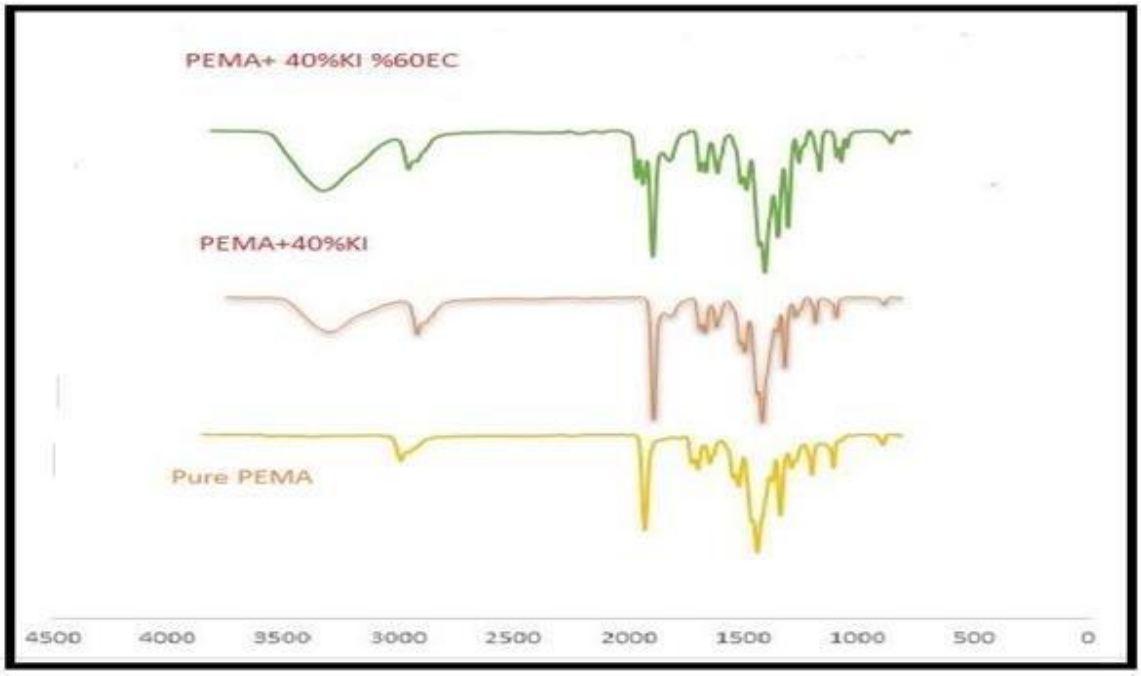

Figure 4.6: FTIR spectra comparison of pure PEMA (yellow colour) (PEMA +40% KI) (red colour) and (PEMA +40% KI+60%EC) (green colour).

4.4. SEM

SEM representations of the pure polymer (a) and the full conducting composite electrolyte sample (b) are seen in figure 4.7. Compared to the rough crystalline appearance found in the standard/pure film, the plasticized film structure is typically finer. Plasticizers may have contributed to this transition by causing the crystalline host polymer film to plasticize, which changed it into an amorphous film. The microstructure is very easy to see in Figure 4.7 (a). The solution casting procedure results in the deposition of PEMA film. The pores indicates that have developed from crystalline to amorphous states because of PEMA conversion in the SEM image of the complex material. In this picture, there are some bright pores and some dark pores. However, above the light area, there is no KI in the film. Additionally, every component was evenly combined. The image makes the surface's roughness very clear to see. Dark pores appear to have formed as PEMA changed from a crystalline to an amorphous state.

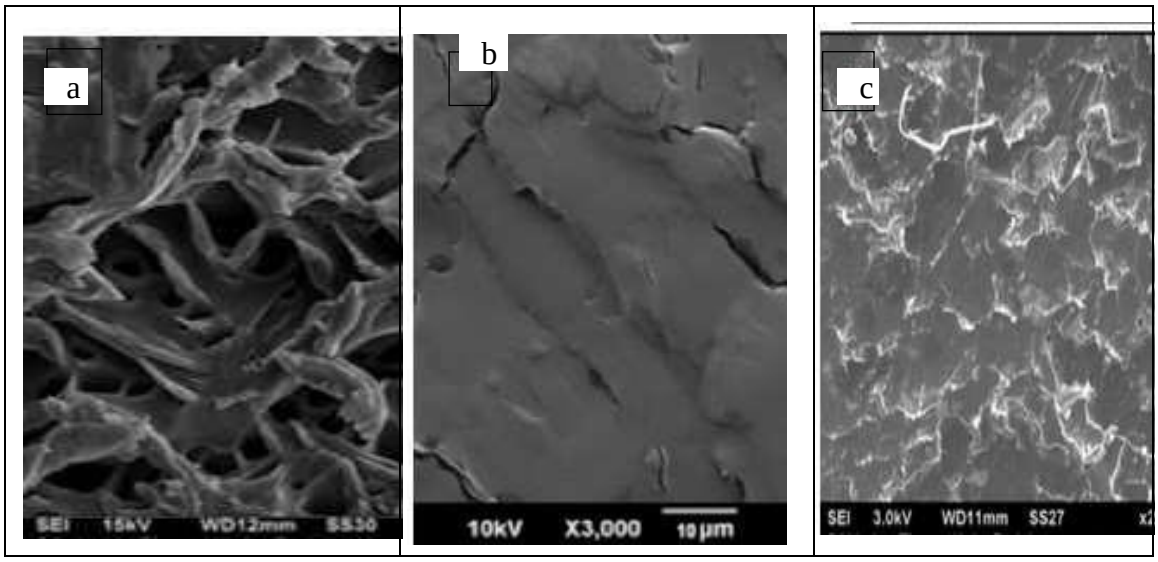

Figure 4.7: SEM micrograph of PEMA (a), PEMA+40%KI (b), PEMA+40%KI+60%EC(c).

4.5. XRD

Shimadzu XRD-6000 diffractometer was used to record the X- ray diffraction (XRD) patterns. To evaluate the complexity and crystallization of the polymer matrix, XRD analysis is used. Figure 4.8 shows that all films have an amorphous form, though the absence of sharp salt-related crystalline peaks in the complexes suggests that the potassium salts have completely dissolved. With a sharp peak at $2\Theta = 43^{o}$, the pure PEMA XRD pattern reveals a nearly amorphous nature. The amorphous peak characteristic of the radial distribution function, which represents the inter-chain distances, is what causes the large peak of pure PEMA.

Figure 4.8 (b) illustrates how the sample's PEMA peak amplitude decreased after the addition of salt. The ordering of polymer side chains causes a decrease in crystallinity, which was visible. Additionally, it was discovered that the peak strength of the plasticizer decreased when EC was added in comparison to PEMA. This suggests that a polymer mixture sample between PEMA, salt KI, and EC was conducted, which also facilitates the polymer structure's amorphous region.

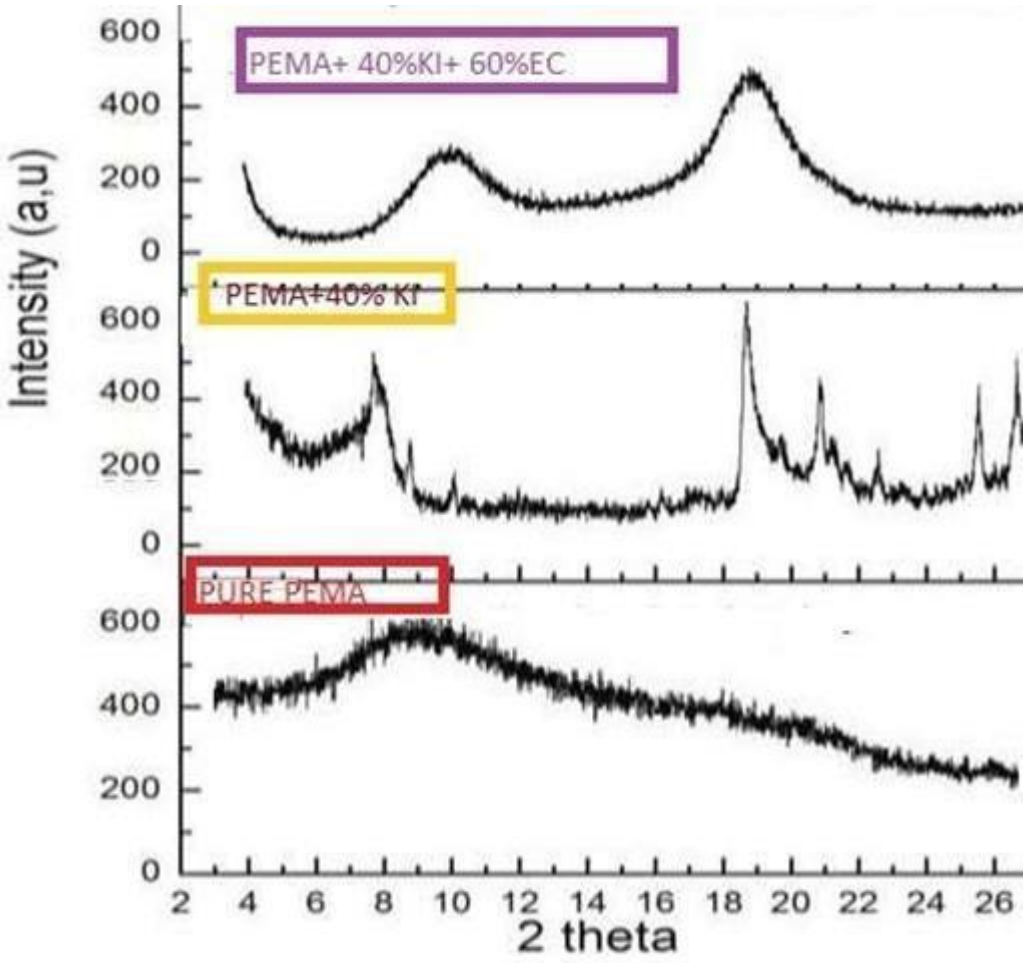

Figure 4.8: XRD analysis of different sample with different salt/material variation.

4.6. CNT EFFECT ON IONIC CONDUCTIVITY

Maximum conducted polymer complex sample PEMA+40% KI +60%EC has conductivity 4.64 x 10^{-5} S/cm. Further conductivity enhanced by adding nanocomposite into the sample. CNT nanocomposite weight percentage variation such as 3% wt., 5% wt., 7% wt., 9% wt., 11%wt., 13% wt., and 15% wt. were added into maximum conducting solution.

The solution of each variation was stirring up to 12 hours and obtained uniform viscous solution. Each solution is put into the Petric plate and dried at room temperature to obtain film. Maximum conductivity obtained 3.5x10^{-4} S/cm at 9% wt. as shown in figure 4.9.

Table 4-3: CNT variation in maximum conductivity sample (PEMA+KI+EC)

S. No	Wt.%	Conductivity(S/cm)
Sample 1	1	$2x10^{-5}$
Sample 2	3	$4 x10^{-5}$
Sample 3	5	$1.4 x10^{-4}$
Sample 4	7	$2.3 x10^{-4}$
Sample 5	9	$3.5 x10^{-4}$
Sample 6	11	$2.5 x10^{-4}$
Sample 7	13	$1.8 x10^{-4}$
Sample 8	15	$1.3x10^{-4}$

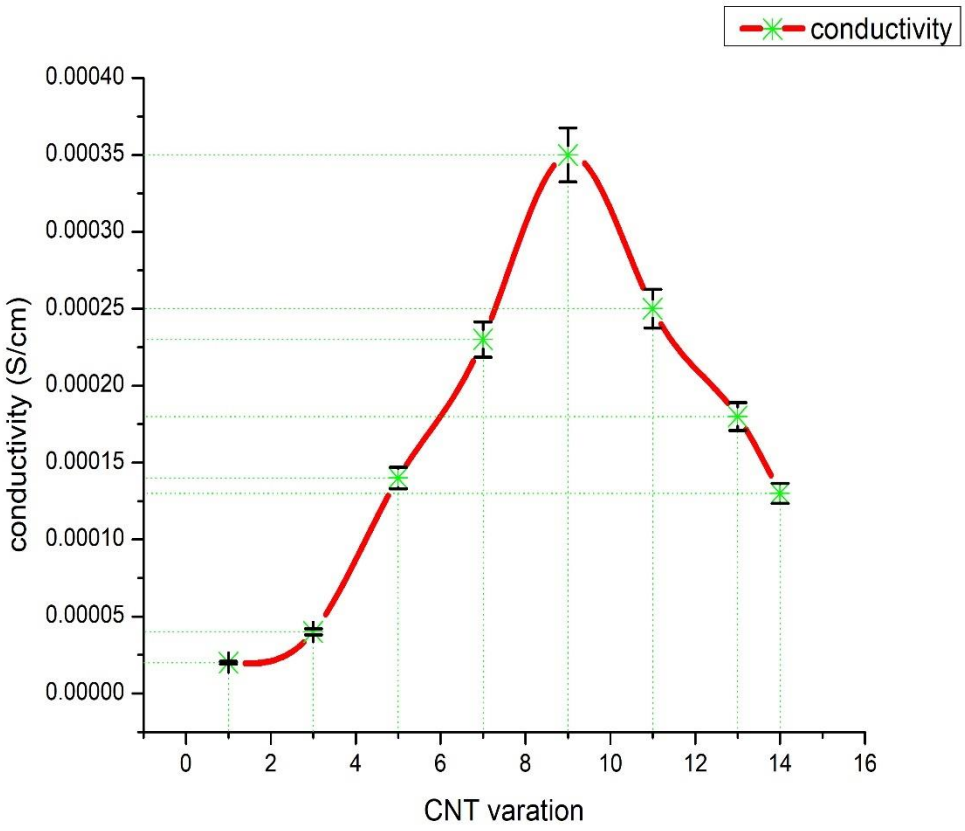

Figure 4.9: Conductivity v/s CNT variation.

4.7. SEM

Solid polymer electrolyte materials morphology was determined by using scanning electron microscopy. First sample coated with gold film to prevent static charging. Surface morphology of pure PEMA, PEMA+KI+EC, PEMA+ KI +EC+CNT(d) are shown in figure 4.10(a-d).

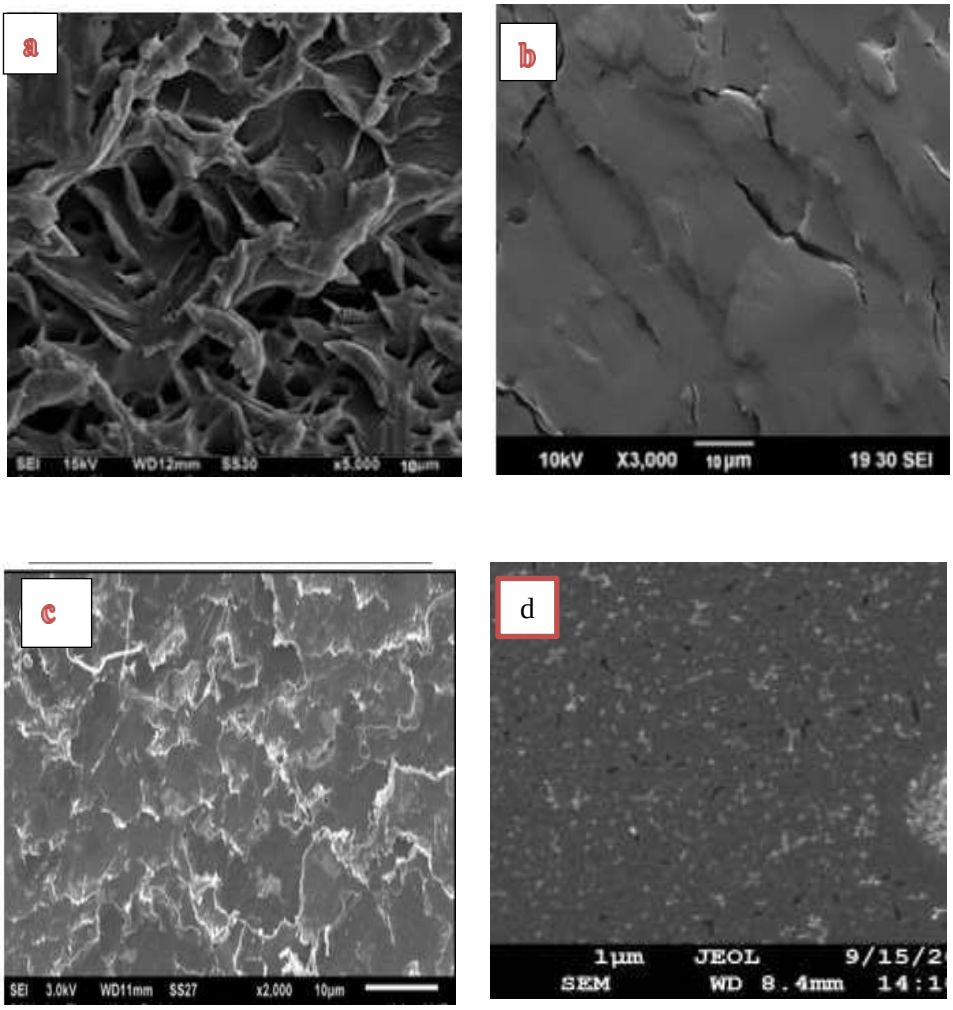

Figure 4.10: Surface morphology of pure PEMA (a), PEMA+KI (b), PEMA+ KI +EC(c)

Due to crystalline nature of PEMA, it was observed that the surface of Pure PEMA was dark in color and rough after adding salt and plasticizer the image was smooth. The change of color and smooth surfacedue to the change of crystalline nature to amorphous nature.

The variation of surface texture of each sample corresponds to its variation of ionic conductivity. Morphological change occurs due to variation of ionic conductivity.

4.8. FTIR Analysis

FTIR characterized technique was used to investigate the information about function group and composite polymer structure. To investigate this test, the Perkin-Elmer spectrophotometer was used to obtain FTIR spectrum about different samples shown in figure 4.11.

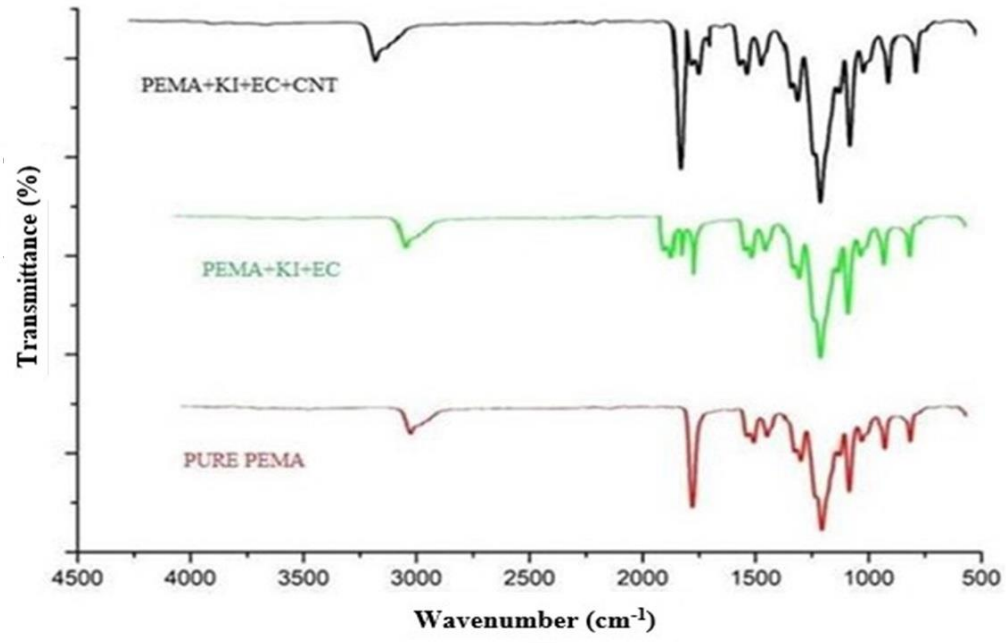

Figure 4.11: FTIR analysis comparison of different polymer composite PEMA, PEMA+KI+EC, PEMA+KI+EC+CNT.

FTIR spectrums were plotted between 500-4500 cm^{-1}wavenumber and vibrational band obtained at wavenumber 2990 cm^{-1} and 2931 cm^{-1} due to symmetric, asymmetric C-H stretching of methylene group present in PEMA. At 3000 cm^{-1} to 3500 cm^{-1} wavenumber -OH and -OOH single bond group was obtained due to hygroscopic nature of solvent THF used. Addition of CNT mixed into maximum conducting sampleof PEMA, KI, and EC some additional peaks of carbon nanomaterial were obtained at 1600cm^{-1} and 1700 cm^{-1}.

4.9. XRD Analysis

XRD technique used to identify the nature of the polymer composite electrolyte whether it is crystalline or amorphous nature. X-Ray diffraction analysis was recorded by using Shimadzu diffractometer XRD. XRD analysis shown in figure 4.8 and following points were observed such as Pure PEMA has crystalline nature shown in figure 4.8.

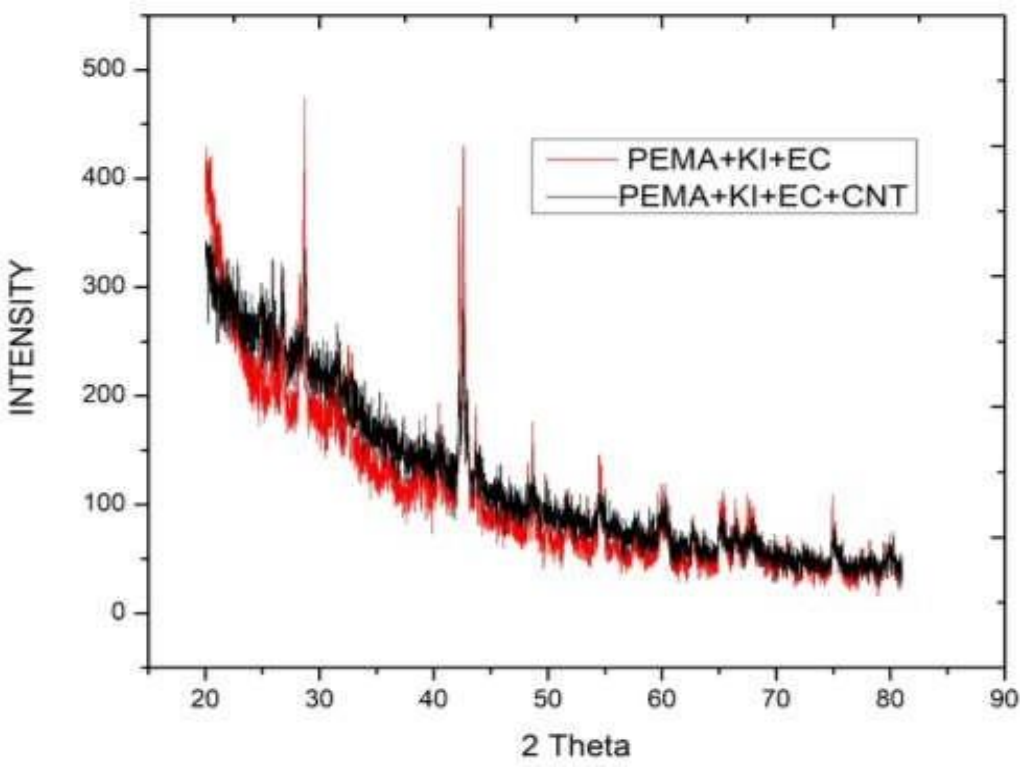

Figure 4.12: XRD comparison of PEMA+KI+EC and PEMA+KI+EC+CNT.

When salt added in pure PEMA composite there was a sharp peak indicating it disturbed the crystalline nature of pure PEMA, it decreases intensity of PEMA and decrease degree of crystallinity. This composite was not amorphous enough for movement of ion in the composite materials. To make the more amorphous nature of polymer composite material EC plasticizer added i.e., shown in figure 4.12 in red colour. Now it was observed the composite was more amorphous shown in figure 4.12 in black colour. It was observed sharp peaks are eliminated when CNT added into the polymer composite. After addition of EC mechanical strength of polymer composite decrease and it improved by adding nano composite

CNT into the polymer matrix shown in blue colour. It observed that the sample was more amorphous than PEMA+KI+EC variation sample.

4.10. Effect of Temperature on conductivity

Concerning temperature variation, the ionic conductivity of the maximum conducting sample was measured. Conductivity has been found to increase further with temperature rises to 90 ^{o}C shown in figure 4.13. It was observed that the increase in temperature also increase in the conductivity plasticized polymer electrolyte upto 3.80 x 10^{-6} Scm^{-1} of sample PEMA+KI. Similarly result obtained in EC and CNT variation sample up to maximum conductive sample 4.65 x 10^{-5}S/cm (PEMA+KI+EC) and 3.5 x 10^{-4}S/cm (PEMA+KI+EC+CNT). Table 4.4, Table 4.5, and table 4.6 show the relationship between log conductivity and 1000/K temperature of various samples of KI, EC, and CNT variation in pure PEMA respectively.

Table 4-4: Effect of temperature on the conductivity on PEMA+40% wt. KI

S. No	Temperature(1000/K)	Log Conductivity(S/cm)
1	3.531697	-7.20482
2	3.411223	-6.31695
3	3.298697	-6.03012
4	3.193358	-5.42022
5	3.094538	-5.61979
6	3.001651	-6.01773
7	2.914177	-6.14267
8	2.831658	-6.25181

Table 4-5: Effect of temperature on the conductivity on PEMA+40% wt. KI +60% wt. EC

S. No	Temperature(1000/K)	Log Conductivity(S/cm)
1	3.41	-5.16622
2	3.19	-4.97881
3	3.09	-4.42481
4	3.00	-4.33348
5	2.91	-4.3439
6	2.83	-4.34679
7	2.75	-4.36653
8	3.41	-5.16622

Table 4-6: Effect of temperature on the conductivity on PEMA+40% wt. KI +60% wt. EC +9% wt. CNT

S. No	Temperature(1000/K)	Log Conductivity(S/cm)
1	3.531697	-4.69897
2	3.411223	-4.39794
3	3.298697	-3.85387
4	3.193358	-3.63827
5	3.094538	-3.45593
6	3.001651	-3.60206
7	2.914177	-3.74473
8	2.831658	-3.88606

The action of Arrhenius was accompanied by an increase in conductivity concerning

increased temperature. The transition from semi-crystalline to amorphous may be what improved temperature conductivity.

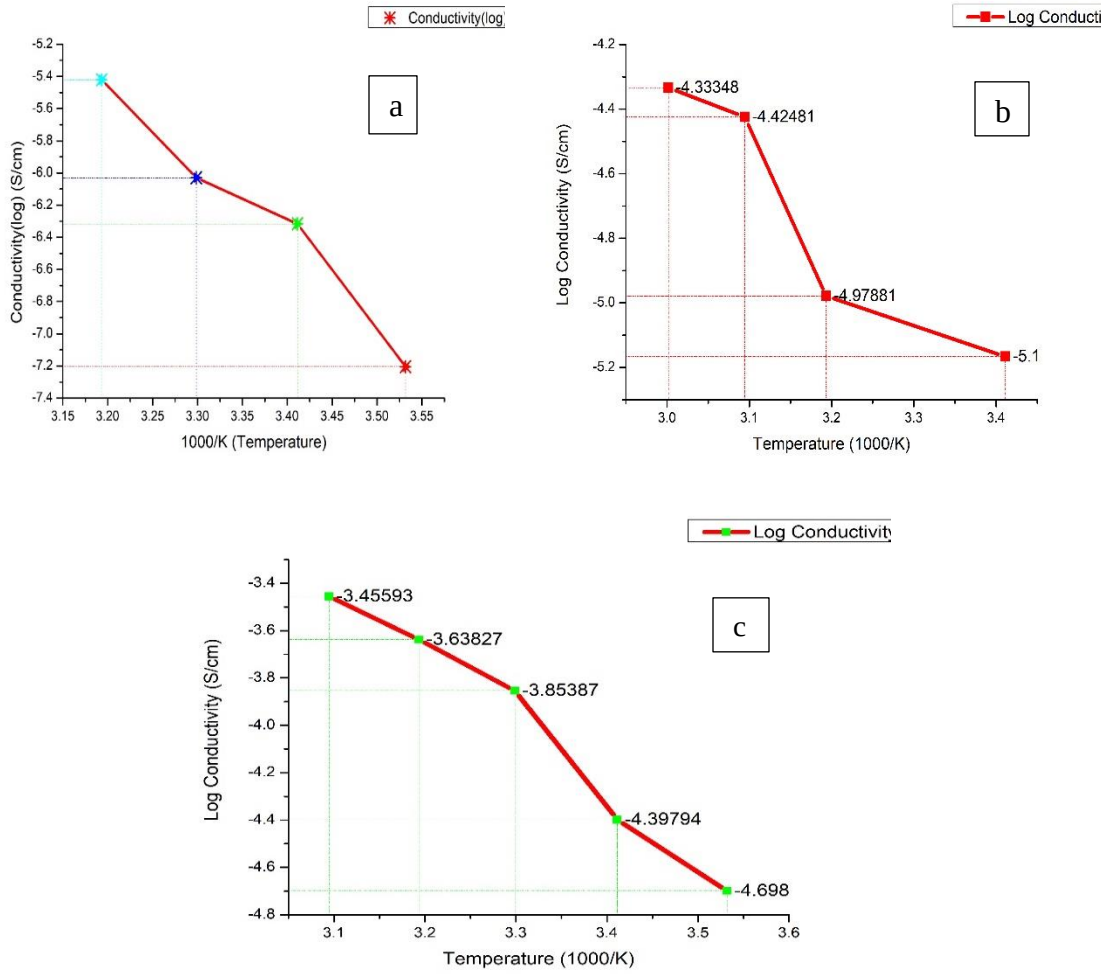

Figure 4.13: Conductivity change due to temperature variation (a) PEMA+KI (b) PEMA+KI+EC (c) PEMA+KI+EC+CNT.

At a certain temperature, polymeric segments rise due to the polymer electrolyte's capacity for vibration. At this temperature, additional energy is needed to compact nearby atoms and make a tiny gap around their volume, which enables vibrational motion.

However, the increased ion mobility brought on by this free volume enhances conductivity

and polymer segments. Similar results are found in the quantity and composites of other polymers.

$$\sigma = \sigma_0 \frac{-E_a}{kT}$$

T is the absolute temperature, k is the Boltzmann constant, and σ_0 is the activation energy., where the proportionality constant is σ.

At a certain temperature, polymeric segments rise due to the polymer electrolyte's capacity for vibration. At this temperature, additional energy is needed to compact nearby atoms and make a tiny gap around their volume, which enables vibrational motion.

The above relationship predicts that log σ and 1000/T have a linear relationship. Multiple curvatures are present at temperatures ranging from 20 to 90 ^{o}C, as shown in Figure 4.13.

4.11. Preparation of DSSC Solar Cell

The required electrodes for the DSSC cell preparation were prepared on 30x30 cm^2 of FTO glass, then cut into pieces having dimensions 2x1.5 cm^2.

DSSB solar cells consist of two electrodes.

1. Blocking Electrode or Working Electrode
2. Counter Electrode

4.11.1 Materials used to prepare DSSC cell

The materials needed to prepare the working electrode, counter electrode, dye, and electrolyte are shown in table 4.7.

4.11.2. Steps to prepare DSSC Cell

Step1) Washing: Both glasses washed properly with acetone.

Step2) Conductivity Check: The conductivity of each surface of the FTO glass was measured using a multimeter, and the conductivity-containing surface was used to prepare the DSSC cell.

Step3) Scotch tape was pasted to the glass's conductivity-containing side, as seen in figure 4.14.

Table 4-7: Material used for preparation of DSSC.

S. No	Components	Material
1	Working Electrode	Titanium oxide (TiO_2)
2	Counter Electrode	Chloroplatinic acid (H_2PtCl_6)
3	Dye solution	N3 Ruthenium

Step 4) TiO2 Coating: TiO2 has previously been produced and applied as a coating on FTO glass. To create a consistent layer on FTO glass, a spin coating device is employed at 1200 rpm for a single minute.

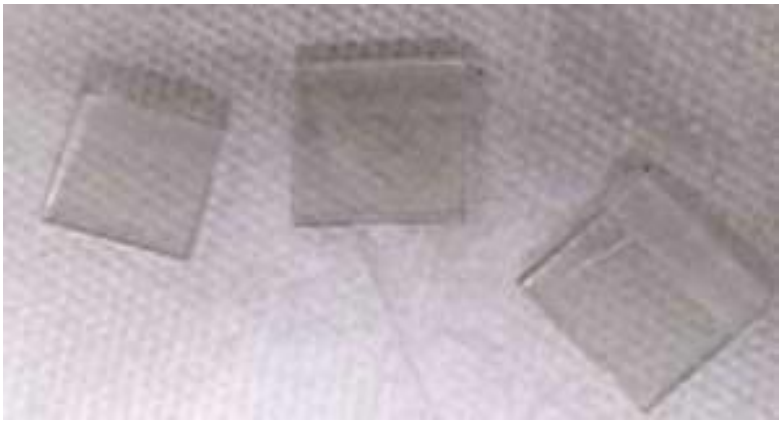

Figure 4.14: Scotch tape at FTO glasses.

Another name for this layer is the blocking layer. Once this is finished, take off the scotch tape. One kind of layer that was added to FTO glass is depicted in figure 4.15. The procedure for creating a counter layer with platinum material is the same. For thirty minutes, place the prepared electrode in a furnace set at 500 ^{o}C. Figure 4.15(a) depicts the TiO_2-coated working electrode and (b) the platinum-coated counter electrode.

Step 5) Doctor blade method: A 50 µm layer was formed on working electrode by pasting a doble scotch tape on it. As seen in figure 4.16, a consistent layer of titania paste was formed on the working electrode using the doctor blade approach. Now, for 30 minutes,

the prepared electrode placed into a furnace at 500 ºC temperature. Figure 4.16 illustrates the entire procedure.

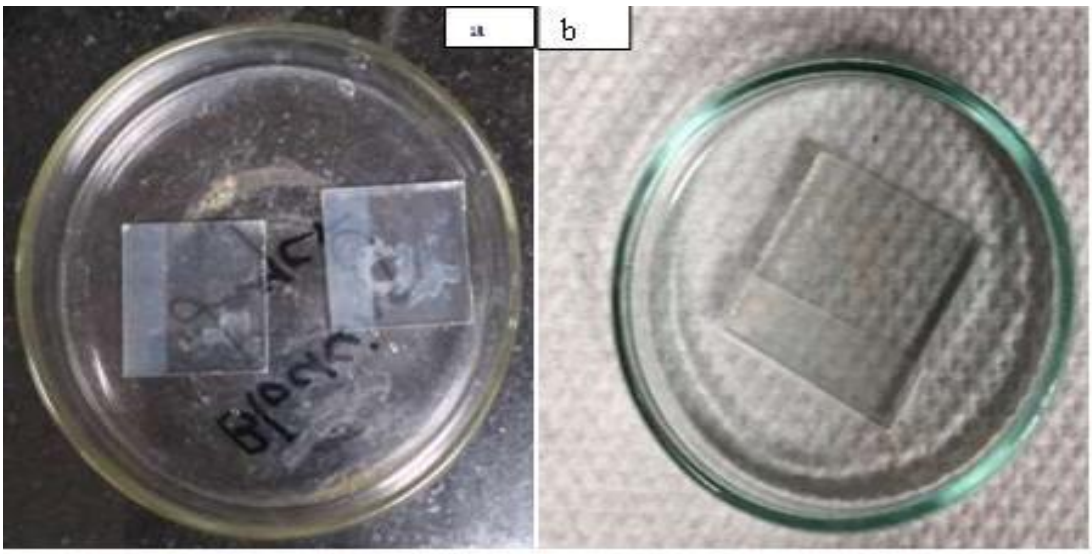

Figure 4.15: (a) TiO_2, (b) Platinum Coating on FTO glasses

Step 6) Dye Sensitization: As seen in figure 4.17, the prepared working electrode was now dipped in silicon paste and left for six hours.

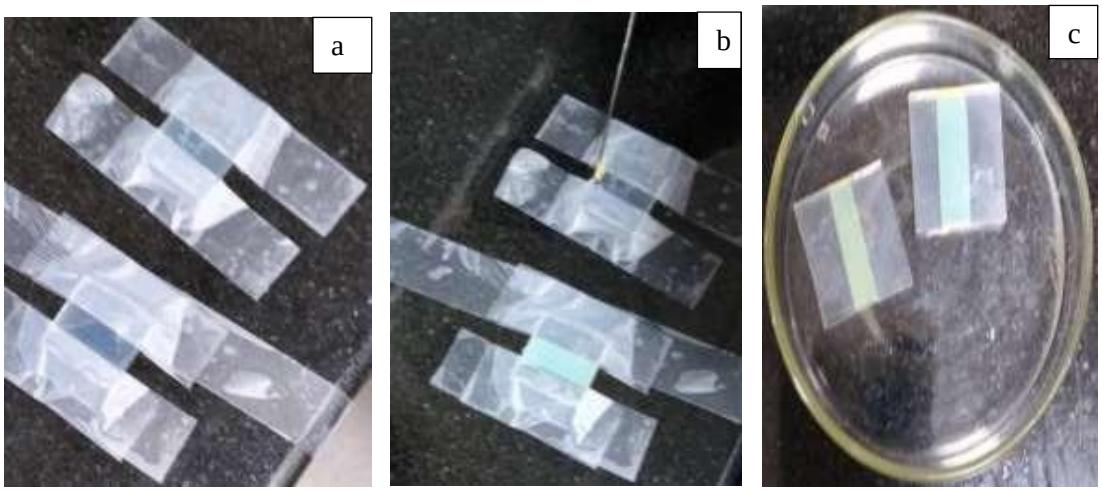

Figure 4.16: (a) Double tapping (b) Apply Titania paste (c) Result after doctor blade method.

Step 7) Polymer Electrolyte layer: Following the process of dye sensitization, polymer electrolyte was added to the dye layer and coupled together using paper clips, resulting in

the final construct DSSC cell depicted in figure 4.18.

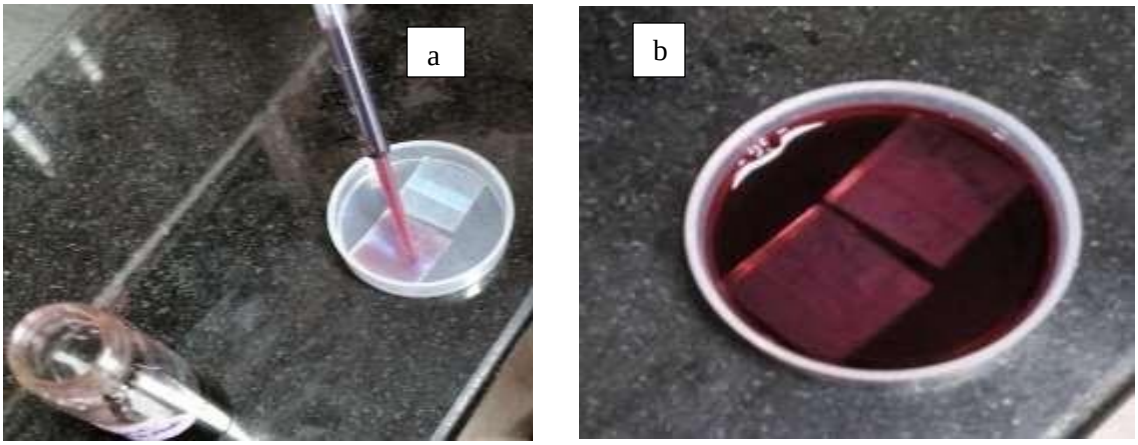

Figure 4.17: (a) Apply dye material (b) doping into dye material.

4.12. V-I characteristics of DSSC Solar Cell

Keysight and a solar simulator were used to measure the I-V characteristics of the dye-sensitized solar cell under a sun 1 condition. For developing redox couple, iodine have added in PEMA+40%KI+60% EC +9% CNT matrix with maximum ionic conducting value. Then polymer electrolyte applied between the already prepared electrode. After 72 hours the performance of DSSC was calculated using the following equations and table 4.4 shows the result.

Figure 4.18: Assembled DSSC Model

$$FF = \frac{V_{max}}{V_{OC}}\frac{I_{max}}{I_{SC}} = \frac{1.93 * 0.56}{1.94 * 0.69} = 81.12$$

$$\eta = FF\frac{V_{OC}J_{sc}}{P_{in}} = \frac{81.12 * 0.69 * 3.88}{100} = 2.26$$

FF stands for fill factor, η photon to electricity conversion efficiency, V_{oc} is open circuit voltage(V), V_{max} & J_{max} (mA/cm^2) are current and voltage in the J-V curve respectively at the point of maximum power output, J_{sc} is the short circuit current density (mAcm^{-2}). Observed parameters are shown in table 4.8. I-V characteristics (photocurrent density – voltage) are shown in figure 4.19.

Table 4-8: Observation parameters of DSSC sample

S. No	J_{SC}(mA/cm^2)	V_{OC}(V)	Fill Factor	Efficiency (%)
1	3.879308	0.688721	81.12	2.26

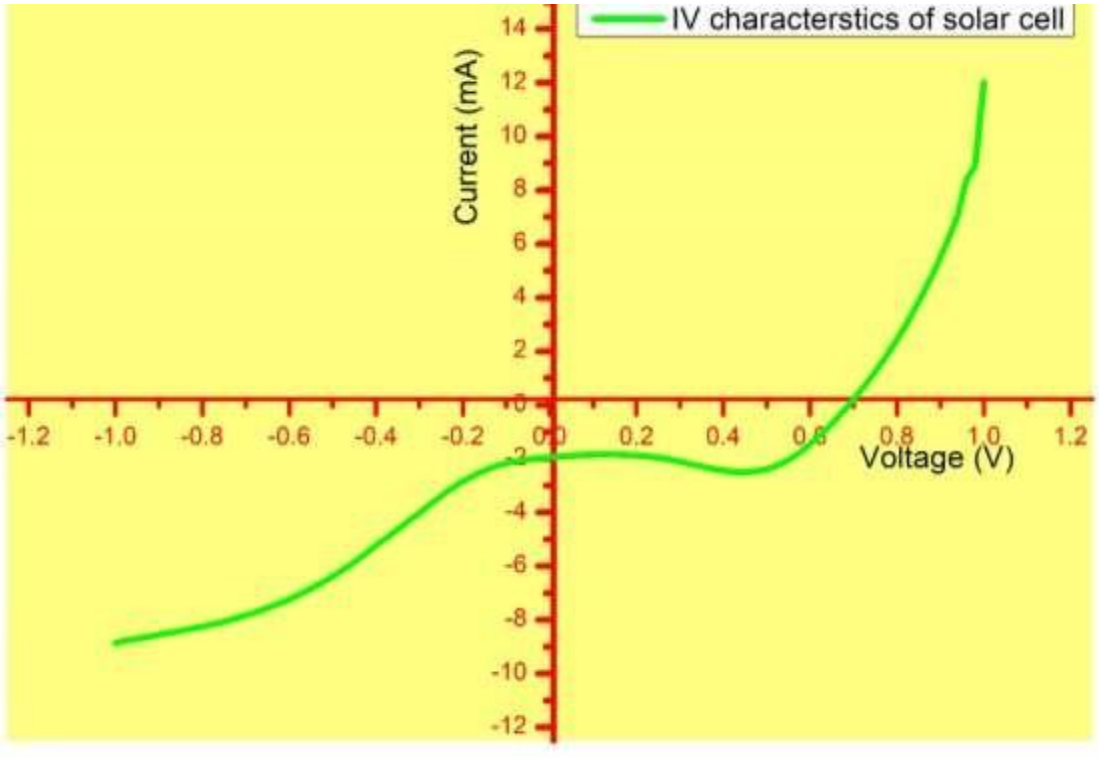

Figure 4.19: I-V characteristics of DSSC solar cell.

4.13. Validation of Result

Obtained result are compared with previous research paper as shown in table 4.9. Fill factor and efficiency of proposed solar cell is compared with previous research publication.

Table 4-9: Comparison with previous research

S.No	V_{oc}(mV)	J_{sc}(mA/cm^2)	FF	η	References
1	660	7.85	66	3.44	[125]
2	591	6.84	56	2.28	[145]
3	720	1.69	35	0.44	[128]
4	670	7.9	65	3.4	[146]
5	524	1.46	26	1.98	[134]
6	148.6	2.98	55.8	0.24	[133]
7	680	11.35	47	3.62	[147]
8	688	3.897	81.12	2.26	Obtained result

In some research paper our result is more effective and optimised. The material used to prepared solar cell also play very important role to enchance the fill factor and efficiency of solar cell [117] that is dicscussed in literature review in table 2.4. In previous research paper the fill factor and efficiency is more than our proposed solar cell. Silicon based solar cell has highest efficiency but the cost of Silicon material is very high. As compared to other research, proposed new material that contain polymer PEMA i.e. plastic form that has semicrystalline struture, high conductivity,high mechnical strength, flexible for packing design, low cost, light weight, no leakage and long life. In this research work Postium iodide used as a salt that is more stable than litium salt because it is not expose in air and environment. Again mechnical strength and amorphicity incresed using EC plastizier.

Conclusion

Polymer Electrolyte composite of PEMA (polyethyl methacrylate) and potassium iodide (KI) was prepared using solution casting technique and obtained maximum conducting sample of PEMA+ 40% wt. percentage of KI having conductivity 3.80 x 10^{-6} S/cm. Further, amorphicity enhancement by adding ethylene carbonate (EC) as plasticizer. The maximum conducting sample was obtained at ratio PEMA+40% wt. percentage + 60% wt. percentage of EC having conductivity 4.65 x 10^{-5} S/cm. Further enhancement of the conductivity of sample by incorporation of carbon nanotubes. At 9% wt. percentage of CNT, polymer composite got maximum conductive sample having conductivity 3.5x10^{-4} S/cm. The maximum conductive sample was characterized using Scanning electron microscopy (SEM), X-ray diffraction (XRD), Complex impedance spectroscopy (CIS), Fourier transform infrared spectroscopy (FTIR). X-Ray diffraction characterization technique was used to identify maximum conducting sample crystalline or amorphous nature. FTIR characterization technique was used to indicate change in interaction between various materials such as KI, EC and CNT. After that the maximum conductivity polymer sample PEMA+40% KI+ 60% EC+ 9% CNT was obtained having conductivity 3.5x10^{-4} S/cm using solution casting technique. Using Doctor Blade Method Dye-Sensitized solar cell was prepared and tested using Keysight instrument and solar simulator at 1 sun condition. Fill factor 81.12 and energy conversion efficiency 2.26% was obtained. The obtained result was compared with the previously reported result. Silicon based solar cells have maximum efficiency and better fill factor. Proposed new material that contain polymer PEMA i.e. plastic form that has semicrystalline struture, high conductivity,high mechnical strength, flexible for packing design, low cost, light weight, no leakage and long life. In this research work Postium iodide as a salt was used that is more stable than litium salt because it is not expose in air and environment. Again mechnical strength and amorphicity incresed using EC plastizier. By enhancing the materials for preparing working electrode, counter electrode, dye further efficiency of DSSCs can be increased.

Future Aspects

Further research should focus on finding optimal parameters to slow down dye degradation and improve dye stability. Exploring the use of new dye structures that can absorb more light at longer wavelengths, particularly in the near-infrared (NIR) region, can enhance dye stability and overall performance. Investigating the chemical stability of oxidized Ru (III) complexes, such as Ru bipyridyl complexes, can contribute to improved dye stability. Developing new dye sensitizers with good absorption properties, long excited-state lifetimes, and efficient metal-to-ligand charge transfer can enhance dye stability. Conducting research on dye and electrolyte additives that can enhance the stability of dye-sensitized solar cells can also contribute to improved dye stability. Improving dye stability and structure to enhance light absorption at longer wavelengths and increase overall efficiency. By enhancing the morphology of semiconductors to improve electronic conduction and reduce dark current. Exploring the use of dye and electrolyte additives to enhance cell performance. Improving the mechanical contact between the two electrodes to optimize cell efficiency. Investigating new materials for the semiconductor oxide, dye sensitizer, and counter electrode to further enhance DSSC performance. Addressing the challenges of low conversion efficiency and stability through research and development.

Exploring the potential of solid-state DSSCs using hole transport materials or solid-state electrolytes. Continuously monitoring and improving the stability and reliability of DSSCs to ensure long-term performance. Further to reduce the cost of materials used instead of platinum for preparing counter electrode researcher can also use carbon material. Carbon materials can be prepared from biowaste and kitchen waste.

Publication

1. Singh, P., Bhargava, C., Kumar, M., Maturia, A. S., Singh, P. K., Sharma, P. K., & Sachdeva, A. "Extraction and comparative study of green energy using different types of biowaste material." *Materials Today: Proceedings* 49 (2022): 3474-3481.
2. Singh, Palvinder, Amit Sachdeva, and Cherry Bhargava. "Polymer Electrolyte a Novel Material for Electrochemical Devices: A Review." *Journal of Physics: Conference Series*. Vol. 2327. No. 1. IOP Publishing, 2022.
3. Singh, P., Sachdeva, A., Bhargava, C., Alheety, M. A., & Sharma, J. "Electrical and Structural Properties of PEMA-Based Plasticized Polymer Electrolyte." *Macromolecular Symposia*. Vol. 407. No. 1. 2023.
4. Singh, P., Sachdeva, A., Bhargava, C., & Kakroo, S. "Effect of TiO_2 Nanoparticle on PEMA-Based Solid Polymer Electrolyte." *Macromolecular Symposia*. Vol. 407. No. 1. 2023.
5. Singh, Palvinder, and Amit Sachdeva. "DSSC Fundamentals and Optimization Materials: A Review." *IOP Conference Series: Earth and Environmental Science*. Vol. 1285. No. 1. IOP Publishing, 2024.
6. Sachdeva, S., Sindhwani, M., Kaur, R., Singh, P., & Sachdeva, A."A 500 km Long Transmission with Coherent Optical OFDM Using Dual Polarization Quadrature Phase Shift Keying (QPSK) and Double Sideband Suppressed-Enhanced Carrier (DSS-EC)." *Macromolecular Symposia*. Vol. 407. No. 1. 2023.
7. Venkatesh, P. S. S., Singh, P., Sachdeva, A., Kumar, R., & Rawal, S "Smart Irrigation System Uses IoT and Blynk App." *Macromolecular Symposia*. Vol. 407. No. 1. 2023.

Copyright:

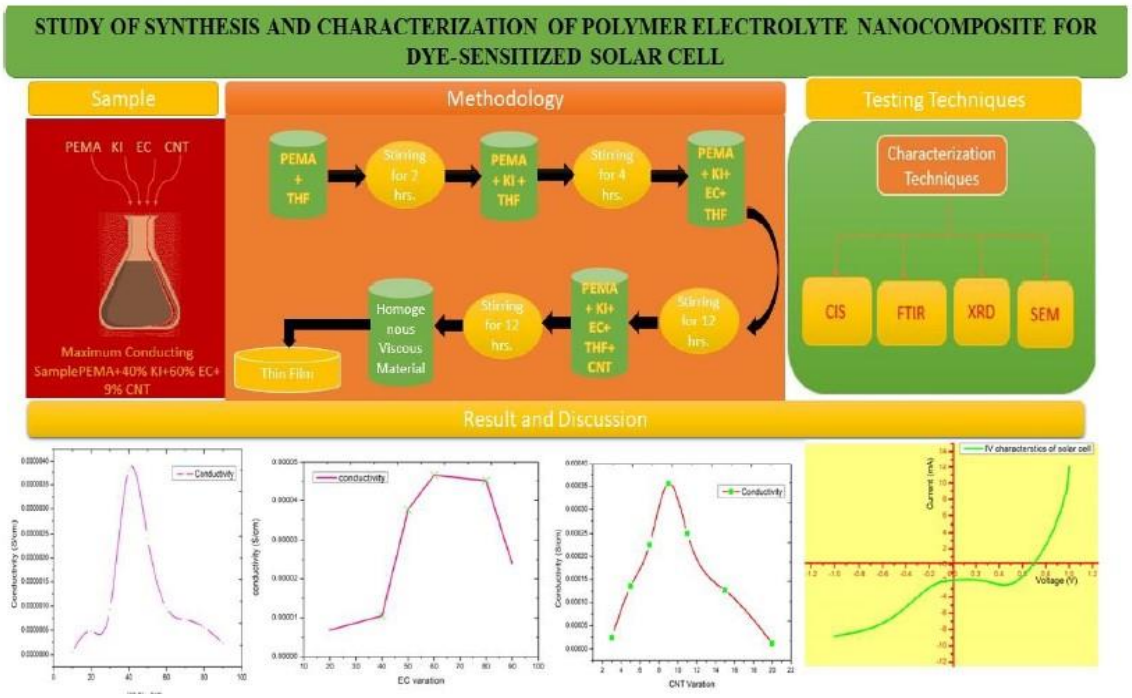

INTELLECTUAL PROPERTY INDIA
PATENTS | DESIGNS | TRADEMARKS | GEOGRAPHICAL INDICATIONS

सत्यमेव जयते

Extracts from the Register of Copyrights

प्रतिलिप्यधिकार कार्यालय, भारत सरकार | Copyright Office, Government Of India

दिनांक/Dated:19/01/2024

1.	पंजीकरण संख्या/Registration Number	:	**L-141806/2024**
2.	आवेदक का नाम, पता तथा राष्ट्रीयता Name, address and nationality of the applicant	:	LOVELY PROFESSIONAL UNIVERSITY , LOVELY PROFESSIONAL UNIVERSITY, JALANDHAR, DELHI-GT ROAD, PHAGWARA PUNJAB-144411 INDIAN
3.	कृति के प्रतिलिप्यधिकार में आवेदक के हित की प्रकृति Nature of the applicant's interest in the copyright of the work	:	OWNER
4.	कृति का वर्ग और वर्णन Class and description of the work	:	LITERARY/ DRAMATIC WORK THE GRAPHICAL ABSTRACT PRESENT THE POLYMER ELECTROLYTE NANOCOMPOSITE FOR DYE SENSITIZED SOLAR CELL.
5.	कृति का शीर्षक Title of the work	:	POLYMER ELECTROLYTE NANOCOMPOSITE FOR DYE SENSITIZED SOLAR CELL.
6.	कृति की भाषा Language of the work	:	ENGLISH
7.	रचयिता का नाम, पता और राष्ट्रीयता तथा यदि रचयिता की मृत्यु हो गई है, तो मृत्यु की तिथि Name, address and nationality of the author and if the author is deceased, date of his decease	:	PALVINDER SINGH , LOVELY PROFESSIONAL UNIVERSITY, JALANDHAR, DELHI-GT ROAD, PHAGWARA PUNJAB-144411 INDIAN DR. AMIT SACHDEVA , LOVELY PROFESSIONAL UNIVERSITY, JALANDHAR, DELHI-GT ROAD, PHAGWARA PUNJAB-144411 INDIAN

REFERENCES

[1] Manthiram, Arumugam, Xingwen Yu, and Shaofei Wang. “Lithium battery chemistries enabled by solid-state electrolytes | Nature Reviews Materials.” Accessed: Sep. 08, 2022. [Online]. Available: https://www.nature.com/articles/natrevmats2016103

[2] K. S. Ngai, S. Ramesh, K. Ramesh, and J. C. Juan, “A review of polymer electrolytes: fundamental, approaches and applications,” *Ionics*, vol. 22, no. 8, pp. 1259–1279, Aug. 2016, doi: 10.1007/s11581-016-1756-4.

[3] B.-S. Cho, J. Choi, and K.-Y. Kim, “Preparation and properties of solid polymer electrolyte based on imidazolium-based ionic liquids for structural capacitors,” *Fibers and Polymers*, vol. 18, no. 8, pp. 1452–1458, 2017.

[4] W. Li, Y. Pang, J. Liu, G. Liu, Y. Wang, and Y. Xia, “A PEO-based gel polymer electrolyte for lithium ion batteries,” *RSC advances*, vol. 7, no. 38, pp. 23494–23501, 2017.

[5] F. M. Gray, *Polymer electrolytes*. Royal Society of Chemistry, 1997.

[6] B. Scrosati and C. A. Vincent, “Polymer electrolytes: the key to lithium polymer batteries,” *Mrs Bulletin*, vol. 25, no. 3, pp. 28–30, 2000.

[7] P. R. Chinnam and S. L. Wunder, “Engineered interfaces in hybrid ceramic–polymer electrolytes for use in all-solid-state Li batteries,” *ACS Energy Letters*, vol. 2, no. 1, pp. 134–138, 2017.

[8] L. Sarojiniamma, “Investigations on the conductivity of organotin-doped polyethyleneoxide polymer system,” PhD Thesis, University of Malaya., 2000.

[9] Y. Zhong *et al.*, “Ultrahigh Li-ion conductive single-ion polymer electrolyte containing fluorinated polysulfonamide for quasi-solid-state Li-ion batteries,” *Journal of Materials Chemistry A*, vol. 7, no. 42, pp. 24251–24261, 2019.

[10] J.-W. Choi *et al.*, “Poly(ethylene oxide)-based polymer electrolyte incorporating room-temperature ionic liquid for lithium batteries,” *Solid State Ionics*, vol. 178, no. 19, pp. 1235–1241, Jul. 2007, doi: 10.1016/j.ssi.2007.06.006.

[11] G. Jiang, S. Maeda, H. Yang, Y. Saito, S. Tanase, and T. Sakai, “All solid-state lithium-polymer battery using poly (urethane acrylate)/nano-SiO2 composite electrolytes,” *Journal of power sources*, vol. 141, no. 1, pp. 143–148, 2005.

[12] W. Liu *et al.*, “Ionic conductivity enhancement of polymer electrolytes with ceramic nanowire fillers,” *Nano letters*, vol. 15, no. 4, pp. 2740–2745, 2015.

[13] B. Kurc and T. Jesionowski, “Modified TiO 2-SiO 2 ceramic filler for a composite gel polymer electrolytes working with LiMn 2 O 4,” *Journal of Solid State Electrochemistry*, vol. 19, pp. 1427–1435, 2015.

[14] Y.-T. Kim and E. S. Smotkin, “The effect of plasticizers on transport and electrochemical properties of PEO-based electrolytes for lithium rechargeable batteries,” *Solid State Ionics*, vol. 149, no. 1–2, pp. 29–37, 2002.

[15] S. M. Tan and M. R. Johan, “Effects of MnO 2 nano-particles on the conductivity of PMMA-PEO-LiClO 4-EC polymer electrolytes,” *Ionics*, vol. 17, pp. 485–490, 2011.

[16] W. Kam, C.-W. Liew, J. Y. Lim, and S. Ramesh, “Electrical, structural, and thermal studies of antimony trioxide-doped poly(acrylic acid)-based composite polymer electrolytes,” *Ionics*, vol. 20, no. 5, pp. 665–674, May 2014, doi: 10.1007/s11581-013-1012-0.

[17] Y. W. Chen-Yang, H. C. Chen, F. J. Lin, and C. C. Chen, “Polyacrylonitrile electrolytes: 1. A novel high-conductivity composite polymer electrolyte based on PAN, LiClO4 and α-Al2O3,” *Solid State Ionics*, vol. 150, no. 3, pp. 327–335, Oct. 2002, doi: 10.1016/S0167-2738(02)00457-5.

[18] Itoh, Takahito, et al. “Composite polymer electrolytes based on poly(ethylene oxide), hyperbranched polymer, BaTiO3 and LiN(CF3SO2)2 - ScienceDirect.” Accessed: Aug. 10, 2020. [Online]. Available: https://www.sciencedirect.com/science/article/abs/pii/S0167273802006823

[19] S. Rajendran, O. Mahendran, and R. Kannan, “Ionic conductivity studies in composite solid polymer electrolytes based on methylmethacrylate,” *Journal of Physics and Chemistry of Solids*, vol. 63, no. 2, pp. 303–307, Feb. 2002, doi: 10.1016/S0022-3697(01)00144-5.

[20] M.-K. Song, Y.-T. Kim, J.-Y. Cho, B. W. Cho, B. N. Popov, and H.-W. Rhee, “Composite polymer electrolytes reinforced by non-woven fabrics,” *Journal of Power*

Sources, vol. 125, no. 1, pp. 10–16, Jan. 2004, doi: 10.1016/S0378-7753(03)00826-7.

[21] J.-K. Kim, G. Cheruvally, X. Li, J.-H. Ahn, K.-W. Kim, and H.-J. Ahn, "Preparation and electrochemical characterization of electrospun, microporous membrane-based composite polymer electrolytes for lithium batteries," *Journal of Power Sources*, vol. 178, no. 2, pp. 815–820, Apr. 2008, doi: 10.1016/j.jpowsour.2007.08.063.

[22] S. Ramesh, T. S. Yin, and C.-W. Liew, "Effect of dibutyl phthalate as plasticizer on high-molecular weight poly(vinyl chloride)–lithium tetraborate-based solid polymer electrolytes," *Ionics*, vol. 17, no. 8, pp. 705–713, Nov. 2011, doi: 10.1007/s11581-011-0568-9.

[23] C.-C. Yang and S.-J. Lin, "Alkaline composite PEO–PVA–glass-fibre-mat polymer electrolyte for Zn–air battery," *Journal of Power Sources*, vol. 112, no. 2, pp. 497–503, Nov. 2002, doi: 10.1016/S0378-7753(02)00438-X.

[24] H. Wang, H. Huang, and S. L. Wunder, "Novel microporous poly (vinylidene fluoride) blend electrolytes for lithium-ion batteries," *Journal of the Electrochemical Society*, vol. 147, no. 8, p. 2853, 2000.

[25] M. Yanilmaz and X. Zhang, "Polymethylmethacrylate/polyacrylonitrile membranes via centrifugal spinning as separator in Li-ion batteries," *Polymers*, vol. 7, no. 4, pp. 629–643, 2015.

[26] M. Rao, X. Geng, Y. Liao, S. Hu, and W. Li, "Preparation and performance of gel polymer electrolyte based on electrospun polymer membrane and ionic liquid for lithium ion battery," *Journal of Membrane Science*, vol. 399–400, pp. 37–42, May 2012, doi: 10.1016/j.memsci.2012.01.021.

[27] K.-H. Lee, K.-H. Kim, and H. S. Lim, "Studies on a new series of cross-linked polymer electrolytes for a lithium secondary battery," *Journal of The Electrochemical Society*, vol. 148, no. 10, p. A1148, 2001.

[28] H. Zhang, X. Ma, C. Lin, and B. Zhu, "Gel polymer electrolyte-based on PVDF/fluorinated amphiphilic copolymer blends for high performance lithium-ion batteries," *RSC Adv.*, vol. 4, no. 64, pp. 33713–33719, Aug. 2014, doi: 10.1039/C4RA04443F.

[29] Z. Wen, T. Itoh, T. Uno, M. Kubo, and O. Yamamoto, “Thermal, electrical, and mechanical properties of composite polymer electrolytes based on cross-linked poly (ethylene oxide-co-propylene oxide) and ceramic filler,” *Solid State Ionics*, vol. 160, no. 1–2, pp. 141–148, 2003.

[30] C. Capiglia, J. Yang, N. Imanishi, A. Hirano, Y. Takeda, and O. Yamamoto, “Composite polymer electrolyte: the role of filler grain size,” *Solid State Ionics*, vol. 154, pp. 7–14, 2002.

[31] S. Ibrahim, S. M. M. Yasin, N. M. Nee, R. Ahmad, and M. R. Johan, “Conductivity, thermal and infrared studies on plasticized polymer electrolytes with carbon nanotubes as filler,” *Journal of Non-Crystalline Solids*, vol. 358, no. 2, pp. 210–216, Jan. 2012, doi: 10.1016/j.jnoncrysol.2011.09.015.

[32] Q. Xu and G. Wan, “Rechargeable Li/LiMn2O4 batteries with a polymeric solid electrolyte,” *Journal of power sources*, vol. 41, no. 3, pp. 315–320, 1993.

[33] E. Quartarone, P. Mustarelli, and A. Magistris, “PEO-based composite polymer electrolytes,” *Solid State Ionics*, vol. 110, no. 1, pp. 1–14, Jul. 1998, doi: 10.1016/S0167-2738(98)00114-3.

[34] C. Capiglia, P. Mustarelli, E. Quartarone, C. Tomasi, and A. Magistris, “Effects of nanoscale SiO2 on the thermal and transport properties of solvent-free, poly (ethylene oxide)(PEO)-based polymer electrolytes,” *Solid state ionics*, vol. 118, no. 1–2, pp. 73–79, 1999.

[35] H. Pitawala, M. Dissanayake, and V. A. Seneviratne, “Combined effect of Al2O3 nano-fillers and EC plasticizer on ionic conductivity enhancement in the solid polymer electrolyte (PEO) 9LiTf,” *Solid State Ionics*, vol. 178, no. 13–14, pp. 885–888, 2007.

[36] P. Zhang, L. C. Yang, L. L. Li, M. L. Ding, Y. P. Wu, and R. Holze, “Enhanced electrochemical and mechanical properties of P (VDF-HFP)-based composite polymer electrolytes with SiO2 nanowires,” *Journal of membrane science*, vol. 379, no. 1–2, pp. 80–85, 2011.

[37] Y. Wu, *Lithium-ion batteries: Fundamentals and Applications*, vol. 4. CRC press,

2015.

[38] M. S. Wilson and S. Gottesfeld, “Thin-film catalyst layers for polymer electrolyte fuel cell electrodes,” *Journal of applied electrochemistry*, vol. 22, no. 1, pp. 1–7, 1992.

[39] M. E. Becquerel, “Mémoire sur les effets électriques produits sous l’influence des rayons solaires,” *Comptes rendus hebdomadaires des séances de l’Académie des sciences*, vol. 9, pp. 561–567, 1839.

[40] B. O’Regan and M. Grätzel, “A low-cost, high-efficiency solar cell based on dye-sensitized colloidal TiO2 films,” *Nature*, vol. 353, no. 6346, pp. 737–740, Oct. 1991, doi: 10.1038/353737a0.

[41] J. Halme, “Dye-sensitized nanostructured and organic photovoltaic cells: technical review and preliminary tests,” 2002.

[42] M. Grätzel, “The advent of mesoscopic injection solar cells,” *Progress in Photovoltaics: Research and Applications*, vol. 14, no. 5, pp. 429–442, 2006.

[43] M. Grätzel, “Solar energy conversion by dye-sensitized photovoltaic cells,” *Inorganic chemistry*, vol. 44, no. 20, pp. 6841–6851, 2005.

[44] D. Cahen, G. Hodes, M. Graetzel, J. F. Guillemoles, and I. Riess, “Nature of photovoltaic action in dye-sensitized solar cells,” *The Journal of Physical Chemistry B*, vol. 104, no. 9, pp. 2053–2059, 2000.

[45] J. H. Kim, M.-S. Kang, Y. J. Kim, J. Won, and Y. S. Kang, “Poly (butyl acrylate)/NaI/I2 electrolytes for dye-sensitized nanocrystalline TiO2 solar cells,” *Solid State Ionics*, vol. 176, no. 5–6, pp. 579–584, 2005.

[46] M. S. Akhtar, J.-G. Park, H.-C. Lee, S.-K. Lee, and O.-B. Yang, “Carbon nanotubes–polyethylene oxide composite electrolyte for solid-state dye-sensitized solar cells,” *Electrochimica Acta*, vol. 55, no. 7, pp. 2418–2423, 2010.

[47] A. F. Nogueira, J. R. Durrant, and M. A. De Paoli, “Dye-sensitized nanocrystalline solar cells employing a polymer electrolyte,” *Advanced Materials*, vol. 13, no. 11, pp. 826–830, 2001.

[48] D. Matthews, P. Infelta, and M. Grätzel, “Calculation of the photocurrent-potential characteristic for regenerative, sensitized semiconductor electrodes,” *Solar Energy*

Materials and Solar Cells, vol. 44, no. 2, pp. 119–155, 1996.

[49] Tarascon, J-M., and Michel Armand. "Issues and challenges facing rechargeable lithium batteries | Materials for Sustainable Energy." Accessed: Sep. 05, 2021. [Online]. Available: https://www.worldscientific.com/doi/abs/10.1142/9789814317665_0024

[50] S. Rajendran, M. R. Prabhu, and M. U. Rani, "Li ion conduction behavior of hybrid polymer electrolytes based on PEMA," *Journal of applied polymer science*, vol. 110, no. 5, pp. 2802–2806, 2008.

[51] T. K. Kwei, G. D. Patterson, and T. T. Wang, "Compatibility in Mixtures of Poly (vinylidene fluoride) and Poly (ethyl methacrylate," *Macromolecules*, vol. 9, no. 5, pp. 780–784, 1976.

[52] H.-S. Han, H.-R. Kang, S.-W. Kim, and H.-T. Kim, "Phase-separated polymer electrolyte based on poly(vinyl chloride)/poly(ethyl methacrylate) blend," *Journal of Power Sources*, vol. 112, no. 2, pp. 461–468, Nov. 2002, doi: 10.1016/S0378-7753(02)00436-6.

[53] T. Fahmy and M. T. Ahmed, "Thermal induced structural change investigations in PVC/PEMA polymer blend," *Polymer testing*, vol. 20, no. 5, pp. 477–484, 2001.

[54] P. Pradeepa, S. Edwinraj, and M. R. Prabhu, "Effects of ceramic filler in poly (vinyl chloride)/poly (ethyl methacrylate) based polymer blend electrolytes," *Chinese Chemical Letters*, vol. 26, no. 9, pp. 1191–1196, 2015.

[55] I. Nicotera, L. Coppola, C. Oliviero, M. Castriota, and E. Cazzanelli, "Investigation of ionic conduction and mechanical properties of PMMA–PVdF blend-based polymer electrolytes☆," *Solid State Ionics*, vol. 177, no. 5–6, pp. 581–588, Feb. 2006, doi: 10.1016/j.ssi.2005.12.028.

[56] Q. Xiao, X. Wang, W. Li, Z. Li, T. Zhang, and H. Zhang, "Macroporous polymer electrolytes based on PVDF/PEO-b-PMMA block copolymer blends for rechargeable lithium ion battery," *Journal of Membrane Science*, vol. 334, no. 1–2, pp. 117–122, 2009.

[57] C.-W. Kuo, W.-B. Li, P.-R. Chen, J.-W. Liao, C.-G. Tseng, and T.-Y. Wu, "Effect of Plasticizer and Lithium Salt Concentration in PMMA- based Composite Polymer

Electrolytes," *Int. J. Electrochem. Sci.*, vol. 8, p. 7, 2013.

[58] A. M. Stephan *et al.*, "A study on polymer blend electrolyte based on PVC/PMMA with lithium salt," *Journal of power sources*, vol. 81, pp. 752–758, 1999.

[59] M. A. Gebreyesus, Y. Purushotham, and J. S. Kumar, "Preparation and characterization of lithium ion conducting polymer electrolytes based on a blend of poly (vinylidene fluoride-co-hexafluoropropylene) and poly (methyl methacrylate)," *Heliyon*, vol. 2, no. 7, p. e00134, 2016.

[60] S. K. Chaurasia, R. K. Singh, and S. Chandra, "Thermal stability, complexing behavior, and ionic transport of polymeric gel membranes based on polymer PVdF-HFP and ionic liquid,[BMIM][BF4]," *The Journal of Physical Chemistry B*, vol. 117, no. 3, pp. 897–906, 2013.

[61] A. L. Saroj and R. K. Singh, "Thermal, dielectric and conductivity studies on PVA/Ionic liquid [EMIM][EtSO4] based polymer electrolytes," *Journal of Physics and Chemistry of Solids*, vol. 73, no. 2, pp. 162–168, Feb. 2012, doi: 10.1016/j.jpcs.2011.11.012.

[62] A. K. Nath and A. Kumar, "Scaling of AC conductivity, electrochemical and thermal properties of ionic liquid based polymer nanocomposite electrolytes," *Electrochimica Acta*, vol. 129, pp. 177–186, May 2014, doi: 10.1016/j.electacta.2014.02.101.

[63] N. K. Anuar, R. H. Y. Subban, and N. S. Mohamed, "Properties of PEMA-NH4CF3SO3 Added to BMATSFI Ionic Liquid," *Materials*, vol. 5, no. 12, Art. no. 12, Dec. 2012, doi: 10.3390/ma5122609.

[64] Y. Kumar, S. A. Hashmi, and G. P. Pandey, "Lithium ion transport and ion–polymer interaction in PEO based polymer electrolyte plasticized with ionic liquid," *Solid State Ionics*, vol. 201, no. 1, pp. 73–80, Oct. 2011, doi: 10.1016/j.ssi.2011.08.010.

[65] C.-W. Liew, S. Ramesh, and A. K. Arof, "Good prospect of ionic liquid based-poly(vinyl alcohol) polymer electrolytes for supercapacitors with excellent electrical, electrochemical and thermal properties," *International Journal of Hydrogen Energy*, vol. 39, no. 6, pp. 2953–2963, Feb. 2014, doi: 10.1016/j.ijhydene.2013.06.061.

[66] X. Zhang *et al.*, “A Flexible Ionic Liquid Gelled PVA-Li2SO4 Polymer Electrolyte for Semi-Solid-State Supercapacitors,” *Advanced Materials Interfaces*, vol. 2, no. 15, p. 1500267, 2015, doi: 10.1002/admi.201500267.

[67] C. Zhu, H. Cheng, and Y. Yang, “Electrochemical Characterization of Two Types of PEO-Based Polymer Electrolytes with Room-Temperature Ionic Liquids,” *J. Electrochem. Soc.*, vol. 155, no. 8, p. A569, Jun. 2008, doi: 10.1149/1.2931523.

[68] S. K. Chaurasia, R. K. Singh, and S. Chandra, “Structural and transport studies on polymeric membranes of PEO containing ionic liquid, EMIM-TY: Evidence of complexation,” *Solid State Ionics*, vol. 183, no. 1, pp. 32–39, Feb. 2011, doi: 10.1016/j.ssi.2010.12.008.

[69] Chaurasia, Sujeet K., Rajendra K. Singh, and S. Chandra. “Dielectric relaxation and conductivity studies on (PEO:LiClO4) polymer electrolyte with added ionic liquid [BMIM][PF6]: Evidence of ion–ion interaction - Chaurasia - 2011 - Journal of Polymer Science Part B: Polymer Physics - Wiley Online Library.” Accessed: Aug. 08, 2020. [Online]. Available: https://onlinelibrary.wiley.com/doi/abs/10.1002/polb.22182

[70] Chaurasia, Sujeet Kumar, and Rajendra Kumar Singh. “Electrical conductivity studies on composite polymer electrolyte based on ionic liquid: Phase Transitions: Vol 83, No 6.” Accessed: Aug. 08, 2020. [Online]. Available: https://www.tandfonline.com/doi/abs/10.1080/01411594.2010.491434

[71] G.-T. Kim, G. B. Appetecchi, F. Alessandrini, and S. Passerini, “Solvent-free, PYR1ATFSI ionic liquid-based ternary polymer electrolyte systems: I. Electrochemical characterization,” *Journal of Power Sources*, vol. 171, no. 2, pp. 861–869, Sep. 2007, doi: 10.1016/j.jpowsour.2007.07.020.

[72] Hellio, Dominique, and Madeleine Djabourov. “Physically and Chemically Crosslinked Gelatin Gel - Macromolecular Symposia - Wiley Online Library.” Accessed: Aug. 08, 2020. [Online]. Available: https://onlinelibrary.wiley.com /doi/abs/10.1002/masy.200650904

[73] S.-H. Wang, S.-S. Hou, P.-L. Kuo, and H. Teng, “Poly(ethylene oxide)-co-

Poly(propylene oxide)-Based Gel Electrolyte with High Ionic Conductivity and Mechanical Integrity for Lithium-Ion Batteries," *ACS Appl. Mater. Interfaces*, vol. 5, no. 17, pp. 8477–8485, Sep. 2013, doi: 10.1021/am4019115.

[74] Y. H. Liao *et al.*, "Self-supported poly(methyl methacrylate–acrylonitrile–vinyl acetate)-based gel electrolyte for lithium ion battery," *Journal of Power Sources*, vol. 189, no. 1, pp. 139–144, Apr. 2009, doi: 10.1016/j.jpowsour.2008.10.027.

[75] G. Girish Kumar and S. Sampath, "Electrochemical and spectroscopic investigations of a gel polymer electrolyte of poly(methylmethacrylate) and zinc triflate," *Solid State Ionics*, vol. 176, no. 7, pp. 773–780, Feb. 2005, doi: 10.1016/j.ssi.2004.11.007.

[76] P. Periasamy *et al.*, "Studies on PVdF-based gel polymer electrolytes," *Journal of Power Sources*, vol. 88, no. 2, pp. 269–273, Jun. 2000, doi: 10.1016/S0378-7753(99)00348-1.

[77] E. Quartarone, C. Tomasi, P. Mustarelli, G. B. Appetecchi, and F. Croce, "Long-term structural stability of PMMA-based gel polymer electrolytes," *Electrochimica Acta*, vol. 43, no. 10, pp. 1435–1439, Apr. 1998, doi: 10.1016/S0013-4686(97)10080-9.

[78] Y. Saito, C. Capiglia, H. Kataoka, H. Yamamoto, H. Ishikawa, and P. Mustarelli, "Conduction properties of PVDF-type polymer electrolytes with lithium salts, LiN(CF3SO2)2 and LiN(C2F5SO2)2," *Solid State Ionics*, vol. 136–137, pp. 1161–1166, Nov. 2000, doi: 10.1016/S0167-2738(00)00612-3.

[79] Choe, H. S., et al. "Preparation and characterization of poly(vinyl sulfone)- and poly(vinylidene fluoride)-based electrolytes - ScienceDirect." Accessed: Aug. 09, 2020. [Online]. Available: https://www.sciencedirect.com/science/article/pii/001346869500180M

[80] Zhu, Yusong, et al. "A Composite Gel Polymer Electrolyte with High Performance Based on Poly(Vinylidene Fluoride) and Polyborate for Lithium Ion Batterie - Advanced Energy Materials - Wiley Online Library." Accessed: Aug. 11, 2020. [Online]. Available: https://onlinelibrary.wiley.com/doi/abs/10.1002/aenm.201300647

[81] Y. Zhang *et al.*, "A gel single ion polymer electrolyte membrane for lithium-ion batteries with wide-temperature range operability," *RSC Advances*, vol. 4, no. 40, pp.

21163–21170, 2014, doi: 10.1039/C4RA02729A.

[82] X. Wang *et al.*, "A single-ion gel polymer electrolyte based on polymeric lithium tartaric acid borate and its superior battery performance," *Solid State Ionics*, vol. 262, pp. 747–753, Sep. 2014, doi: 10.1016/j.ssi.2013.09.007.

[83] P. Hu *et al.*, "A composite gel polymer electrolyte with high voltage cyclability for Ni-rich cathode of lithium-ion battery," *Electrochemistry Communications*, vol. 61, pp. 32–35, Dec. 2015, doi: 10.1016/j.elecom.2015.09.026.

[84] Deng, Fangli, et al. "Microporous polymer electrolyte based on PVDF/PEO star polymer blends for lithium ion batteries - ScienceDirect." Accessed: Aug. 09, 2020. [Online]. Available: https://www.sciencedirect.com/science/article/abs/pii/S0376738815004433

[85] D.-W. Kim, "Electrochemical characterization of poly(ethylene-co-methyl acrylate)-based gel polymer electrolytes for lithium-ion polymer batteries," *Journal of Power Sources*, vol. 87, no. 1, pp. 78–83, Apr. 2000, doi: 10.1016/S0378-7753(99)00363-8.

[86] M. Sivakumar, R. Subadevi, S. Rajendran, H.-C. Wu, and N.-L. Wu, "Compositional effect of PVdF–PEMA blend gel polymer electrolytes for lithium polymer batteries," *European Polymer Journal*, vol. 43, no. 10, pp. 4466–4473, Oct. 2007, doi: 10.1016/j.eurpolymj.2007.08.001.

[87] Agrawal, lS L., and Arvind Awadhia. "DSC and conductivity studies on PVA based proton conducting gel electrolytes | SpringerLink." Accessed: Aug. 09, 2020. [Online]. Available: https://link.springer.com/article/10.1007/BF02707280

[88] X. Ma, X. Huang, J. Gao, S. Zhang, Z. Deng, and J. Suo, "Compliant gel polymer electrolyte based on poly(methyl acrylate-co-acrylonitrile)/poly(vinyl alcohol) for flexible lithium-ion batteries," *Electrochimica Acta*, vol. 115, pp. 216–222, Jan. 2014, doi: 10.1016/j.electacta.2013.10.169.

[89] F. Lian, Y. Wen, Y. Ren, and H. Guan, "A novel PVB based polymer membrane and its application in gel polymer electrolytes for lithium-ion batteries," *Journal of*

Membrane Science, vol. 456, pp. 42–48, Apr. 2014, doi: 10.1016/j.memsci.2014.01.010.

[90] W. Xiao, X. Li, Z. Wang, H. Guo, Y. Li, and B. Yang, "Performance of PVDF-HFP-based gel polymer electrolytes with different pore forming agents," *Iran Polym J*, vol. 21, no. 11, pp. 755–761, Nov. 2012, doi: 10.1007/s13726-012-0081-7.

[91] A. Manuel Stephan, "Review on gel polymer electrolytes for lithium batteries," *European Polymer Journal*, vol. 42, no. 1, pp. 21–42, Jan. 2006, doi: 10.1016/j.eurpolymj.2005.09.017.

[92] Y. W. Chen-Yang, Y. T. Chen, H. C. Chen, W. T. Lin, and C. H. Tsai, "Effect of the addition of hydrophobic clay on the electrochemical property of polyacrylonitrile/LiClO4 polymer electrolytes for lithium battery," *Polymer*, vol. 50, no. 13, pp. 2856–2862, Jun. 2009, doi: 10.1016/j.polymer.2009.04.023.

[93] A. Mejía *et al.*, "Scalable plasticized polymer electrolytes reinforced with surface-modified sepiolite fillers – A feasibility study in lithium metal polymer batteries," *Journal of Power Sources*, vol. 306, pp. 772–778, Feb. 2016, doi: 10.1016/j.jpowsour.2015.12.099.

[94] B. Liang, Q. Jiang, S. Tang, S. Li, and X. Chen, "Porous polymer electrolytes with high ionic conductivity and good mechanical property for rechargeable batteries," *Journal of Power Sources*, vol. 307, pp. 320–328, Mar. 2016, doi: 10.1016/j.jpowsour.2015.12.127.

[95] B. Liang *et al.*, "Preparation and characterization of PEO-PMMA polymer composite electrolytes doped with nano-Al2O3," *Electrochimica Acta*, vol. 169, pp. 334–341, Jul. 2015, doi: 10.1016/j.electacta.2015.04.039.

[96] Y. Ma, L. B. Li, G. X. Gao, X. Y. Yang, and Y. You, "Effect of montmorillonite on the ionic conductivity and electrochemical properties of a composite solid polymer electrolyte based on polyvinylidenedifluoride/polyvinyl alcohol matrix for lithium ion batteries," *Electrochimica Acta*, vol. 187, pp. 535–542, Jan. 2016, doi: 10.1016/j.electacta.2015.11.099.

[97] Sharma, A. L., and Awalendra K. Thakur "Plastic separators with improved properties for portable power device applications | SpringerLink." Accessed: Aug. 09, 2020. [Online]. Available: https://link.springer.com/article/10.1007/s11581-012-0760-6

[98] "Improvement in voltage, thermal, mechanical stability and ion transport properties

in polymer-clay nanocomposites - Sharma - 2010 - Journal of Applied Polymer Science - Wiley Online Library." Accessed: Aug. 09, 2020. [Online]. Available: https://onlinelibrary.wiley.com/doi/abs/10.1002/app.32677

[99] Lin, Dingchang, et al. "High Ionic Conductivity of Composite Solid Polymer Electrolyte via In Situ Synthesis of Monodispersed SiO2 Nanospheres in Poly(ethylene oxide) | Nano Letters." Accessed: Aug. 09, 2020. [Online]. Available: https://pubs.acs.org/doi/abs/10.1021/acs.nanolett.5b04117

[100] T. Dam, N. K. Karan, R. Thomas, D. K. Pradhan, and R. S. Katiyar, "Observation of ionic transport and ion-coordinated segmental motions in composite (polymer-salt-clay) solid polymer electrolyte," *Ionics*, vol. 21, no. 2, pp. 401–410, Feb. 2015, doi: 10.1007/s11581-014-1181-5.

[101] S. Klongkan and J. Pumchusak, "Effects of Nano Alumina and Plasticizers on Morphology, Ionic Conductivity, Thermal and Mechanical Properties of PEO-LiCF3SO3 Solid Polymer Electrolyte," *Electrochimica Acta*, vol. 161, pp. 171–176, Apr. 2015, doi: 10.1016/j.electacta.2015.02.074.

[102] F. A. Amaral *et al.*, "Preparation and characterization of the porous solid polymer electrolyte of PAN/PVA by phase inversion," *J Appl Electrochem*, vol. 45, no. 8, pp. 809–820, Aug. 2015, doi: 10.1007/s10800-015-0816-1.

[103] P. Tamilselvi and M. Hema, "Structural, thermal, vibrational, and electrochemical behavior of lithium ion conducting solid polymer electrolyte based on poly(vinyl alcohol)/poly(vinylidene fluoride) blend," *Polym. Sci. Ser. A*, vol. 58, no. 5, pp. 776–784, Sep. 2016, doi: 10.1134/S0965545X16050199.

[104] H. Zhang *et al.*, "Lithium bis(fluorosulfonyl)imide/poly(ethylene oxide) polymer electrolyte," *Electrochimica Acta*, vol. 133, pp. 529–538, Jul. 2014, doi: 10.1016/j.electacta.2014.04.099.

[105] Karthik, Sekar, et al. "Polyvinyl Alcohol Based Solid Electrolyte Film: Synthesis, Characterization and Electrical Properties - Macromolecular Symposia - Wiley Online Library." Accessed: Aug. 09, 2020. [Online]. Available:

https://onlinelibrary.wiley.com/doi/abs/10.1002/masy.201400230

[106] S. Rajendran, M. R. Prabhu, and M. U. Rani, “Characterization of PVC/PEMA Based Polymer Blend Electrolytes,” *Int. J. Electrochem. Sci.*, vol. 3, p. 9, 2008.

[107] C. S. Ramya, T. Savitha, S. Selvasekarapandian, and G. Hirankumar, “Transport mechanism of Cu-ion conducting PVA based solid-polymer electrolyte,” *Ionics*, vol. 11, no. 5–6, pp. 436–441, Sep. 2005, doi: 10.1007/BF02430262.

[108] Y. Li, J. Wang, J. Tang, Y. Liu, and Y. He, “Conductive performances of solid polymer electrolyte films based on PVB/LiClO4 plasticized by PEG200, PEG400 and PEG600,” *Journal of Power Sources*, vol. 187, no. 2, pp. 305–311, Feb. 2009, doi: 10.1016/j.jpowsour.2008.11.126.

[109] L. Liu, Z. Wang, Z. Zhao, Y. Zhao, F. Li, and L. Yang, “PVDF/PAN/SiO2 polymer electrolyte membrane prepared by combination of phase inversion and chemical reaction method for lithium ion batteries,” *J Solid State Electrochem*, vol. 20, no. 3, pp. 699–712, Mar. 2016, doi: 10.1007/s10008-015-3095-1.

[110] P. G. Bruce, “Structure and electrochemistry of polymer electrolytes,” *Electrochimica Acta*, vol. 40, no. 13, pp. 2077–2085, Oct. 1995, doi: 10.1016/0013-4686(95)00144-4.

[111] J. Wu *et al.*, “Electrolytes in Dye-Sensitized Solar Cells,” *Chem. Rev.*, vol. 115, no. 5, pp. 2136–2173, Mar. 2015, doi: 10.1021/cr400675m.

[112] S. V. Kumar, K. A. Razak, H. K. Madhusudhana, A. Buradi, A. Afzal, and C. A. Saleel, “Preparation of dye (Bala gidda) for DSSC application,” *Materials Today: Proceedings*, vol. 47, pp. 6153–6157, 2021.

[113] J. Gong, K. Sumathy, Q. Qiao, and Z. Zhou, “Review on dye-sensitized solar cells (DSSCs): Advanced techniques and research trends,” *Renewable and Sustainable Energy Reviews*, vol. 68, pp. 234–246, 2017.

[114] J. Gong, J. Liang, and K. Sumathy, “Review on dye-sensitized solar cells (DSSCs): Fundamental concepts and novel materials,” *Renewable and Sustainable Energy Reviews*, vol. 16, no. 8, pp. 5848–5860, 2012.

[115] M. Yanagida, N. Onozawa-Komatsuzaki, M. Kurashige, K. Sayama, and H.

Sugihara, “Optimization of tandem-structured dye-sensitized solar cell,” *Solar Energy Materials and Solar Cells*, vol. 94, no. 2, pp. 297–302, 2010.

[116] M. Alhamed, A. S. Issa, and A. W. Doubal, “Studying of natural dyes properties as photo-sensitizer for dye sensitized solar cells (DSSC),” *Journal of electron Devices*, vol. 16, no. 11, pp. 1370–1383, 2012.

[117] K. Sharma, V. Sharma, and S. S. Sharma, “Dye-Sensitized Solar Cells: Fundamentals and Current Status,” *Nanoscale Res Lett*, vol. 13, no. 1, p. 381, Dec. 2018, doi: 10.1186/s11671-018-2760-6.

[118] H. Iftikhar, G. G. Sonai, S. G. Hashmi, A. F. Nogueira, and P. D. Lund, “Progress on electrolytes development in dye-sensitized solar cells,” *Materials*, vol. 12, no. 12, p. 1998, 2019.

[119] M. Sokolskỳ and J. Cirák, “Dye-sensitized solar cells: materials and processes,” *Acta Electrotechnica et Informatica*, vol. 10, no. 3, pp. 78–81, 2010.

[120] P. Gu *et al.*, “Influence of electrolyte proportion on the performance of dye-sensitized solar cells,” *AIP Advances*, vol. 7, no. 10, 2017, Accessed: Dec. 07, 2023. [Online]. Available: https://pubs.aip.org/aip/adv/article/7/10/105219/977765

[121] J. Song *et al.*, “Improved utilization of photogenerated charge using fluorine-doped TiO2 hollow spheres scattering layer in dye-sensitized solar cells,” *ACS applied materials & interfaces*, vol. 4, no. 7, pp. 3712–3717, 2012.

[122] J. Lin, J. Chen, and X. Chen, “High-efficiency dye-sensitized solar cells based on robust and both-end-open TiO2 nanotube membranes,” *Nanoscale research letters*, vol. 6, no. 1, pp. 1–5, 2011.

[123] A. Latini *et al.*, “Efficiency improvement of DSSC photoanode by scandium doping of mesoporous titania beads,” *The Journal of Physical Chemistry C*, vol. 117, no. 48, pp. 25276–25289, 2013.

[124] Z. Tong, T. Peng, W. Sun, W. Liu, S. Guo, and X.-Z. Zhao, “Introducing an intermediate band into dye-sensitized solar cells by W6+ doping into TiO2 nanocrystalline photoanodes,” *The Journal of Physical Chemistry C*, vol. 118, no. 30, pp. 16892–16895,

2014.

[125] A. Subramanian and H.-W. Wang, “Effects of boron doping in TiO2 nanotubes and the performance of dye-sensitized solar cells,” *Applied Surface Science*, vol. 258, no. 17, pp. 6479–6484, 2012.

[126] A. M. Bakhshayesh and N. Farajisafiloo, “Efficient dye-sensitised solar cell based on uniform In-doped TiO2 spherical particles,” *Applied Physics A*, vol. 120, no. 1, pp. 199–206, 2015.

[127] Y. Tabari-Saadi and M. R. Mohammadi, “Efficient dye-sensitized solar cells based on carbon-doped TiO 2 hollow spheres and nanoparticles,” *Journal of Materials Science: Materials in Electronics*, vol. 26, pp. 8863–8876, 2015.

[128] S. S. Sharma, K. Sharma, and V. Sharma, “Nanographite-TiO2 photoanode for dye sensitized solar cells,” in *AIP Conference Proceedings*, AIP Publishing LLC, 2016, p. 020515.

[129] Q. Yang *et al.*, “Ternary platinum alloy counter electrodes for high-efficiency dye-sensitized solar cells,” *Electrochimica Acta*, vol. 190, pp. 85–91, 2016.

[130] Q. Tang, H. Zhang, Y. Meng, B. He, and L. Yu, “Dissolution engineering of platinum alloy counter electrodes in dye-sensitized solar cells,” *Angewandte Chemie International Edition*, vol. 54, no. 39, pp. 11448–11452, 2015.

[131] P. Yang and Q. Tang, “A branching NiCuPt alloy counter electrode for high-efficiency dye-sensitized solar cell,” *Applied Surface Science*, vol. 362, pp. 28–34, 2016.

[132] J. Balamurugan, T. D. Thanh, N. H. Kim, and J. H. Lee, “Nitrogen-doped graphene nanosheets with FeN core–shell nanoparticles as high-performance counter electrode materials for dye-sensitized solar cells,” *Advanced Materials Interfaces*, vol. 3, no. 1, p. 1500348, 2016.

[133] Z. Shi *et al.*, “Efficient p-type dye-sensitized solar cells with all-nano-electrodes: NiCo2S4 mesoporous nanosheet counter electrodes directly converted from NiCo2O4 photocathodes,” *Nanoscale research letters*, vol. 9, no. 1, pp. 1–6, 2014.

[134] S. K. Prakash, R. K. Sharma, M. S. Roy, and M. Kumar, “Carbon coated stainless steel as counter electrode for dye sensitized solar cells,” in *AIP Conference Proceedings*,

American Institute of Physics, 2014, pp. 218–222.

[135] A. A. Arbab, K. C. Sun, I. A. Sahito, M. B. Qadir, Y. S. Choi, and S. H. Jeong, "A novel activated-charcoal-doped multiwalled carbon nanotube hybrid for quasi-solid-state dye-sensitized solar cell outperforming Pt electrode," *ACS Applied Materials & Interfaces*, vol. 8, no. 11, pp. 7471–7482, 2016.

[136] C.-H. Tsai, P.-H. Fei, and C.-H. Chen, "Investigation of coral-like Cu2O nano/microstructures as counter electrodes for dye-sensitized solar cells," *Materials*, vol. 8, no. 9, pp. 5715–5729, 2015.

[137] Yang, Jiabao, et al. "Influence of the Donor Size in D−π–A Organic Dyes for Dye-Sensitized Solar Cells | Journal of the American Chemical Society." Accessed: Jun. 21, 2023. [Online]. Available: https://pubs.acs.org/doi/abs/10.1021/ja500280r

[138] K.-M. Lee *et al.*, "A high-performance counter electrode based on poly (3, 4-alkylenedioxythiophene) for dye-sensitized solar cells," *Journal of Power Sources*, vol. 188, no. 1, pp. 313–318, 2009.

[139] G. K. R. Senadeera, P. V. V. Jayaweera, V. P. S. Perera, and K. Tennakone, "Solid-state dye-sensitized photocell based on pentacene as a hole collector," *Solar energy materials and solar cells*, vol. 73, no. 1, pp. 103–108, 2002.

[140] N. Puspitasari, S. S. N. Amalia, and G. Yudoyono, "Effect of Mixing Dyes and Solvent in Electrolyte Toward Characterization of Dye Sensitized Solar Cell Using Natural Dyes as The Sensitizer," in *IOP Conference Series: Materials Science and Engineering*, IOP Publishing, 2017, p. 012022.

[141] N. Metri *et al.*, "Processable star-shaped molecules with triphenylamine core as hole-transporting materials: Experimental and theoretical approach," *The Journal of Physical Chemistry C*, vol. 116, no. 5, pp. 3765–3772, 2012.

[142] K. C. Sun *et al.*, "Highly efficient and durable dye-sensitized solar cells based on a wet-laid PET membrane electrolyte," *Journal of Materials Chemistry A*, vol. 4, no. 2, pp. 458–465, 2016.

[143] E. L. Unger *et al.*, "Contribution from a hole-conducting dye to the photocurrent in

solid-state dye-sensitized solar cells," *Physical Chemistry Chemical Physics*, vol. 13, no. 45, pp. 20172–20177, 2011.

[144] M. Patel, K. G. Chandrappa, and A. J. Bhattacharyya, "Increasing ionic conductivity and mechanical strength of a plastic electrolyte by inclusion of a polymer," *Electrochimica Acta*, vol. 54, no. 2, pp. 209–215, Dec. 2008, doi: 10.1016/j.electacta.2008.08.010.

[145] L. B. Patle and A. L. Chaudhari, "Performance of DSSC with Cu Doped TiO2 electrode prepared by dip coating technique," *Int J Sci Eng Res*, vol. 7, no. 8, pp. 1004–1009, 2016.

[146] N. Ibrayev, E. Seliverstova, R. Dzhanabekova, and T. Serikov, "Photovoltaic properties of DSSC with composite counter electrodes based on Pt and SLGO," in *IOP Conference Series: Materials Science and Engineering*, IOP Publishing, 2018, p. 012009.

[147] C.-H. Tsai, P.-H. Fei, and C.-H. Chen, "Investigation of coral-like Cu2O nano/microstructures as counter electrodes for dye-sensitized solar cells," *Materials*, vol. 8, no. 9, pp. 5715–5729, 2015.